



universität
wien

MASTERARBEIT / MASTER'S THESIS

Titel der Masterarbeit / Title of the Master's Thesis

„On the conversion of selected anticancer Thiosemicarbazones to their respective potent copper complexes in human serum – An incubation study and analysis using SEC HPLC – ICP-QqQ MS“

verfasst von / submitted by

Tomáš PRSTEK, BSc

angestrebter akademischer Grad / in partial fulfilment of the requirements for the degree of
Master of Science (MSc)

Wien, 2021 / Vienna, 2021

Studienkennzahl lt. Studienblatt /
degree programme code as it appears on
the student record sheet:

UA 066 862

Studienrichtung lt. Studienblatt /
degree programme as it appears on
the student record sheet:

Masterstudium Chemie

Betreut von / Supervisor:

Univ.-Prof. Dr. Gunda Köllensperger

Declaration of originality

I hereby declare that this Master's thesis was originated and composed entirely by me. I confirm that the informations derived from published and unpublished works of others have been acknowledged in the text and that corresponding sources are given in section 5.References respectively.

Vienna, July 2021

Signature: _____

Tomáš Prstek

Acknowledgments

I would like to express my sincere gratitude to my supervisors Martin Schaier, MSc., Anna Schoeberl, MSc., Dr. Sarah Theiner and Andreas Schweikert, MSc. for providing their direct guidance, help, suggestions and comments throughout the course of my project. I would like to thank Univ.-Prof. Dr. Gunda Köllensperger for giving me the opportunity to be part of her brilliant research team. Also, I would like to thank my whole family for being a great support throughout my entire graduate education.

Table of Contents

Declaration of originality.....	I
Acknowledgments.....	II
List of abbreviations.....	V
Abstract.....	VIII
Zusammenfassung.....	IX
1. Introduction.....	1
1.1 Thiosemicarbazones.....	1
1.2 Inductively coupled plasma – Mass spectrometry.....	6
1.3 Size exclusion High-performance liquid chromatography.....	18
2. Experimental section.....	23
2.1 Reagents and other chemical materials.....	23
2.1.1 Basic chemicals, solvents and standards.....	23
2.1.2 Preparation of solutions.....	24
2.1.3 Samples.....	25
2.1.4 Other chemical materials.....	27
2.2 Consumables.....	27
2.3 Instrumentation.....	28
2.3.1 Mass spectrometer.....	28
2.3.1.1 Agilent 7800 mass spectrometer.....	28
2.3.1.2 Agilent 8800 mass spectrometer.....	30
2.3.2 Liquid Chromatography system.....	32
2.4 Cleanroom.....	33
2.5 Experimental setups and sample preparations.....	33
2.5.1 Assessment of contaminations in cell Culture media.....	33
2.5.2 Selection of viable solvent system for optimal measurement performance and background reduction (Cell culture media and Thiosemicarbazones in flow injection experiments).....	34
2.5.3 Experimental setup and preparation of alternative quantitation standard – bovine CuZn Superoxid Dismutase).....	35
2.5.4 Selection of appropriate analytical column – separation experiment with human blood serum (proteins).....	35

2.5.5 Description of main experiments - incubation studies.....	36
2.5.6 Preparation of Cu-Selective ion exchange resin (CHELEX® ion exchange) and experimental setup for subsequent measurements of filtered cell culture media components.....	37
2.5.5 non-lethal in-vivo experiments with Triapine in mouse.....	38
2.6 Data handling.....	38
2.6.1 General handling of outputs.....	38
2.6.2 Multilinear regression (MLR)	39
3. Results and discussion.....	40
3.1 Assessment of contaminations in cell culture media.....	40
3.1.1 Contamination analysis using a digestion method.....	40
3.1.2 Contamination analysis using a flow-injection method.....	44
3.2 Analysis of Thiosemicarbazones in flow injection analysis mode.....	48
3.3 Analytical column choice for main experiments	49
3.4 Analysis of human blood protein standards	56
3.5 Multilinear regression.....	61
3.6 Main experiments – Incubation studies.....	65
3.6.1 Baseline measurements (Buffered human blood plasma).....	65
3.6.2 Incubation experiments of Thiosemicarbazones with buffered human blood serum	71
3.7 Free TSC elution experiment using MabPac analytical column	87
3.8 Alternative quantitation using bovine Cu-Zn Superoxide Dismutase.....	88
3.9 In vivo Incubation (Mouse) – a short metabolic study.....	89
3.10 CHELEX® ion exchange for background reduction in cell culture media	90
4. Conclusions.....	91
5. References.....	93
List of tables.....	98
List of figures.....	99

List of Abbreviations

3AP	Triapine; 3-Aminopyridine-2-carboxaldehyde-thiosemicarbazone
5-HP	5-hydroxyl-2-formyl-pyridine-thiosemicarbazone
A	Ampere (Unit of electrical amperage) [A]
AC	Alternating current
Ar	Argon
bar	Bar (Unit of pressure) [$*10^5 \text{ kg} \cdot \text{m}^{-1} \cdot \text{s}^{-2}$]
bCuZnSoD	Bovine Copper-Zinc Superoxide Dismutase (Enzyme)
COTI2	4-(pyridine-2-yl)-N-([(8E)-5,6,7,8-tetrahydroquinolin-8-ylidene]amino)piperazine-1-carbothioamide
Cu	Copper
Cu-TSC	Copper-Thiosemicarbazone complex
CRM	Certified reference material
Da	Dalton (Unit of atomic mass)
DC	Direct current
DMF	Dimethyl Formamide
DNA	Deoxyribonucleic acid
Dp44mT	Di-2-pyridylketone-4,4,-dimethyl-3-thiosemicarbazone
DpC	Di-2-pyridylketone-4-cyclohexyl-4-methyl-3-thiosemicarbazone
<i>F</i>	abbreviation for Force (Unit) [$\text{kg} \cdot \text{m} \cdot \text{s}^{-2}$]
<i>f</i>	abbreviation for Frequency (Unit) [s^{-1}]
FA	Formic Acid
FBS	Fetal bovine serum
HEPES	(4-(2-hydroxyethyl)-1-piperazineethanesulfonic acid) – Buffering Agent
HPLC	High performance liquid chromatography or high-pressure liquid chromatography
HRSF-MS	High resolution sector field mass spectrometry
Hz	Hertz (Unit of frequency) [s^{-1}]
ICP	Inductively coupled plasma
ICP-MS	Inductively coupled plasma – Mass spectrometry
ICP-OES	Inductively coupled plasma – optical emission spectroscopy
IgA	Immunoglobuline A

IgG	Immunoglobuline G
IgM	Immunoglobuline M
IKF-MUW	Institut für Krebsforschung der Medizinischen Universität Wien
IPA	Isopropanol
K	Kelvin (Unit of temperature) [K]
k	kilo- (Prefix *10 ³)
kDa	kiloDalton (Unit) derived from Da – Dalton
LA	Laser ablation
LA-ICP-MS	Laser ablation inductively coupled plasma – mass spectrometry
LC	Liquid chromatography
M	Molar concentration (Unit) [mol*L ⁻¹] or Mega- (Prefix *10 ⁶)
<i>m</i>	abbreviation for Mass (Unit) [kg] or milli- (Prefix *10 ⁻³)
Me ₂ NNMe ₂	3-(Dimethylamino)pyridine-2-carbaldehyde N,N-Dimethyl-thiosemicarbazone
MEME	Minimal essential medium eagle
MHz	Megahertz (Unit of frequency) derived from Hz – Hertz [10 ⁶ *Hz]
MLR	Multilinear Regression
MS	Mass spectrometry
ms	Millisecond (Unit of time) derived from s - second
m/z	Mass over charge ratio (mass spectrometric Unit)
PEEK	Polyetheretherketon
PFA	Perfluoroalkoxy alkane
q	Denotation for a single quadrupole, usually deployed in “ion pass-through” mode
QqQ	Denotation for triple quadrupole setup in mass spectrometry; Q being analyzer Quadrupole
RF	Radiofrequency (used in quadrupole applications to refer to AC voltage)
RNA	Ribonucleic acid
RR	Ribonucleotide reductase (enzyme)
s	Second (Unit of time) [s]
SAR	Structure-Activity relationship
SEC	Size exclusion chromatography (Subtype of liquid chromatography)
STDDEV	Standard deviation (statistics)
TOF	Time of flight

TRA	Time resolved analysis
TSC	Thiosemicarbazones
V	Volt (Unit of electrical voltage) [$\text{kg}\cdot\text{m}^2\cdot\text{A}^{-1}\cdot\text{s}^{-3}$]
W	Watt (Unit of power) [$\text{kg}\cdot\text{m}^2\cdot\text{s}^{-3}$]
μ	micro- (Prefix $\cdot 10^{-6}$)
μM	(micro-)molar concentration (Unit with prefix) [$10^{-6}\cdot\text{mol}\cdot\text{L}^{-1}$]
Ω	Ohm (Unit of electrical resistance) [$\text{kg}\cdot\text{m}^2\cdot\text{A}^{-2}\cdot\text{s}^{-3}$]
ω	Angular frequency (Unit) [$2\pi\text{f}$; $\text{rad}\cdot\text{s}$]

Abstract

In the last around 70 years, Thiosemicarbazones were investigated extensively due to their multifaceted properties. In fact, several specific members of the thiosemicarbazone family were tested in preclinical and clinical trials for medical conditions like Rheumatism, Psoriasis, Tuberculosis, Malaria, Leprosy and many other bacterial, viral and zoonotic infections. The efficacy of thiosemicarbazones was mediocre and flawed in the beginning, but due to extensive research efforts few highly interesting applications of the agents were elucidated. One subgroup, namely α -N-heterocyclic thiosemicarbazones were found to be excellent candidates for cancer treatment. The key parameter of α -N-heterocyclic thiosemicarbazones is their cytotoxicity against rapidly dividing cells. Exploiting several crucial cellular pathways for growth, survival and cellular integrity, α -N-heterocyclic thiosemicarbazones can effectively target rapidly progressing cancer cells.

The Aim of this master's thesis is to further deepen the already broad understanding of anticancer Thiosemicarbazones and their molecular-mechanistic mode of action. It is generally known that thiosemicarbazones act as strong chelating agents; their chelating properties in fact are so strong, that analytical attempts like chromatographic separations using steel columns may become very difficult as shall be demonstrated in later parts of this work. For the mode of action of Thiosemicarbazones there is a rather large consensus that free Thiosemicarbazones have relatively low biological activity, but upon complexation with copper, iron or possibly other metals, their cytotoxic activity raises by orders of magnitude in some cases. Therefore, the main part of this master's thesis deals with measurement strategies on detecting interactions between free thiosemicarbazones and proteins in human blood serum (mainly copper and iron proteins). The question I want to answer is whether free Thiosemicarbazones can pull copper or iron from blood proteins like ceruloplasmin, albumin, transcuprein (α 2-Macroglobulin) etc. and if so, what is the timeframe for this process? The main method for this experiment series is a standard incubation study using buffered human blood serum at physiological temperature of 37°C and selected free and copper-bound thiosemicarbazones. For protein separations a size exclusion chromatography was chosen. The main analytical information is facilitated by means of ICP-MS/MS (elemental analysis).

Zusammenfassung

In den letzten rund 70 Jahren wurden Thiosemicarbazone aufgrund ihrer vielfältigen biologischen Eigenschaften vielfach wissenschaftlich untersucht. Tatsächlich wurden sehr früh mehrere spezifische Mitglieder der Klasse der Thiosemicarbazone in präklinischen und klinischen Studien gegen Erkrankungen wie Rheuma, Psoriasis, Tuberkulose, Malaria, Lepra und viele andere bakterielle, virale und zoonotische Infektionen getestet. Die Wirksamkeit von Thiosemicarbazonen war anfangs unzureichend, aber aufgrund umfangreicher Forschungsanstrengungen wurden einige wenige hochinteressante praktische Anwendungen dieser Wirkstoffe identifiziert. Eine Unterklasse, nämlich die α -N-heterocyclische Thiosemicarbazone, erwiesen sich als ausgezeichnete Kandidaten für die Behandlung von Krebserkrankungen. Der wichtigste Schlüssel-parameter von α -N-heterocyclischen Thiosemicarbazonen ist ihre Zytotoxizität gegen sich schnell teilende Zellen. α -N-heterocyclische Thiosemicarbazone stören essenzielle zelluläre Pathways für Wachstum, Überleben und zelluläre Integrität und können effektiv gegen sich schnell vermehrende Krebszellen wirken.

Das Ziel dieser Masterarbeit ist es, weitere wissenschaftliche Beiträge zum bereits breiten Fachwissen über Thiosemicarbazone in der Krebsforschung zu liefern. Es ist bereits bekannt, dass Thiosemicarbazone starke Chelatoren von einigen Übergangsmetallen sind. Diese Eigenschaft der Thiosemicarbazone ist in manchen Fällen so stark, dass analytische Versuche wie chromatographische Trennungen mit Stahlsäulen sehr schwierig werden können, wie in späteren Teilen dieser Arbeit gezeigt werden soll. Über die Wirkungsweise von Thiosemicarbazonen besteht ein wissenschaftlicher Konsens, dass freie Thiosemicarbazone eine relativ geringe biologische Aktivität aufweisen, aber bei Komplexbildung mit Kupfer, Eisen oder möglicherweise anderen Metallen ihre zytotoxische Aktivität in einigen Fällen um Größenordnungen ansteigt. Der Hauptteil dieser Masterarbeit befasst sich daher mit Messstrategien, um Wechselwirkungen zwischen Thiosemicarbazonen und Proteinen im menschlichen Blutserum (hauptsächlich Kupfer- und Eisenproteine) analytisch zugänglich zu machen und zu bestimmen. Die Frage, die ich beantworten möchte, ist, ob freie Thiosemicarbazone Kupfer oder Eisen aus Blutserumproteinen wie Ceruloplasmin, Albumin, Transcuprein (α 2-Macroglobulin) usw. komplexieren können und wenn ja, wie ist der Zeitrahmen für diesen Prozess. Die Hauptmethode für diese Versuchsreihe ist eine standard-Inkubationsstudie. Verwendet wird gepuffertes menschlichem Blutserum bei der physiologischen Temperatur von 37°C. 5 ausgewählte freie und kupfergebundene Thiosemicarbazone werden dabei untersucht. Die Analyse erfolgt über die Größenausschlusschromatographie gekoppelt mit der ICP-MS / MS (Elementaranalyse).

1. Introduction

1.1 Thiosemicarbazones

Thiosemicarbazones (TSC) represent a broad class of organic compounds which have the general structure as shown in figure 1 below. TSCs were found as more or less strong metal chelating agents – this is due to their unique geometry, the placement and distance of sulfur and nitrogen atoms that allow for bidentate coordination of metals like iron, zinc, copper and many more.[1,2] Several thiosemicarbazones were additionally found to possess interesting medicinal properties, which sparked a wide research interest. There are plentiful mentions in the literature of thiosemicarbazone derivatives being at least partly effective against medical conditions such as tuberculosis, leprosy, bacterial and viral infections, psoriasis, rheumatism, trypanosomiasis, coccidiosis and among many others, also against malignant diseases.[1,3] It is for the cytostatic and cytotoxic activity, which can eventually be effectively directed against cancerous cells that is currently a topic of high interest and a part of this master's thesis. Presently, the most promising subclass of TSCs in cancer treatment is α -N-heterocyclic thiosemicarbazones (more specifically, α -pyridyl thiosemicarbazones) and their metal complexes (see figure 2: Pyridyl in α -position to the thiosemicarbazide denoted with an arrow).[3, 4]

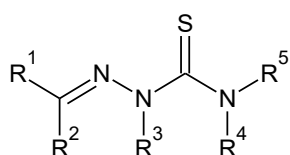


Figure 1: General structure of Thiosemicarbazones

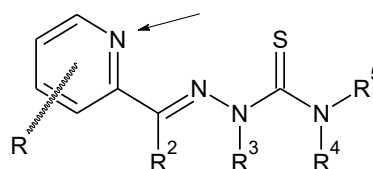


Figure 2: General structure of α -N-Heterocyclic TSCs

α -N-heterocyclic TSCs are generally more potent metal chelators than other simply-derived TSCs. This is due to their ability to undergo complexation reactions with metals in a tridentate manner.[2] An extensive summary of research on complexation properties of TSCs is given by *Tarlok S. Lobana, Rekha Sharma, Gagandeep Bawa and Sonia Khanna* in their review “*Bonding and structure trends of thiosemicarbazone derivatives of metals—An overview*” from 2008. This highly relevant work contains physicochemical data on stability properties of almost every metal complex of TSC, spectroscopic data thereof and much more.

To explain the cytotoxic activity, TSCs were found to act (at least) partly as ribonucleotide reductase (RR) inhibitors.[5]

Ribonucleotide reductase, briefly, is an enzyme found in all living organisms. It is responsible for converting ribonucleotides (building units of RNA) into deoxyribonucleotides (building units of DNA).

There are currently 3 known classes of RR: class II and III being anaerobic and only relevant to prokaryotic organisms and archaea.[6] For our discussion class I RR is oxygen dependent, and the only one which is found in eukaryotic organisms including humans and, therefore, relevant in this work. The dimeric enzyme consists of two asymmetrical substructures and its core functional unit is an iron atom in close proximity to a tyrosine side chain. The iron cycles between +II and +III state providing reductive electrons to tyrosine, generating tyrosyl radical. Tyrosyl radical then funnels reductive electrons into the reaction site of the enzyme where a ribonucleotide is bound and converted to deoxyribonucleotide.[7] The inhibition of this enzyme causes a cell to arrest in its cell cycle. This is generally not a very big issue for cells that do not divide further, i.e. cells that stay in stationary G_0 of their cell cycle. However, cells that are quickly reproducing like blood-forming cells, small intestine epithelial cells[8], but also cancerous cells are susceptible to RR inhibition. The effects of RR inhibition may range depending on agent's concentration and its effective half-life from slowdown in growth to cell death by deprivation of DNA building units.[9] Importantly, cancerous cells often overproduce their RR to further increase their rate of reproduction. Therefore, RR was quickly recognized to be an important possible target for cancer treatment.[10] Many research groups tested various α -N-heterocyclic TSC derivatives for their anti-cancer properties since at least 1950's. The search for relevant literature is difficult as many sources are not digitalized and references from old publications disappear into unpublished works. However, one of the first mentions of competent research on α -N-heterocyclic TSCs can be found in "*Observations on the Antileukemic Activity of Pyridine-2-carboxaldehyde Thiosemicarbazone and Thiocarbohydrazone*" by R.W. Brockman, J.Richard Thomson, Martelia J. Bell and Howard E. Skipper from 1956. This work clearly identifies α -N-heterocyclic TSCs as potential anticancer drugs.[11] Since then, tens to hundreds other α -N-heterocyclic TSCs were proposed and tested. One of the more prominent TSC anticancer agents of the early research was 5-hydroxyl-2-formyl-pyridine thiosemicarbazone (5-HP) which entered clinical trials in 1972 but failed due to fast metabolization and low efficacy against solid tumors.

Also, severe side effects such as gastrointestinal intolerance and methemoglobinemia prevented the drug from further testing in its contemporary form.[12] Two years prior, in 1970 the molecular target was elucidated to be primarily ribonucleotide reductase.[13] However, partly contradictory and confusing results on molecular target were obtained in the following years to decades thereafter. While (to current knowledge) RR is in fact inhibited to various degrees by TSCs, other, possibly more important mechanisms of action seemed very well be involved too. Noteworthy, iron - α -N-heterocyclic TSC complexes shifted into the spotlight of research for their enhanced activity. In the published work by *Antholine, William, et al. "Studies of the reaction of 2-formylpyridine thiosemicarbazone and its iron and copper complexes with biological systems."* from 1977 there is a strong suggestion that it is the redox activity of Iron-TSCs rather than RR inhibition alone that results in cytotoxic effects.[14] In fact, some researchers in recent years investigated the possibility of iron, copper or other metal redox cycling while coordinated by TSC ligands and concluded that such redox cycling processes ($\text{Fe}^{\text{II}}/\text{Fe}^{\text{III}}$, $\text{Cu}^{\text{I}}/\text{Cu}^{\text{II}}$ and others) might very well contribute to oxidative stress in cells or damage essential redox active enzymatic sites.[15,16] Historically, another promising candidate was 3-Aminopyridine-2-carboxaldehyde-thiosemicarbazone (Triapine or 3AP). 3AP is one of the simplest of α -N-heterocyclic TSCs and, furthermore, one of the few substances of its class that was extraordinarily promising as to be tested in several clinical trials on oncological patients.[17,18,19] 3AP entered clinical trials in 2003 and showed results worth of further investigation and research into Triapine-like drugs. In the subsequent publication "*Phase I and pharmacodynamic study of Triapine[®], a novel ribonucleotide reductase inhibitor, in patients with advanced leukemia*", *Francis J. by Giles et al.* underlined the partial efficacy against leukemia, prominent RR-inhibiting activity in patients and the necessity of further elucidating of mechanism of action possibly in a follow up study with Triapine in combination therapy. [18] 3AP was then deployed in several other clinical trials.[19] Ultimately, however, 3AP was proven ineffective against solid tumors due to its short plasma half-life and rapid metabolic inactivation.[20] Although many research groups tested dozens of α -N-heterocyclic TSCs before, a proper systematical approach to understand structure – activity relations (SAR) of α -N-heterocyclic TSCs in respect to the cytotoxicity (RR inhibition potential) was done by *Christian Kowol et al.* in their publication "*Impact of Stepwise NH_2 -Methylation of Triapine on the Physicochemical Properties, Anticancer Activity, and Resistance Circumvention*" from 2016, that laid the framework on further synthesis strategies as well as by stepwise

methylation, elucidating the molecular sites on TSC moiety (see figure 3) which had the highest activity response on cancer cell lines SW480, A2780 and on several other treatment resistant cell lines.[21]

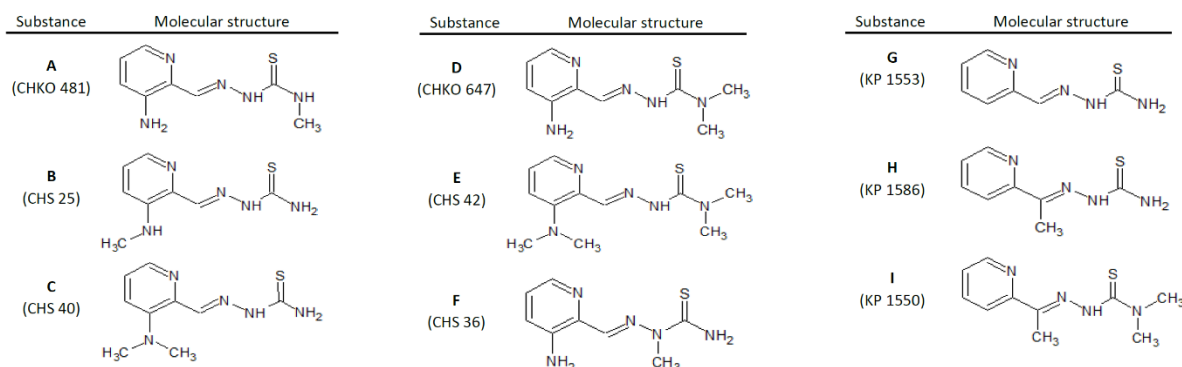


Figure 3: Structures of several methyl-derivated TSCs from the publication “Impact of Stepwise NH₂-Methylation of Triapine on the Physicochemical Properties, Anticancer Activity, and Resistance Circumvention” by C. Kowol et al. that were systematically tested for anticancer activity on cancer cell lines

A major step in elucidating the sought after exact molecular mechanism of action of TSCs was laid down by Karla Pelivan et al. in their publication “Understanding the metabolism of the anticancer drug Triapine: electro-chemical oxidation, microsomal incubation and in vivo analysis using LC-HRMS” from 2017. The aim of this work was to analyze the metabolic pathway of 3AP in living organisms. 3AP as a rather simple molecule was excellently suitable for preliminary suggestions on what chemical modifications does this drug undergo before it is completely inactivated and excreted. The research group was able to work out the molecular structure of several metabolites and pointed out major flaws of the drug such as low stability in biological environments and fast metabolization end excretion. As can be expected, the metabolization pathway of Triapine involves metabolic water solubility increase e.g. by introducing hydrophilic -OH groups and by conjugation with hydrophilic groups such as acetate, glucuronate etc. Surprisingly, a rather complex oxidation-cyclization reactions were also found that probably prevent 3AP from metal complexation or neutralize the already formed metal-3AP complexes.[20] This finding along with earlier equally important research underlines the significance of metal-TSC complexes.

After 3AP, two more successful candidates entered clinical trials recently, namely 4-(pyridine-2-yl)-N-([(8E)-5,6,7,8-tetrahydroquinolin-8-ylidene]amino)piperazine-1carbothio-amide (COTI-2) in 2015 and Di-2-pyridylketone-4-cyclohexyl-4-methyl-3-thiosemicarbazone (DpC) in 2016.

Both agents are highly active; concretely in a target concentration range of tens to hundreds of nanomoles per liter (10^{-9} mol/L). For comparison 3AP's active concentration range is in tens of micromoles per liter (10^{-6} mol/L).[21,22]

Both nanomolar agents were deployed clinically against advanced or recurrent malignancies. COTI-2 was found effective against solid epithelial cancer while well tolerated.

Using advanced biomolecular assays, a suggested molecular mechanism involving Hsp90¹ kinase and ATPase inhibition was ruled out. Furthermore, COTI-2 did not inhibit over 200 additional kinases involved in common cancer survival pathways. However, recent research suggests that secondary mechanisms of COTI-2 may interfere with mutated p53 protein and AKT/AMPK/mTOR² pathways.[25] Furthermore, some interesting synergistic properties of COTI-2 with other anticancer agents - mainly metallodrugs can be exploited in further clinical trials.[26]

As for DpC, this agent together with the previously described COTI-2 represent next generation thiosemicarbazones that possess superior properties. DpC was found to be effective against multiple cancer cell lines that are otherwise extremely hard to treat. Further interesting synergies were found and the result of a very recent research from *Sundus N. Maqbool et al.* in their publication "*Overcoming tamoxifen resistance in oestrogen receptor-positive breast cancer using the novel thiosemicarbazone anti-cancer agent, DpC*" gives a close attention to endocrinologic status of patients, which was very often overlooked or was very hard to be accounted for in the past research.[27,28]

To summarize the topic, large amount of ongoing research is being done to elucidate the mechanisms by which cancer, or more specifically cancer types evade the body's own defense mechanisms and evade drug treatment. There are currently many good candidates for several cancer types that are being developed, thiosemicarbazones among them, but as can be seen it is very hard to pinpoint the molecular target and mechanism of action of those drugs. It is, hence, very hard to understand why exactly a certain candidate is better suitable for a specific application in cancer treatment. For example, as already mentioned, TSCs were thought to solely inhibit RR. The mechanism of TSCs doing so was suggested to take place by depriving

¹ Hsp90 is a member of a protein family called "heat-shock proteins" (HSPs). HSPs were found to be a special type of proteins called chaperons, which facilitate the folding of other proteins. In recent years, several small-molecule drugs that target the molecular chaperone Hsp90 were identified as potential anticancer agents. [23]

² AKT/AMPK/mTOR are all intracellular and extracellular signaling pathways that serve as central regulators of cell metabolism, growth, proliferation and survival. [24]

the enzyme of its core functional metal – the iron through a complexation process or via “redox cycling” causing oxidative damage to the enzyme. This scientific position lost its significance partly as the research methods got advanced and sophisticated over time, discovering other possible targets - serious advancements were done in recent years (protein- and pathways targets elucidation) for at least some of the TSC anticancer agents. However, even to this point, as of writing this master’s thesis the ultimate question on the exact molecular mode of action remains still unanswered and further research must be done.

1.2 Inductively coupled plasma – Mass spectrometry

Inductively coupled plasma – mass spectrometry (ICP-MS) is a technique commonly deployed in the branch of analytical chemistry, more specifically, in the field of elemental analysis.[29] The setup consists, as its name suggests, of two complicated parts, which deserve a profound introduction each.

Inductively coupled plasma (ICP) is a stable source of a directed beam of plasma. The plasma is generated by argon gas that is continuously supplied in high quantities through a torch with a special electrical solenoid around it. This solenoid is generally powered with a high voltage alternating current (with relevant frequencies of up to about 40 MHz) drawing up to 2000W of electrical power.[30, 31]

The formation of plasma takes place when the electric and magnetic fields generated by the solenoid are sustainably high enough to strip off electrons from argon atoms. Historically, ICP was rather quickly recognized as a method of potentially great analytical value, mainly for the extraordinary high temperatures reached in the burning plasma. The plasma can easily reach temperatures of up to 6 000K (or even 10 000K according to many sources)[30,31,32] and can thereby ionize around 85% of all known elements at least to a relevant extent.[33] All metals are generally well ionizable (40% - 100% charge transfer efficiency in formation of M^+ or M^{2+} at 7 500K), while mainly light non-metals (C, N, O, F, etc.) are not easily ionizable (0.1% – 5% charge transfer efficiency in formation of M^+ or M^{2+} at 7 500K) and thus not detectable as monoatomic ionic species in ICP ionization (see figure 4 on the next page).[34,35]

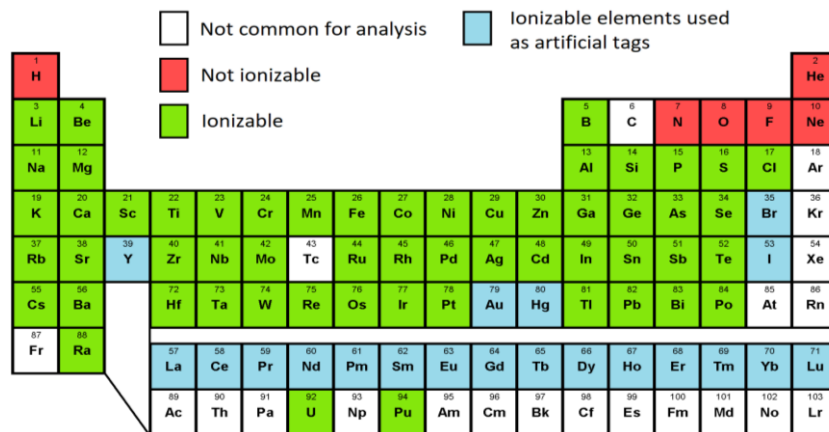


Figure 4: Periodic table of elements with denotation about ionizability by means of ICP. Table redrawn and altered from: Pröfrock, Daniel, and Andreas Prange. "Inductively coupled plasma-mass spectrometry (ICP-MS) for quantitative analysis in environmental and life sciences: a review of challenges, solutions, and trends." *Applied spectroscopy* 66.8 (2012): 843-868.

To utilize this method in an analytically meaningful way, a diluted spray of aqueous solution containing substances of interest can be introduced into the plasma torch (see figure 5 below) from a spray chamber.

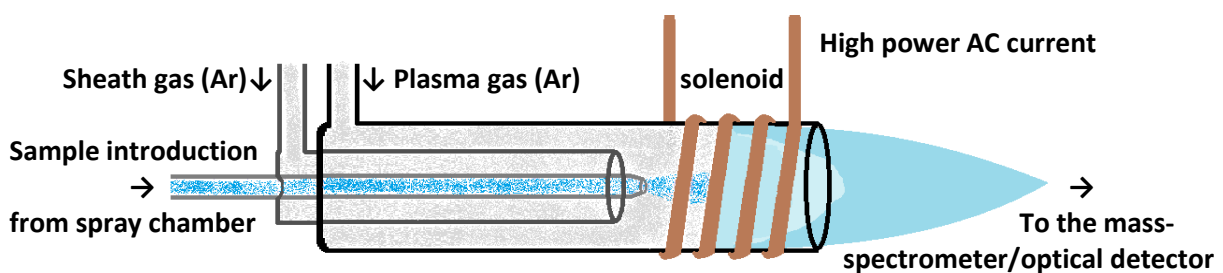


Figure 5: General construction of the ICP torch. Sample introduction tube being in the center, concentrically encased in a sheath gas tube and, lastly, the nebulizer tube. The tubes are generally made from zirconia.

A spray chamber is a piece of glassware, where a continuously supplied solution is sprayed from a thin capillary using a nebulizer gas (Ar) in a process called pneumatic nebulization (see figure 6 on the next page – Scott double pass spray chamber depicted here is currently one of two most common spray chamber construction types, the other one being cyclonic nebulizer, which has equal capability and performance).[36]

The sample can be transported to the spray chamber directly using a peristaltic pump or it can be fed in using a high-performance liquid chromatography pump (HPLC; usually also performing a separatory experiment at the same time – further description is in section 1.3 Size exclusion HPLC). An overflow from the spray chamber always needs to be pumped to waste – for this reason ICP setups usually have a peristaltic pump attached to it allowing for easy waste management.

After the nebulization, the fine watery spray reaches the torch via a short sample introduction tube.

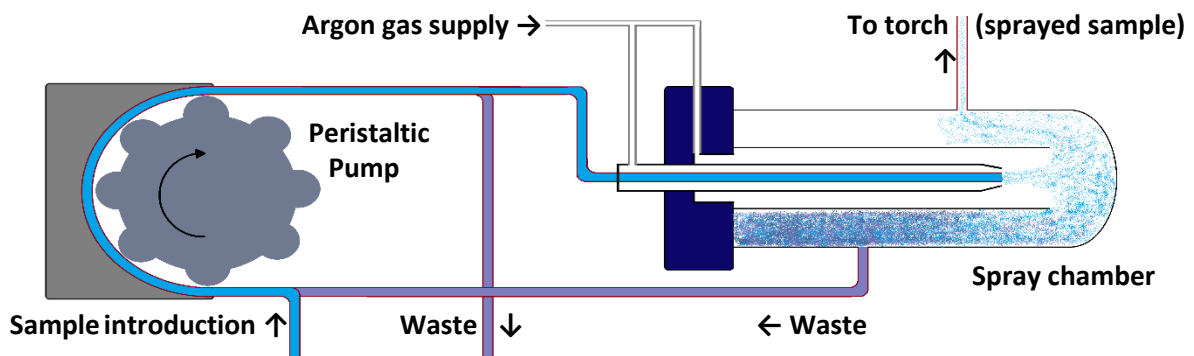


Figure 6: General construction of a spray chamber being fed via peristaltic pump. The construction type shown here is a very common “Scott double-pass spray chamber”. The waste of the spray chamber is also pumped away via peristaltic pump.

As a result of very harsh electronic conditions and high temperatures in the plasma gas the more complex molecules fragment into atoms and then the atoms become energetically excited and/or ionized. When the excited atoms reverse to their electronic ground state, an electromagnetic atomic emission occurs which can then be registered and analyzed (in the simplest case) optically – in a detecting setup called optical emission spectroscopy (OES).[37] The versatility of ICP is very broad and out of the scope of this brief general introduction.

As far as it is of concern for this Master’s thesis, however, an introduction to inductively coupled plasma - mass spectrometry will be given in the next lines.

As previously described, the electronically harsh conditions in the burning plasma cause most atoms to become ionized. Given this condition, ICP can be deployed in mass spectrometry as means of ionization (ion source). The major drawback, or major advantage lies in the fact that analyte molecules typically fragment into atoms. Therefore, only elements or more specifically, element isotopes can be analyzed – restricting the meaningful spectrometric mass range from $7m/z$ (Li) to around $245m/z$ (Pu).

There are currently many types of mass spectrometers that employ ICP as means of ionization. The most prominent and interesting ones presently are the ICP-(triple)Quadrupole-MS (ICP-QqQ-MS), High resolution sector field MS (HRSF-MS) and ICP-(q)TOF-MS.[10] There are, however, trade-offs when considering each of the mentioned mass spectrometric techniques – for example ICP-QqQ MS suits best for exact quantitative analyses for its unapproached sensitivity. It struggles, on the other hand, at capturing the atomic signature of a given analyte,

where in turn, ICP-(q)TOF excels in its fast and simultaneous elemental screening capabilities with high enough resolution to overcome most interferences (more detail on possible interferences in MS is given on page 14).[38,39] For this reason, ICP-(q)TOF is currently of high interest in the now emerging field of single particle analytics and laser ablation analysis, where elemental screenings need to be completed in a time-span of milliseconds.[40,41] The choice of the mass spectrometric technique must always be made according to the encountered analytical task as there is no all-in-one solution. As ICP-QqQ MS is the main analytical tool used in the course of this master's thesis, the next description will be primarily concerning general quadrupole function in the field of mass spectrometry.

The quadrupole is an old and relatively simple design of a mass analyzer. It utilizes 4 metal rods³ arranged in the corners of an imaginary square or equilateral diamond as shown in figure 8.[42] When subjected to an alternating voltage – in the way such as depicted in figures 7 and 8, some interesting properties of the quadrupole emerge.

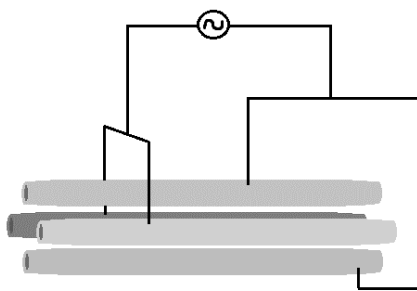


Figure 7: schematic construction of a quadrupole. Two opposing rods sharing the same potential resulting in quadrupole electric field as shown in figure 3

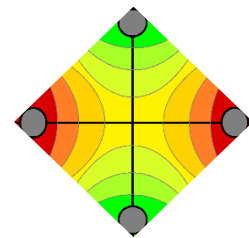
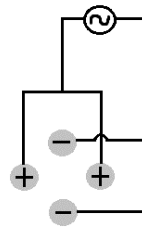


Figure 8: Electrical fields of a quadrupole

The electric potential on a certain coordinate inside the quadrupole can be expressed by linear combination of the potentials produced by the rods. The equation (1.1) expresses the relationship between the electrical potential ϕ and its coordinates; where Π_0 is a position-independent factor or function of time (which may depend on an alternating voltage) and λ , σ , γ are weighing (bias) constants.[42,43]

$$\phi(x, y, z) = -\frac{1}{2}\Pi_0(\lambda x^2 + \sigma y^2 + \gamma z^2) \quad (1.1)$$

The electrical potentials and fields have restraints dictated by physics that result in a simplification shown in equation (1.2) below.

$$\lambda + \sigma + \gamma = 0 \quad (1.2)$$

³ The rods of a quadrupole mass analyzer, nowadays, are constructed such as their cross sections resemble hyperbolas rather than exact circles. This construction ensures better performance.

The electric field on a single coordinate is exactly the same along the long z-axis of the quadrupole, so only a 2-dimensional slice (perpendicular plane in respect to the z-axis) of the quadrupole needs to be considered. The simplest solution for λ , σ and γ which results from the aforementioned simplification is displayed in equation (1.3).

$$\lambda - \sigma = 0; \quad \gamma = 0 \quad (1.3)$$

Combination of equations (1.1), (1.2) and (1.3) results in an expression of potential shown in equation (1.4)

$$\phi(x, y) = -\frac{1}{2} \Pi_0 \lambda (x^2 - y^2) \quad (1.4)$$

Next, the potential of a theoretical monopole is considered having an AC voltage (denoted U) superimposed on a constant DC voltage (denoted V). ω denotes the angular frequency of the applied AC voltage.

$$\Pi_0 = 2[U + V * \cos(\omega t)] \quad (1.5)$$

Plugging equation (1.5) into (1.4) a general equation for electric potential in the quadrupole is obtained (1.6).

$$\phi_0(x, y) = \lambda(x^2 - y^2) * [U + V * \cos(\omega t)] \quad (1.6)$$

To arrive at a meaningful expression for potentials in a quadrupole, two special but relevant cases are presented in equations (1.7) and (1.8) where the coordinates x and y are kept constant at 0 respectively. r represents the distance from the center of the quadrupole.

$$\phi(x, 0) = \frac{\phi_0 x^2}{2r^2} \quad \text{and} \quad \phi(0, y) = \frac{\phi_0 y^2}{2r^2} \quad (1.7 \text{ and } 1.8)$$

The electric field along x or y axis is the derivative of the respective potential function

$$E_x = \frac{d\phi}{dx} = \frac{\phi_0 x}{r^2} \quad \text{and} \quad E_y = \frac{d\phi}{dy} = \frac{\phi_0 y}{r^2} \quad (1.9 \text{ and } 1.10)$$

Finally, from equations of field along x and y axis (1.9 and 1.10), the corresponding forces on a singular point charge e in that field can be calculated:

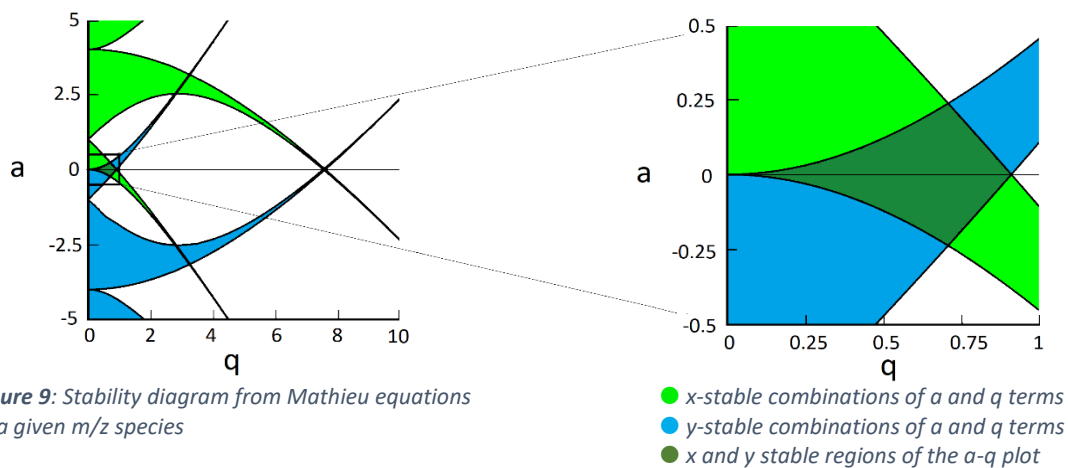
$$F_x = -eE_x = \frac{-e\phi_0 x}{r^2} = ma \quad \text{and} \quad F_y = -eE_y = \frac{-e\phi_0 y}{r^2} = ma \quad (1.11 \text{ and } 1.12)$$

The equations of acting force on a singular charged particle with a charge e and mass m (1.11 and 1.12) is the last step before arriving at the Mathieu equations which separate the main equation into a term "a" with a sole variable being a DC voltage "U" (equation 1.13) and a term "q" with a sole variable being an AC voltage "V" (equation 1.14)

$$a = \frac{8zeU}{m\omega^2 r_0^2} \quad (1.13)$$

$$q = \frac{4zeV}{m\omega^2 r_0^2} \quad (1.14)$$

These expressions are of interest, because the combination of them dictates, whether a singular charged particle in a quadrupole field experiences a net zero force or a net force over time along a given axis – a so called Mathieu stability diagram can be constructed for every charged particle with a given mass over charge ratio m/z (see figure 9) [43]



Graph redrawn from Heinrich, Johannes. "A Be⁺ ion trap for H₂⁺ spectroscopy." Diss. Sorbonne université, (2018), p.15

Now being equipped with the mathematical background the important properties of a quadrupole become apparent. As mentioned, there are combinations of "a" and "q" terms which result in a zero net force acting on a singular charged particle of mass m and charge ze along either of the axis. There are, luckily, also stable regions where both x and y become stable simultaneously.[42,43] This means that a given charged particle can remain stable in such a field.

This property of the quadrupole allows for analytical utilization as ion analyzer, as there are infinitely many stability conditions for each m/z value. In practice the ion analyzer function is used such as only one m/z species has a stable path along the quadrupole at a time.

This is achieved by setting the "a"(DC) and "q"(AC) parameters accordingly (see figure 10 – linear increase of both "a" and "q" voltages results in a quadrupole function that allows successively heavier ions to pass through when being continuously injected as ion cloud). Alternatively, setting the DC voltage term "a" to zero, all charged species will have stable paths along the quadrupole. Hence, the quadrupole becomes an ion pass-through device.[42,43]

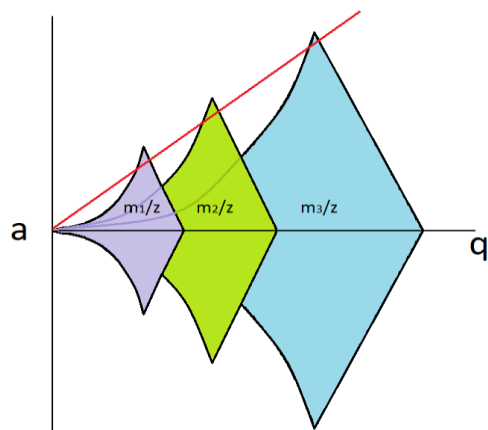


Figure 10: Stability diagrams of three theoretical charged species with ascending order of their m/z values. The red line (---) denotes a possible scanning function of a quadrupole that needs to be employed in order to separate the three theoretical charged species.

In a simplest setup a quadrupole used in a “single quad” mode (see figure 11 below) is usually located behind the sample introduction cones in a high vacuum to prevent atomic collisions and may possess both of the aforementioned functions - it can be operated either in a scanning mode (i.e. it sets its U and V voltages to pass through ions of each discrete m/z value sequentially with a integration time window for each.), or in a fixed m/z mode. The former is usually used to assess the mass spectrometric fingerprint of an analyte, the latter is used to perform quantitation experiments on a known analyte.

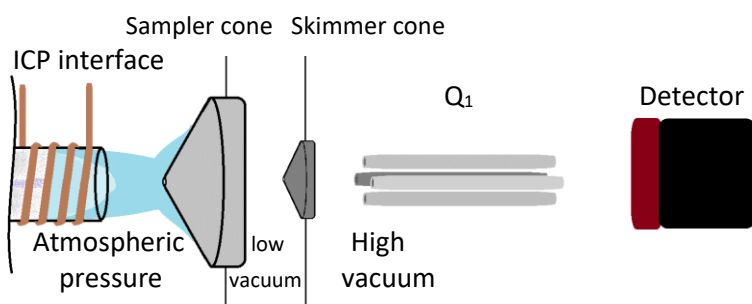


Figure 11: Schematic graph of a single quadrupole mass analyzer setup and ICP as means of ionization.

Single quadrupole setups are powerful analytical tools, however, when used with an ICP interface as means of ionization, they are prone to interferences (more detail on possible interferences is described later on page 14).

Another powerful setup is the so-called triple quadrupole mass analyzer – See figure 12 below. The first quadrupole, which is located after sample introduction cones in high vacuum is usually named “Q₁”. It can be operated in scanning mode or fixed m/z mode.

The second quadrupole “q” is located in close proximity behind Q₁ and is usually operated in an ion pass-through mode (also called “RF-only”, because all charged species are passed through when quadrupole is subjected to AC voltage only, hence radiofrequency-only).[42]

Additionally, q can be located inside a collisional gas chamber where either a collisional or reactant gas can be deployed. The last quadrupole “Q₂” is located behind q and can be operated in scanning mode or fixed m/z mode.

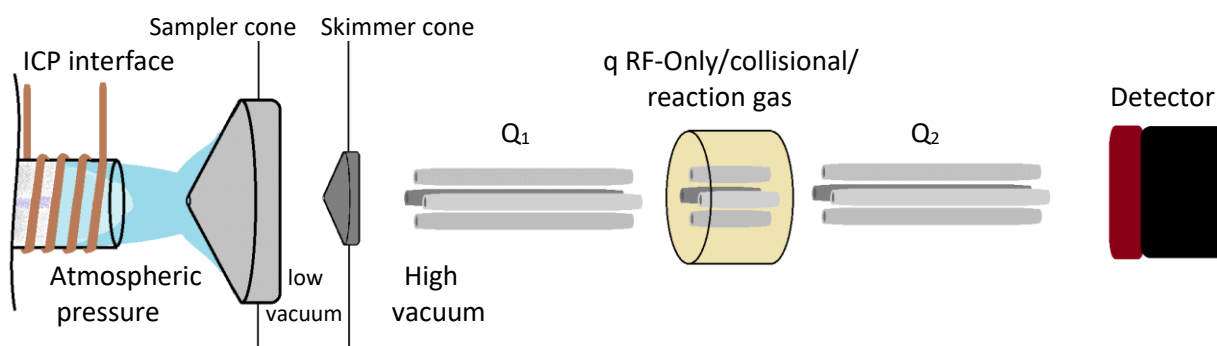


Figure 12: Schematic graph of a triple quadrupole mass analyzer and ICP as means of ionization

The triple quadrupole setup as a whole can be operated in following modes:

- 1) Product Ion scan: Q₁: set at $m/z = m_{\text{analyte}}$ q: RF-only/collisional fragmentation Q₂: scanning mode. In this mode a fragmentation pattern of an analyte is obtained. This mode is not of interest, when ICP is deployed as means of ionization. However, in the field of organic mass spectrometry, where softer ionization methods are being deployed that do not cause complete atomization of analytes, product ion scan is a viable option for elucidating the molecular structure of an analyte.[44,45]
- 2) Precursor Ion scan: Q₁: scanning mode q: RF-only/collisional fragmentation Q₂: set at $m/z = m_{\text{analyte}}/\text{fragmented}$. In this mode, one usually seeks for precursor ions which lose a certain functional group (for example certain fatty acid loss, benzyl loss, phenyl loss etc.)[45,46]

- 3) Neutral loss scan: Q₁: scanning mode q: RF-only/collisional fragmentation
Q₂: scanning mode with an m/z offset of a neutral molecule. In neutral loss scan, both analyzing quadrupoles are scanning together with a constant offset in mass. In this way a loss of a neutral fragment (mass offset) can be found. Neutral losses are usually small fragments such as H₂O, CO₂, Acetate, but also larger fragments like side chains of an organic molecule.[45,46]
- 4) Selected reaction/fragmentation monitoring: Q₁: set at m/z=m_{analyte}
q: RF-only/collisional fragmentation Q₂: set at m/z=m_{analyte+reactant}. This mode is employed when the fragmentation or reaction of a certain analyte is known.[45]
An example of a reaction gas in the ICP mass spectrometry is oxygen. When reacting with an analyte ion, oxygen causes a mass shift of +16m/z. This technique is also used in the field of ICP-QqQ MS as means of mitigating interferences (which will be discussed in the next lines).[45,46]

As far as actual measurements with ICP as means of ionization are concerned, one major challenge has to be further mentioned now. For one, ICP inherently produces among monoatomic charged species also di- and triatomic charged species which emerge from fast radical-like gas reactions. It is for such interfering species that measurements of some analytes are difficult or even impossible without additional measures.[47]

The critical interference of polyatomic species stems from their similar-to-analytes masses i.e. they are isobaric to some analytes.

An extensive overview on all possible isobaric interferences is for example given by *Thomas W. May* and *Ray H. Wiedmeyer* in their publication "A Table of Polyatomic Interferences in ICP-MS" from 1998. Mass similarities of under 1m/z can generally be distinguished with a high enough resolution setup. This is, however, not the case with quadrupoles, which only allow for unit resolution (i.e. quadrupoles resolve nominal m/z values).

Some polyatomic interferences sharing the same nominal mass as atomic analytes relevant to this master's thesis are tabulated in table 1 on the next page.[48]

Table 1: Interferences of some relevant analyte ions.
excerpt from Thomas W. May and Ray H. Wiedmeyer, A Table of Polyatomic Interferences in ICP-MS (1998)

Isotope	Abundance	Interference
³² S	95.02 %	¹⁶ O ₂ ⁺ , ¹⁴ N ¹⁸ O ⁺ , ¹⁵ N ¹⁷ O ⁺ , ¹⁴ N ¹⁷ OH ⁺ , ¹⁵ N ¹⁶ OH ⁺ , ¹⁴ N ¹⁶ OH ₂ ⁺
³⁴ S	4.21 %	¹⁵ N ¹⁸ OH ⁺ , ¹⁶ O ¹⁸ O ⁺ , ¹⁷ O ₂ ⁺ , ¹⁶ O ¹⁷ OH ⁺ , ³³ SH ⁺
⁵⁶ Fe	91.33 %	⁴⁰ Ar ¹⁶ O ⁺ , ⁴⁰ Ca ¹⁶ O ⁺ , ⁴⁰ Ar ¹⁵ NH ⁺ , ³⁸ Ar ¹⁸ O ⁺ , ³⁸ Ar ¹⁷ OH ⁺ , ³⁷ Cl ¹⁸ OH ⁺
⁵⁷ Fe	2.19 %	⁴⁰ Ar ¹⁶ OH ⁺ , ⁴⁰ Ca ¹⁶ OH ⁺ , ⁴⁰ Ar ¹⁷ O ⁺ , ³⁸ Ar ¹⁸ OH ⁺ , ³⁸ Ar ¹⁹ F ⁺ ,
⁶³ Cu	69.1 %	³¹ P ¹⁶ O ₂ ⁺ , ⁴⁰ Ar ²³ Na ⁺ , ⁴⁷ Ti ¹⁶ O ⁺ , ²³ Na ⁴⁰ Ca ⁺ , ⁴⁶ Ca ¹⁶ OH ⁺ , ³⁶ Ar ¹² C ¹⁴ NH ⁺ , ¹⁴ N ¹² C ³⁷ Cl ⁺ , ¹⁶ O ¹² C ³⁵ Cl ⁺
⁶⁵ Cu	30.9 %	⁴⁹ Ti ¹⁶ O ⁺ , ³² S ¹⁶ O ₂ H ⁺ , ⁴⁰ Ar ²⁵ Mg ⁺ , ³⁶ Ar ¹⁴ N ₂ H ⁺ , ³² S ³³ S ⁺ , ³² S ¹⁶ O ¹⁷ O ⁺ , ³³ S ¹⁶ O ₂ ⁺ , ¹² C ¹⁶ O ³⁷ Cl ⁺ , ¹² C ¹⁸ O ³⁵ Cl ⁺ , ³¹ P ¹⁶ O ¹⁸ O ⁺

To reduce the interferent species during measurements, several dispersive methods⁴ were developed that can be categorized into roughly two classes:

- 1) Dispersion in Time methods make use for example of an inert (collisional) gas that is supplied under a given pressure to a field-free pass-through chamber of the spectrometer. There the incoming analytes and polyatomic interferences interact with the collisional gas. Polyatomic interferences have usually larger collisional cross-sections than monoatomic analytes. Thus, there is a tendency that larger polyatomic interferences will be slowed down much more than analytes and reach the detector later, hence, they become dispersed in time. There are also other dispersive methods that use complicated electronic equipment to exclude ions based on their momenta.[49] These techniques, however, are out of the scope of this master's thesis.
- 2) Dispersion in Space methods usually deploy advanced procedures where analytes and interferences are subjected to complex electric fields in the collisional cell while an inert gas may or may not be present. If done optimally, large polyatomic interferences react differently to applied electric fields than analytes and become dispersed in space reaching the detector in a reduced number or not reaching the detector at all.[50]

The interference mitigating method used while working on this master's thesis was a simple collisional reaction cell used in a triple quadrupole apparatus, in which a supplied collisional reactant gas reacted with the interfering species or the analytes causing a mass shift.

⁴ Dispersive methods are usually used in analyses involving larger, unfragmented molecules like in -omics disciplines. However, some time-dispersive methods are well applicable in the field of ICP-MS.

This mass shift could be selected or omitted in the triple quadrupole mass spectrometry. Hence this method does not rely on any dispersion, but rather on a deliberate gas phase reaction.[51]

In particular, in this master's thesis relevant ions were ^{32}S , ^{56}Fe , ^{57}Fe , ^{63}Cu and ^{65}Cu . All of the aforementioned ions were measured during main incubation experiments using the oxygen reaction gas. Therefore, Q_1 was set to scan the nominal masses of the ions of interest (32, 56, 57, 63 and 65).

In q_2 , an oxygen reaction took place - ^{32}S reacted to $^{32}\text{S}^{16}\text{O}$; ^{56}Fe and ^{57}Fe reacted to $^{56}\text{Fe}^{16}\text{O}$ and $^{57}\text{Fe}^{16}\text{O}$ respectively while ^{63}Cu and ^{65}Cu do not react with oxygen. Hence, the Q_2 was set to scan nominal masses of $32+16m/z$ for sulfur, $56+16m/z$ and $57+16m/z$ for iron, $63m/z$ and $65m/z$ for copper respectively.

Lastly, brief introductory topic regarding ICP-MS to cover here is the construction of the ion detector. The most often used detector type in quadrupole mass analyzer devices is the so-called "Faraday cup". Faraday cup is a simple equipment consisting of a conductive metal surface shaped in a concave cup form that is part of an electric circuit. Incoming ions that hit the surface of the Faraday cup transfer their charge, thus become neutralized. This charge transfer can be detected as electric current in the circuitry of the faraday cup.[52] Additionally, a special type of electrodes is used to amplify the signal of incoming ions. These electrodes ("Dynodes") emit electrons when hit by charged particles. When several dynodes are constructed in series a multiplication of the number of electrons that can be emitted will be achieved. Such amplified charged particles can ultimately be counted by a Faraday cup, effectively increasing the sensitivity of the detector system.[53]

Other more advanced detector type (mainly used in TOF instruments) are the so-called channeltron and multichannel plate.

The function of these types of detectors is essentially the same in principle as faraday cup with amplifying dynodes, but in a more compact form factor.[54]

In order to use ICP-MS, an extraordinarily powerful analytical method in an even more versatile way there is an over a decade long research and development on coupling separatory techniques like liquid chromatography, Gas chromatography or even (capillary) electrophoresis to MS systems. This setup is usually used to perform analyses of complex mixtures, quantify them, and determine the molecular (or atomic) identity of mixture constituents, if proper techniques and standards are used.

The latter application can be found in the literature in the context of ICP mass spectrometry under the term “speciation analysis”. To describe speciation analysis in detail IUPAC’s glossary of terms specifies “a chemical species” as a defined specific form of an element defined as isotopic composition, electronic or oxidation state, and/or complex or molecular structure - hence, an exactly defined molecular or atomic entity. Chromatographic techniques coupled to ICP-MS is a particularly well-equipped device for speciation analysis as chromatography (liquid or gas) provides molecular/atomic information while ICP-MS functions as exceptional isotopic detector that additionally allows for exact quantitations.[55]

As for new advancements in the field of ICP-MS a potentially very powerful method needs to be mentioned briefly in this introduction: The Laser ablation – inductively coupled plasma mass spectrometry, LA-ICP-MS for short. This method uses a finely focused laser beam to ablate a preselected spot or area of a given sample.[56]

This samples may be organic such as a tissue or even single cells, or inorganic in nature such as lithological rock samples.

The former being of great interest for applications in the field of (single-)cell mass spectrometry and the latter being of great interest for structural and lithological research in the fields of geosciences and enviro-sciences.[57] In chemical applications single cell mass spectrometric methods gained popularity in the last years, and, currently an accelerated research output can be observed. An extensive review was given by *Sarah Theiner et al.* in the publication “*Single-cell analysis by use of ICP-MS*” from 2020 describing state of the art methods and hardware and addressing some hurdles but also approaches to solutions of the immense analytical and statistical challenges of measuring transient single cell signals by means of ICP-MS.

It is therefore, expected that there will be a gigantic progress and a development of new interdisciplinary fields that allow for broader method application range in the coming next years to decades.

1.3 Size exclusion High-performance liquid chromatography

High-performance liquid chromatography (HPLC) or liquid chromatography (LC) describes one sub-type of chromatography techniques; i.e. a separatory technique that is generally used in the field of analytical chemistry.[58] The prefix “high-performance” stems from the fact that liquid chromatography experienced a major development over the time and went from a technique reliant on gravity driven flux of a solvent (see figure 13 below) to pump-facilitated flux of solvent that is used today (see figure 14 below). Hence, a HPLC setup generally consists of a solvent reservoir, a pump or pumps, a sample introduction device and an analytical column packed with the so-called “stationary phase”.[59] During a separatory experiment a sample mixture is introduced into the analytical column in small quantity and passed through it using pressurized solvent. Optimally, every component in the sample mixture interacts differently with the stationary phase.

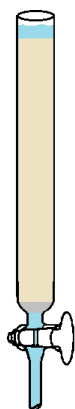


Figure 13: Schematic figure of a gravity-driven liquid chromatography column packed with stationary phase



Figure 14: Schematic figure of a pump-driven HPLC system

The separation of each component takes place as each component will pass through the stationary phase with a different rate, or in other words, after a different elution time.[59,60] In practice the choice of an optimal stationary phase and an optimal solvent or combination of solvents always needs to be considered carefully. For example, in order to separate a mixture of polar substances such as alcohols, small organic substances with a high degree of hydrophilic substitution, amino acids etc. a normal (polar) stationary phase with a nonpolar solvent would be employed. In order to separate a mixture of nonpolar substances such as fatty acids, a reverse (nonpolar) stationary phase with a rather polar solvent would be employed.

Presently, there is a myriad of types of stationary phases, each exploiting different properties of analytes.[60]

Normal (polar) stationary phase is essentially finely pulverized silica material. Having its silyl -OH groups free (see figure 15 below), the stationary phase mainly interacts with highly polar substances. In order to maximize the interactions between analytes and stationary phase a non-polar solvent like hexane is used. To facilitate the elution of analytes/wash out the column a more polar solvent is used (e.g. Dichloromethane, isopropanol, methanol...).[61] It must be pointed out that normal stationary phase only has historic relevance and is outdated today as more capable stationary phases become widely available. Nevertheless, normal phase stationary phase in liquid chromatography was once one of the most important tools in analytical research. And even recently novel powerful techniques implementing normal stationary phase are being developed.[62]

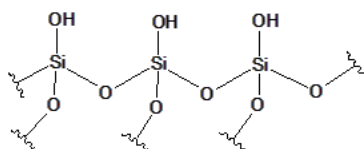


Figure 15: Chemical structure of silica (normal stationary phase)

Reversed stationary phase mainly consists of fine silica material which was chemically modified. Free -OH groups are usually converted to silyl ether carrying alkane chains such as C18 or C8 (number referring to the length of alkane chain – See figure 16 below).[63]

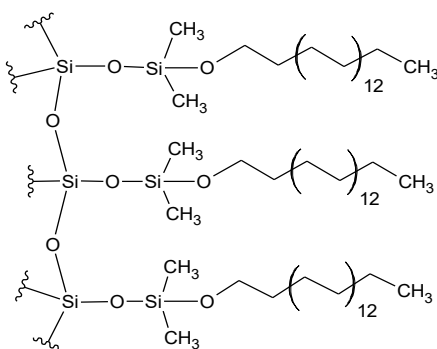


Figure 16: chemical structure of silica modified with alkyl-silyl chains, that allow hydrophobic interactions on the surface of the stationary phase (reversed stationary phase)

Historically, major breakthroughs were achieved by using normal phase stationary phases and later reversed phase stationary phases, the latter of which is to these days the most common stationary phase in the field of liquid chromatography.

There are some more stationary phase types like HILIC, Ion exchange stationary phases for cations or anions etc., but it is out of the scope of this brief introduction to describe all of them in great detail.

The next paragraphs will, therefore, focus on Size exclusion liquid chromatography, which was exclusively deployed throughout the course of this master's thesis and hence, deserves a more profound introduction for better understanding.

Size exclusion chromatography uses a fine inert stationary phase with pores of fixed size (or more precisely, pore size with a narrow size variance) such as only analytes with certain molecular dimensions can access those pores.[64] The general elution trend in size exclusion chromatography is: small molecules that are able to access and diffuse into the pores of the stationary phase elute later than large molecules that cannot access the pores. As mentioned earlier the stationary phase is generally inert so the separation takes place solely due to small molecules having access to more volume inside the column while large molecules don't have any means for volume-based retention.[65]

The most common type of analytes for size exclusion chromatography are rather large (bio)molecules like proteins, in some cases DNA or RNA macromolecules, but also synthetic polymers and others.[66] These analytes can, however, vary in their size drastically. For example proteins be as small as few tens to <100 aminoacids such as some Metallothioneins⁵, or as large as 10'000 to even 27'000 aminoacids such as an extreme case: Titin⁶. [69] For such large variance in analyte sizes there simply is no stationary phase that can successfully provide variable pore volume for each size and hence provide satisfactory separatory performance in the whole possible range. Therefore, there are myriads of size exclusion stationary phases on the market available that provide an exceptional separatory performance for protein size cohorts. For proteins, as a rule of thumb the molecular weight can be assumed as the main separatory parameter. The real criterion for separatory performance of any protein cohort, however, is the so-called hydrodynamic radius.[70] This parameter is not generally used in the scientific field very widely mainly due to its uncertainty and due to its dependency on the

⁵ Metallothionein is a family of mostly low molecular protein species that can be found in a wide range of species in animal kingdom. Metallothioneins function mainly as chelators of toxic metals (such as mercury, cadmium, arsenic etc.), but also as chelators of essential metals when present in excess quantities, essentially rendering bioactive metals inactive.[67]

⁶ Titin is a large human protein that provides muscle with enhanced elasticity [68]

solvent system. Hence, manufacturers will almost exclusively specify the suitable molecular weight range of analytes in units of Dalton (Da) or kilodalton (kDa).

As for the analytical column material, there are currently two main structural designs. For one, plastic columns made from special inert material such as Polyetheretherketones (PEEK, see figure 18 below) can be purchased for niche applications where inert column material is needed to prevent unwanted reactions (such as adherence of some proteins or other substances to the walls of a column, that would result in strange elution behavior). One major disadvantage of PEEK columns is their brittleness. PEEK columns cannot be subjected to high pressures, because they would burst under high pressure. Therefore, their column packing is not very tight - suffering a loss in separatory performance. PEEK columns combined with inert HPLC systems are an optimal solution to high metal backgrounds in high sensitivity applications like ICP-MS. Ultimately, the choice must be made according to an analytical problem encountered. The next few lines are dedicated to the second major type of an analytical column, which is commonly more powerful in terms of separatory performance – The steel type (see figure 17 below).

This column material is extremely robust and resilient. The stationary phase is packed very densely, which allows for high separatory performance and high operational pressures (high flow rates). Common steel columns can easily support pressures of up to 700bar and modern special columns even more depending from its exact form factor. The column (wall) material, however, is not completely inert and aside from possible interactions with analytes the analyses exhibit higher backgrounds of some elements (mainly iron and possibly copper and other metals).[71]



Figure 17: Common steel analytical column Source: https://www.waters.com/webassets/cms/category/media/snapshot/sec_hplc_group_yellow_fobs.jpg

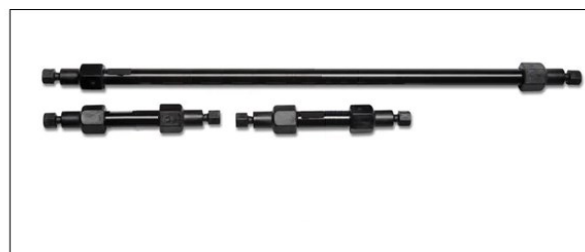


Figure 18: An analytical column made from PEEK Source: <https://assets.thermofisher.com/TFS-Assets/CMD/product-images/MabPac%20SCX%20Columns%20Horizontal%20white.jpg-650.jpg>

Currently, there are new manufacturing processes in development that allow for combination of the advantages of the two aforementioned materials – PEEK coated steel columns might exhibit both the inertness of the PEEK material and superb performance and pressure resistance of the steel material that is much needed in advanced research areas like high sensitivity analytical chemistry, proteomics and others.[72] These columns are not widely available as of writing this master’s thesis. However, they are clearly making an entry into the analytical-chemical market in big leaps. In the context of this master’s thesis this kind of analytical columns might be of high interest as for the complicated chromatographic analyses of thiosemicarbazones – Further discussion in section 4. Conclusions starting on page 91.

2. Experimental Section

2.1 Reagents other chemical material

2.1.1 Basic chemicals, solvents and standards

For all sample preparations and measurements, when available, ultra-pure grade reagents were used. All necessary water dilutions were performed using ultra-pure Water (18.2 MΩ.cm) from an in-house water purifying device Milli-Q Advantage (Darmstadt, Germany). A detailed overview of all used chemicals is given in table 2 below.

Table 2: All basic chemicals and solvents that were used in the course of this research thesis

Reagent	Formula	CAS	Purity	Company	Storage conditions (Comments)
Nitric acid 69%	HNO ₃	7697-37-2	Suprapur	Sigma Aldrich (USA)	Sufficiently ventilated storage
Acetic acid 100%	CH ₃ COOH	64-19-7	Suprapur	Sigma Aldrich (USA)	Sufficiently ventilated storage
Formic acid 100% (FA)	HCOOH	64-18-6	Suprapur	Sigma Aldrich (USA)	Sufficiently ventilated storage
Methanol	CH ₃ OH	67-56-1	>99.9% for HPLC	Sigma Aldrich (USA)	Sufficiently ventilated storage
Isopropanol 70% (IPA)	C ₃ H ₇ OH	67-63-0			Sufficiently ventilated storage
Ammonia 25%	NH ₃	1336-21-6	Suprapur	Sigma Aldrich (USA)	Sufficiently ventilated storage
Citric Acid (Monohydrate)	C ₆ H ₈ O ₇ * H ₂ O	5949-29-1		Sigma Aldrich (USA)	
Monosodium Phosphate	NaH ₂ PO ₄ * 2 H ₂ O	13472-35-0		Sigma Aldrich (USA)	(Hygroscopic, difficult to weigh)
Disodium Phosphate (Dihydrate)	Na ₂ HPO ₄ * 2 H ₂ O	10028-24-7		Sigma Aldrich (USA)	(Hygroscopic, difficult to weigh)
Dimethyl Formamide (DMF)	C ₃ H ₇ NO	68-12-2	97%	Sigma Aldrich (USA)	Sufficiently ventilated storage. (Hygroscopic)
Argon (pressurized)	Ar	7440-37-1	99.999%	Messer (Germany)	
Hydrogen peroxide 30%	H ₂ O ₂	7722-84-1	Suprapur	Sigma Aldrich (USA)	Sufficiently ventilated storage at +4°C
Human blood serum				Sigma Aldrich (USA)	Frozen -20°C (long term storage) or refrigerated +4°C (short term storage)

A certified reference material (CRM) of blood serum - Seronorm™ was purchased from LabMark Inc.(USA). Another CRM TM-28.4 – Lake Ontario water was obtained from Environment and Climate Change (Burlington, Canada).

Pure protein standards were kindly provided by research group Dr.Christian Kowol (presolubilized, watery solutions in various specified concentrations – see numbered list below).

- | | |
|--------------------------------|-------------------------|
| 1) Albumin 100μM | 2) Fibrinogen 100μM |
| 3) Transferrin 100μM | 4) α1-Antitrypsin 100μM |
| 5) α1- Acid glycoprotein 100μM | 6) IgG 100μM |
| 7) Haptoglobin 40μM | 8) Ceruloplasmin 30μM |
| 9) IgA 10μM | 10) IgM 1,1μM |

Method calibrations were performed using multielement standard solutions and single element standard solutions for Fe and Cu, all of which were purchased from LabKings (Hilversum, Netherlands).

In the special case of one side experiment described in section 2.5.3 Experimental setup and preparation of alternative quantitation standard – bovine CuZn Superoxide Dismutase on page 35 a standard bovine CuZn Superoxide Dismutase (lyophilized protein) purchased from Sigma Aldrich (USA) was used.

2.1.2 Preparation of solutions

50mM Ammonium Acetate pH 6.8: This solution was prepared from its suprapure precursors, namely Ammonia (25 w%) and Acetic Acid (100 w.%). First a 500mM Stock solution was prepared by adding 37,6mL of Ammonia and 28,5mL of Acetic Acid to around 800mL of ultra-pure Water (18.2 MΩ.cm). After mixing, more ultra-pure Water was added to a final volume of 1L. The pH of this solution was controlled with a pH meter and adjusted with respective solution (either Ammonia or Acetic Acid) to pH 6.8. This solution was diluted 1:10 with ultra-pure Water to produce 50mM Ammonium Acetate solution.

10mM Citric Acid: The Citric acid solution was produced by weighing 0.1052g of Citric acid monohydrate into a 50mL Falcon Tube and diluting it to 50mL with ultra-pure Water.

Buffered Human blood serum pH 7.4: The buffered serum for incubation studies was produced by pipetting 5mL of human blood serum (Sigma Aldrich, USA) into a 10mL FalconTube® and adding a mixture of 19mg NaH₂PO₄ dihydrate and 111mg Na₂HPO₄ dihydrate. The exact pH of 7,4 was adjusted by adding a respective amount of either NaH₂PO₄ or Na₂HPO₄ to the serum and checking with a pH meter.

Bovine CuZn Superoxide dismutase calibration standard: For alternative copper quantification standard solution, 1,95g of a bovine CuZn-Superoxide dismutase (bCuZn-SoD) was dissolved in 1mL of ultra-pure water. This resulted in a copper content in the solution of about 8mg/L. This solution was then diluted with 50mM pH 6.8 Ammonium Acetate 8-fold (0.125 mL bCuZn-SoD solution + 0.875 mL 50mM Ammonium acetate) to obtain 1mg/L (1ppm) of a theoretical copper standard. Further dilutions were performed using 50mM Ammonium-acetate solution pH 6.8.

Calibration Standards: For main calibrations, own 10ppm standard stock solution was produced, consisting of multielement standard solution (1:10 diluted from 100ppm) and an additional sulfur standard solution (diluted 100-fold from 1000ppm). From the 10ppm stock standard solution a calibration series was produced for calibration range of 1000ppb to 0.01ppb. All dilutions were performed using 0.3% HNO₃ solution.

2.1.3 Samples

Samples of cell culture media (components): The cell culture medium or its precursors were kindly provided by the Institute of cancer research - medical university of Vienna (Institut für Krebsforschung der Medizinischen Universität Wien – IKF-MUW). The Components of cell culture medium provided were:

- Minimal essential medium Eagle (MEME)
- Fetal bovine serum (FBS)
- Sodium bicarbonate (NaHCO₃)

Mouse serum: The mouse serum for investigation on the behavior of Triapine in an *in-vivo* system was kindly provided by the Institute of Cancer Research (IKF - MUW)

Mouse urine: The mouse urine for investigation on the behavior of Triapine in an *in-vivo* system was kindly provided by the Institute of Cancer Research (IKF - MUW).

2.1.4 Other chemical materials

Copper-selective Ion exchange resin: In order to reduce copper background in several samples a copper-selective Ion exchange resin CHELEX® (Sigma Aldrich, USA) provided by Dr.Christian Kowol was investigated (further details and results in section 3.10 CHELEX® ion exchange for background reduction in cell culture on page 91).

2.2 Consumables

In order to keep contaminations low, clean plastic disposable FalconTube® (Fisher Scientific, USA) were used in the chain of all sample preparations. Also, clean Eppendorf® tubes were used for preparation or storage of small volumes of samples or solutions. The final solutions intended for measurements were filled into disposable 1,5mL plastic vials (Macherey-Nagel GmbH, Duren, Germany) and closed with plastic caps (Macherey-Nagel GmbH, Duren, Germany) with perforated membrane to allow for easy needle insertion in the sample introduction system. For pipetting, ultra clean pipette tips from Eppendorf® were purchased. All handling of samples, labware and chemicals was done using clean nitrile gloves (without glove powder).

2.3 Instrumentation

2.3.1 Mass spectrometer

2.3.1.1 Agilent 7800 mass spectrometer

For multielemental measurements a MS setup consisting of **Agilent 7800 single quadrupole mass spectrometer** (Agilent Technologies, Tokyo, Japan) was used. As means of ionization an integrated inductively coupled plasma torch was deployed.

The liquid samples were introduced from an on-site autosampler system (Agilent Technologies SPS 4 Autosampler) to a nebulizer chamber of the mass spectrometer using a peristaltic pump (Direct infusion – See figure 20 below). Additionally, internal standard solution containing Indium and Rhenium was introduced to every sample via a T-junction which was installed about 3 cm upstream of the peristaltic pump.

An extensive overview of the exact measurement parameters is summarized in Table 3 on the next page.

All data were recorded and processed using the Agilent own software “MassHunter” (Workstation Software, Version C.01.03, 2016). Further informations on the data processing steps are described in more detail in section 2.6 Data handling on page 38.

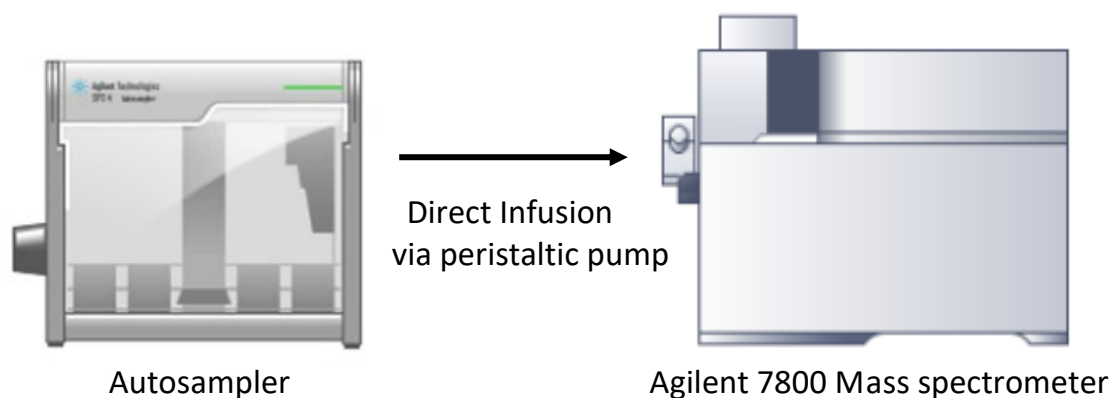


Figure 20: A schematic figure on the measurement method. The sample is introduced from the onsite autosampler via a direct infusion method to the Agilent 7800 mass spectrometer

Table 3: A tabular overview on the general setup and settings of the 7800 mass spectrometer in the direct infusion experiments (samples: CRMs, Cell culture media)

Parameter	Value
RF Power	1500 W
Sampling depth	6.3 mm
Nebulizer	MicroMist
Spray chamber	Scott double-pass
Monitored isotopes	⁹ Be, ¹¹ B, ²³ Na, ²⁴ Mg, ²⁷ Al, ²⁸ Si, ³¹ P, ³⁹ K, ⁴³ Ca, ⁴⁴ Ca, ⁴⁷ Ti, ⁵¹ V, ⁵³ Cr, ⁵⁵ Mn, ⁵⁶ Fe, ⁵⁹ Co, ⁶⁰ Ni, ⁶³ Cu, ⁶⁶ Zn, ⁷⁵ As, ⁷⁷ Se, ⁷⁸ Se, ⁸² Se, ⁹⁵ Mo, ¹⁰⁷ Ag, ¹¹¹ Cd, ¹²¹ Sb, ¹²⁷ Ba, ¹⁹⁵ Pt, ²⁰⁵ Tl, ²⁰⁶ Pb, ²⁰⁸ Pb, Std: ¹¹⁵ In, ¹⁸⁵ Re
Measured m/z (Q1)	9, 11, 23, 24, 27, 28, 31, 39, 43, 44, 47, 51, 53, 55, 56, 59, 60, 63, 66, 75, 77, 78, 82, 95, 107, 111, 121, 127, 195, 205, 206, 208, 115, 185
Plasma gas (Flow rate)	Argon (15 L.min ⁻¹)
Nebulizer gas (Flow rate)	Argon (1.1 L.min ⁻¹)
Auxiliary gas (Flow rate)	Argon (0.9 L.min ⁻¹)
Reaction gas	Helium (collisional gas)
Cones	Nickel
Cell entrance lens voltage	-60 V
Cell exit lens voltage	-110 V
Mode	TRA
Integration time	0.1 s for each Element

2.3.1.2 Agilent 8800 mass spectrometer

For main experiments (exploratory and incubation studies) an **Agilent 8800 triple quadrupole mass spectrometer** (Agilent Technologies, Tokyo, Japan) with integrated inductively coupled plasma torch as means of ionization was used (See figure 21 below).

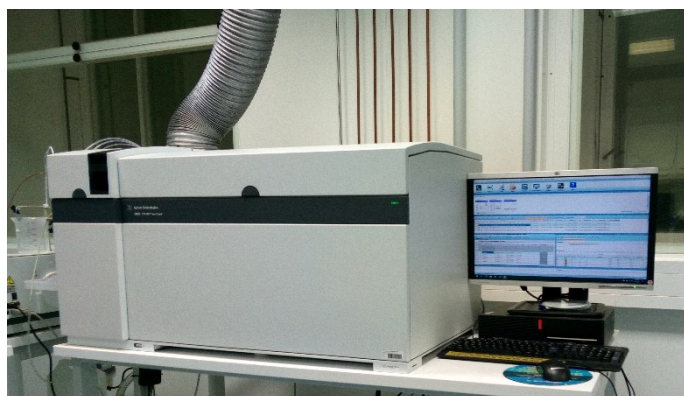


Figure 21: Agilent 8800 triple quadrupole setup

With this setup 4 elements were measured, namely Sulphur-32, Iron-56, Copper-63 and Zinc-66, each in Oxygen reaction gas mode. The mass spectrometer was operated in triple quadrupole mode (reaction monitoring). The first analyzing quadrupole was set to allow masses 32m/z (S), 56m/z (Fe), 63m/z (Cu) and 66m/z (Zn) to pass. The second analyzing quadrupole was set such as a mass shift of one oxygen atom (16m/z) can be detected for Sulfur (48m/z) and for iron (72m/z). For copper and zinc no mass shifts are feasible to set up in the second quadrupole, because those two elements do not readily react with oxygen. Therefore, the masses were set to 63m/z and 66m/z respectively.

The **Agilent 8800 triple quadrupole mass spectrometer** was always coupled to a HPLC setup (see figure 22 on the next page - described in section 2.3.2 Liquid Chromatography system on page 32 in greater detail) and operated either in flow injection mode or in HPLC column separatory mode (this is dependent on the concrete measurement and will be described in each result section accordingly).

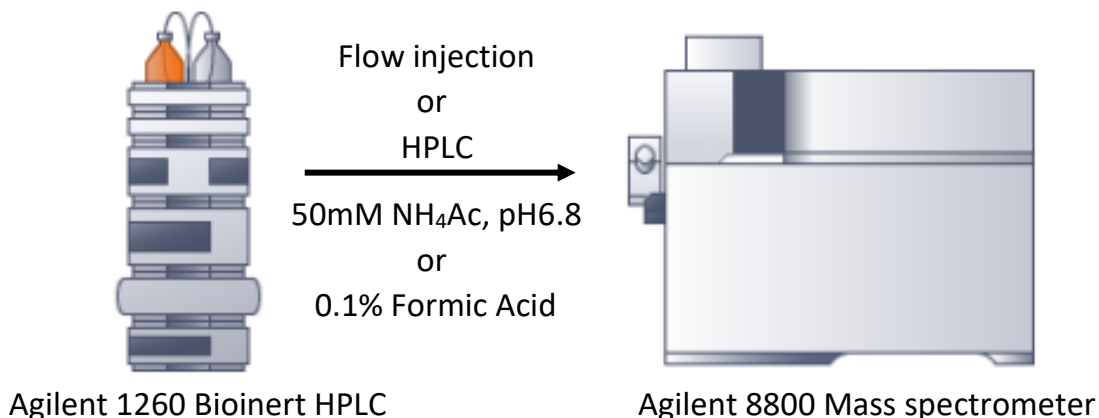


Figure 22: A schematic depiction of the measurement setup consisting of the Agilent 1260 Bioinert HPLC interfaced with Agilent 8800 Mass spectrometer. The measurement mode is either Flow-injection mode bypassing an analytical column or HPLC mode with an installed analytical column

A more extensive overview of all relevant measurement parameters is summarized in Table 4 below. All data were recorded and processed using the Agilent own software “MassHunter” (Workstation Software, Version C.01.03, 2016). Further informations on the data processing steps are described in more detail in section 2.6 Data handling on page 38.

Table 4: A tabular overview on the general setup and settings of the 8800 mass spectrometer in The main experiments (Flow-injection and HPLC-MS/MS Experiments)

Parameter	Value
RF Power	1500 W
Sampling depth	6.3 mm
Nebulizer	MicroMist
Spray chamber	Scott double-pass
Monitored isotopes	³² S, ⁵⁶ Fe, ⁶³ Cu, ⁶⁶ Zn
Measured m/z (Q1 → Q2)	³² S (32→46) ³² S ¹⁶ O ⁵⁶ Fe (56→72) ⁵⁶ Fe ¹⁶ O ⁶³ Cu (63→63) ⁶³ Cu ⁶⁶ Zn (66→66) ⁶⁶ Zn
Plasma gas (Flow rate)	Argon (15 L.min ⁻¹)
Nebulizer gas (Flow rate)	Argon (1.1 L.min ⁻¹)
Reaction gas	Oxygen reaction gas
Cones	Nickel
Cell entrance lens voltage	-60 V
Cell exit lense voltage	-110 V
Mode	TRA
Integration time	0.1s for each element (0.4s for all)

2.3.2 Liquid Chromatography system

The analytical separations were performed on an **Agilent 1260 infinity BioInert system** (Agilent Technologies, Waldbronn, Germany). The sample introduction volume was always set to 5 μ L. All measurements were conducted either using an analytical column or were conducted in flow-injection-mode bypassing the analytical column. An injection duration in flow injection experiments of 1 min (flow rate 0.2mL.min⁻¹) was set.

As for the analytical column, after several experiments (as described in Section 3.3 Analytical column choice for main experiments on page 49), for our purpose the most optimal available candidate was Acquity UPLC Protein BEH SEC 200Å; 1,7 μ m; 4,8mm x 300mm (Waters, Milford, Massachusetts, USA). The system was set to operate at a constant flow rate of 0,4ml/min, which generated a pump pressure of around 500bar (max allowed pressure for this setup: 600bar). The HPLC needle was washed after every injection by dipping 5 times into a separate wash vial filled with 70% isopropanol. The duration of one chromatographic experiment was set to 12min as for the last observable analyte eluted after about 11min.

However, due to a complicated chemical behavior of Thiosemicarbazones with steel columns, elution time shifts were observed and even became a serious issue over time of use.

For more detailed informations on the HPLC parameters see Table 5 below.

Table 5: A tabular overview on the used settings of the HPLC setup in the main experiments part

Parameter	Value
Autosampler temperature	4°C
Injection volume	5 μ L
Flowrate (pump pressure)	0.4 mL.min ⁻¹ (500 bar)
Column	Acquity UPLC Protein BEH SEC
Pore size	200 Å
Particle size	1.7 μ m
Column type	Size Exclusion (protein range 10 kDa – 500 kDa)
Column temperature	Ambient (no temperature control)
Eluent	50 mM Ammonium Acetate pH 6.8
Elution mode	Isocratic

2.4 Cleanroom

In order to keep all possible contaminations from the surroundings low the preparation and handling of samples and reagents intended for measurements on the **Agilent 8800 mass spectrometer** was always carried out in an ISO class 8 cleanroom. The sample measurements were then performed without leaving the cleanroom in the neighboring ISO class 7 Cleanroom at the faculty of chemistry – department of analytical chemistry, Koellensperger Lab.

2.5 Experimental setups and sample preparations

2.5.1 Assessment of contaminations in cell culture media

The assessment of contaminations in cell culture media components was performed on **Agilent 7800 mass spectrometer** in direct infusion mode.

10 samples were precisely weighted into precleaned PFA (Perfluoroalkoxy alkane) digestion Tubes and digested using 2mL 20% Nitric Acid and 100 μ L Hydrogen peroxide. The weighing of the samples was performed on a micro balance CPA 225D (Sartorius AG, Göttingen, Germany). The digestion was done using automated hot plate with a standard digestion program of 7 hours at max temp. 200°C. The samples denoted with “MEME” are Minimal essential media eagle (Available from Merck, Germany) provided by research group around Dr. Christian Kowol and Institut für Krebs-Forschung (IKF) of Medical University of Vienna. The abbreviation “FBS” stands for Fetal bovine serum which was obtained from Sigma Aldrich (USA). There were also additional 6 samples which contained essentially 3% Nitric Acid, which were digested as well to obtain digestion blank values.

- | | |
|--|--|
| 1) MEME (Powder) | 6) MEME + NaHCO ₃ (IKF) |
| 2) MEME (Cleanroom) | 7) MEME + NaHCO ₃ , FBS (IKF) |
| 3) MEME + NaHCO ₃ (Cleanroom) | 8) FBS |
| 4) MEME + NaHCO ₃ , FBS (Cleanroom) | 9) Human Serum |
| 5) MEME (IKF) | 10) Mouse Serum |

After digestion the cooled samples were quantitatively transferred into clean 15mL FalconTubes[®]. Each PFA tube was additionally cleaned two times with 4mL of milli-Q Water (18.2 M Ω .cm) and this solution was also transferred into respective sample FalconTube[®].

Resulting weights of the diluted samples were recorded for more precise calculations. The samples were then mixed thoroughly and put into the on-site Autosampler (Agilent Technologies SPS4 Autosampler) for the measurements. Every sample was introduced (direct infusion) to the ICP interface using a peristaltic pump (detailed description in Section 2.3.1.1 Agilent 7800 Mass Spectrometer on page 28). The sample preparations and measurements were performed in a normal laboratory (no cleanroom) at the faculty of inorganic chemistry – Währinger Straße 42, 1090 Vienna. The data processing and evaluation was done as described in section 2.6 Data handling on page 38.

An analogous assessment of contaminations in the aforementioned samples was also performed using **Agilent 8800 mass spectrometer** omitting the digestion step. This experiment will be described in more detail in the next chapter.

2.5.2 Selection of viable solvent system for optimal measurement performance and background reduction (Cell culture media and Thiosemicarbazones in flow injection experiments)

In this experiment, an alternative quantification of contaminants in cell culture media was carried out to cross-validate the two possible methods – Direct infusion method on the Agilent 7800 and flow-injection method on the Agilent 8800.

The samples were the same as previously described.

- | | |
|--|--|
| 1) MEME (Powder) | 6) MEME + NaHCO ₃ (IKF) |
| 2) MEME (Cleanroom) | 7) MEME + NaHCO ₃ , FBS (IKF) |
| 3) MEME + NaHCO ₃ (Cleanroom) | 8) FBS |
| 4) MEME + NaHCO ₃ , FBS (Cleanroom) | 9) Human Serum |
| 5) MEME (IKF) | 10) Mouse Serum |

Simultaneously, all thiosemicarbazones (in a concentration of 10µM in 0.3% HNO₃) were measured alongside as well to test their quantizability in simple analytical setup.

As means of calibration – a standard calibration solution series was produced using a multielement stock solution as described in section 2.1.2 Preparation of Solutions paragraph “**Calibration Standards**” on page 25.

The experiment was performed on the **Agilent 1260 HPLC** setup ran in flow injection mode (no analytical column – description in section 2.3.2 Liquid Chromatography system on page 32). The eluent was 0,1% formic acid solution. The setup was coupled to **Agilent 8800 mass spectrometer** (settings described in section 2.3.1.2 Agilent 8800 mass spectrometer on page 30). The duration of one flow injection experiment was set to 1 minute as this was sufficient for complete elution.

Several preliminary experiments showed that there are very serious problems with the sample measurability and therefore, all samples were additionally dissolved in following solvent systems:

1) 0.1% Formic acid 2) 0.3% HNO₃ 3) 1% HNO₃ 4) 10mM Citric acid
in 1:1 ratio to facilitate better measurability of copper ions.

2.5.3 Experimental setup and preparation of alternative quantitation standard – bovine CuZn Superoxide Dismutase

In this side experiment an alternative quantitation of copper was attempted using a standard bovine Copper-Zinc Superoxide Dismutase (bCuZn-SoD) on the **Agilent 8800 Mass spectrometer** in a flow injection mode (as described section 2.3.1.2 Agilent 8800 mass spectrometer on page 30 and in section 2.3.2 Liquid Chromatography system on page 32). The stock standard solution of bCuZn-SoD was produced as described in Section 2.1.2 Preparation of Solutions in paragraph “**Bovine CuZn Superoxide dismutase calibration standard**” on page 25.

2.5.4 Selection of appropriate analytical column – separation experiment with human blood serum (proteins)

For the main experiments - incubation studies, an analytical column capable of separating the most components of human blood serum proteins needed to be selected. For this purpose, 4 available size exclusion chromatographic columns were tested, namely:

-) Acquity UPLC Protein BEH, 4.8mm x 300mm, 1.7um, 200Å - **AcqUHPLC_200Å/300mm**
-) Acquity UPLC Protein BEH, 4.6mm x 150mm, 1.7um, 200Å - **AcqUHPLC_200Å/150mm**
-) Acquity UPLC Protein BEH, 4.6mm x 150mm, 1.7um, 125Å - **AcqUHPLC_125Å/150mm**
-) ThermoScientific MAbPac SEC-1, 4mm x 300mm, 5um, 450Å - **MAbPac_450Å/300mm**

All columns were tested according to their specified operation limits without additional temperature control i.e. in ambient temperature. The results and discussion of the separation performance of each column is described in section 3.3 Analytical column choice for main experiments - starting on page 49.

2.5.5 Description of main experiments - incubation studies

All provided thiosemicarbazones (See section 2.1.3 Samples paragraph “**Samples for Incubation studies**” on page 26) were dissolved, if possible, in minimal amount of DMF. 100µL was usually sufficient for 1mg of the substance. However, for Cu-Dp44mT 900µL DMF were necessary and Cu-COTI-2 was not fully dissolved even after adding 1300µL DMF.⁷ Further dilutions of the substances were performed using 50mM Ammonium Acetate solution such as the resulting concentration of each thiosemicarbazone was 2000µM, 200µM and 20µM.

These solutions were directly used for incubation with human blood serum by diluting them 20-fold with the buffered human blood serum (8µL TSC + 152µL serum) such as the resulting concentration of the agent during measurements was 100µM / 10µM / 1µM accordingly.

As for the parameters of the measurement, the incubation study was carried out using the **8800 Agilent Mass spectrometer** coupled to **1290 Agilent HPLC setup**. The Temperature of the autosampler was set to 37°C in order to simulate physiological conditions. The HPLC setup was set using an analytical column (Acquity UPLC Protein BEH, 4.8mm x 300mm, 1.7µm, 200Å) as described in section 2.3.2 Liquid Chromatography system on page 32. The settings of the mass spectrometer were set as described in section 2.3.1.2 Agilent 8800 mass spectrometer on page 30.

A blank sample (50 mM Ammonium acetate) was always injected first in order to assess any possible contaminations. The second injection was always buffered human blood serum as a reference before incubation. As for the duration of one chromatographic analysis of 12min, the best possible time resolution of the incubation studies is equal to about 12min.

⁷ To carry out the measurements with Cu-COTI2 nevertheless, the suspension of undissolved substance was mixed thoroughly, and a small aliquot was quickly pipetted for further dilutions with 50mM Ammonium Acetate pH 6.8. The resulting dilutions did not show any “cloudiness” which meant that Cu-COTI2 could be used for the intended incubation studies.

2.5.6 Preparation of Cu-Selective ion exchange resin (CHELEX® ion exchange) and experimental setup for subsequent measurements of filtered cell culture media - components

To assess the possibility of lowering the copper background in cell culture media components (MEME, NaHCO₃ and FBS), a Cu-selective CHELEX® ion exchange material was used and tested. First, a small amount of the CHELEX® material was transferred into a clean 50mL FalconTube® and suspended in ultra-pure Water. Using a 10mL Eppendorf® pipette the suspended material was transferred into a Pasteur pipette with small piece of glass wool stucked into its thin part such as the CHELEX® material stays in the pipette but solutions can pass through.

The Pasteur pipette was filled halfway with the CHELEX® material (2-3cm) – See figure 23 below. This preparation was repeated for each of the media intended to be filtered through CHELEX® ion exchanger.

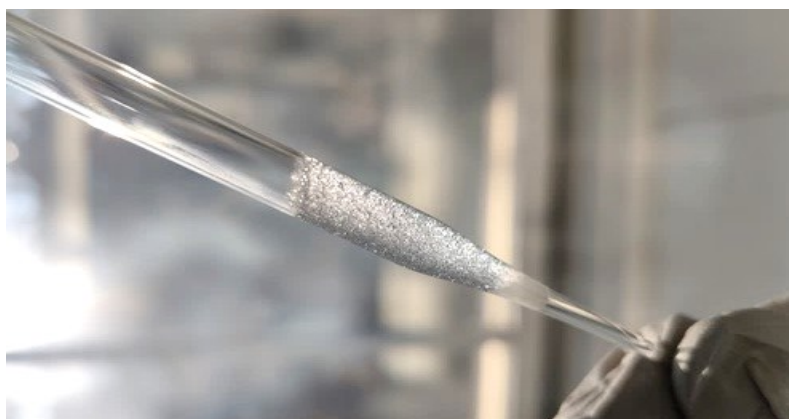


Figure 23: A Pasteur pipette filled with CHELEX® ion exchanger material for background reduction experiment with cell culture media.

The filtration was performed first, by passing about 3mL of the respective medium to wash out excess water. This effluent was discarded. Then 10mL of the respective medium was filtered in small portions through the CHELEX® material and combined into clean FalconTube®. After that 2mL of each sample was transferred into precleaned PFA (Perfluoroalkoxy alkane) digestion Tubes and digested using 2mL 20% Nitric Acid and 100µL Hydrogen peroxide. The digestion of the samples was performed using automated hot plate with a standard digestion program of 7 hours at max temp. 200°C. (analogous as described in section 2.5.1 assessment of contaminations in cell culture media on page 33).

2.5.7 non-lethal *in-vivo* experiments with Triapine in mouse

To obtain further data on the behavior of Thiosemicarbazones, a small non-lethal *in-vivo* experiment was conducted on two mice with Triapine Agent. A small amount of blood and urine was first drawn from tested mice A and B. Then, mice A and B were injected a solution of Triapine such as the resulting concentration of the drug in both mouses blood stream was around 15mM. 10 minutes after the injection, blood and urine was drawn from both animals. The experiments were performed according to the Federation of Laboratory Animal Science Association guidelines for the use of experimental animals.

2.6 Data handling

2.6.1 General handling of outputs

The recorded mass spectrometric data were handled by the integrated software package from Agilent "MassHunter" (Workstation Software, Version C.01.03, 2016). In every measurement series blank samples containing only 50mM Ammonium Acetate or 0.3% HNO₃ were also prepared and measured along with other samples. The blank values were used to calculate Limits of detection (3*standard deviation) and Limits of quantification (10*standard deviation).

- The output of measurements performed on the **7800 Agilent mass spectrometer** was an average of counts per second of every respective element and measurement mode (no gas or He). Additionally, the measured data were automatically divided by the signal of the internal standard - This accounts for plasma- and flow instabilities und further improves the measurement accuracy. The data were then exported from the MassHunter software as *.csv and further data treatment was done using Microsoft Excel. An average blank value from several blank measurements for every element was calculated and subtracted from every measured sample. The same procedure was repeated with a digestion blank (ultra-pure water digested along with other samples) to obtain the final results, every concentration from every sample was multiplied with its respective dilution factor. For plotting the results, a freeware software SciDAVis was used.

- The output of measurements performed on the **8800 Agilent mass** spectrometer were raw counts per second raw data (always time resolved analysis mode) The internal algorithms handled the quantitation using data from measurements of calibration series. As far as raw data are concerned, no further data handling was necessary. The data were then exported from the MassHunter software as *.csv and further data treatment (organizing) was done using Microsoft Excel. For plotting simple result graphs, a freeware software SciDAVis was used. For plotting the results of incubation studies – a registered Software OriginPro 2019 was used. Concretely, the traces of incubation studies were plotted as stacked waterfall plot.

2.6.2 Multilinear Regression (MLR)

For Multilinear Regression a short python scrip was written (see figure 24 below) to conduct matrix operations on measured data matrices.⁸ Concretely this method was used to estimate the concentrations of proteins in human blood serum. As the chromatogram of human blood serum as well as chromatograms of 10 protein standards commonly found in human blood serum were available from measurements, the concentrations can be obtained from simple matrix calculations. MLR is usually used in the field of spectrometry, but this analytical problem has the same attributes as spectrometric data. Therefore, MLR can be employed here.

```
# -*- coding: utf-8 -*-
"""
Spyder Editor
Author: Tom
"""
import numpy

components=numpy.loadtxt("components.txt") #Loads chromatograms of the 10 protein standards (sulfur trace)
target=numpy.loadtxt("target.txt")       #Loads chromatogram of the human blood plasma (sulfur trace)

target=numpy.reshape(target, (1730,1))   #Creates matrix array from list
components=numpy.reshape(components, (1730,10)) #Creates matrix array from list

C=(numpy.linalg.inv((numpy.transpose(components)
    .dot(components))).dot((numpy.transpose(components).dot(target)))) #Matrix operations for calculating C
```

Figure 24: The Python code used for Multilinear regression employed in a side experiment with protein standards commonly found in human blood serum emulating human blood serum chromatogram measured separately.

⁸ For context reasons more information on the basics of multilinear regression is discussed in section 4.5 Multilinear regression – protein standards on page 47.

3. Results and Discussion

3.1 Assessment of contamination in Cell culture media

3.1.1 Contamination analysis using a digestion method

First, a standard calibration series was performed on an **Agilent 7800 single quadrupole** using a multielement standard. For most of the elements a good linearity was obtained. Further improvements could be achieved by deleting outlier values, particularly from the lower concentration range of 0.1ppb – 1 ppb. This was performed on a case-to-case basis for several elements.

Using the standard calibration curve the LOD / LOQ values were calculated from 10 blanks (1% HNO₃).

$$\text{LOD} = 3 \cdot \text{STDDEV} \quad \text{LOQ} = 10 \cdot \text{STDDEV}$$

Respective values of the most worthwhile elements are summarized in Table 6 below.

Table 6: A tabular overview on selected metals and their respective limits of detection and limit of quantitation in the direct infusion experiments performed on the Agilent 7800 mass spectrometer

Measured Isotope	[⁵² Cr] ⁺	[⁵⁵ Mn] ⁺	[⁵⁶ Fe] ⁺	[⁵⁹ Co] ⁺	[⁶⁰ Ni] ⁺	[⁶³ Cu] ⁺	[⁶⁶ Zn] ⁺	[⁹⁵ Mo] ⁺	[¹¹¹ Cd] ⁺	[²⁰⁸ Pb] ⁺
Measurement mode	[He]	[no gas]	[He]	[He]	[no gas]	[no gas]	[He]	[He]	[He]	[He]
LOD [µg/kg]	0.0244	0.0074	0.0975	0.0054	0.0134	0.0016	0.0362	0.0025	0.0017	0.0019
LOQ [µg/kg]	0.0814	0.0245	0.3250	0.0181	0.0447	0.0053	0.1207	0.0084	0.0057	0.0063

The calibration functions of the two metals of upmost interest, namely iron and copper are depicted in Figures 25 and 26 on the next page.

For the most abundant iron isotope (91.66%)[20] with its nominal mass of 56m/z, generally high background from polyatomic species like ⁴⁰Ar¹⁶O, ⁴⁰Ca¹⁶O and several more are expected. Therefore, in order to eliminate these interferences iron generally must be measured using a collisional gas. In our case using Helium as collisional gas, the background signal of ⁵⁶Fe was reduced significantly (around 90-fold). Copper with its nominal mass of 63m/z or 65m/z on the other hand does not suffer from any excessive polyatomic interferences (minor interferences include ⁴⁰Ar²³Na for ⁶³Cu and ⁴⁰Ar²⁵Mg for ⁶⁵Cu) and can, therefore, be measured either with or without a collisional gas.

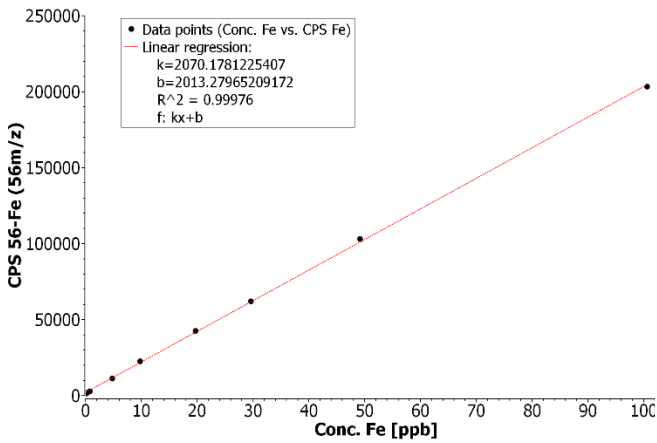


Figure 25: Analytical function plot: Concentration of iron in ppb against counts per second in the experiments on 7800 mass spectrometer. Linear regression performed using SciDAVis

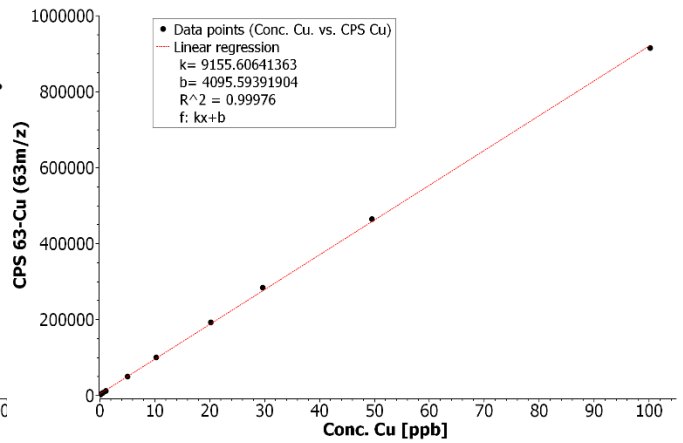


Figure 26: Analytical function plot: Concentration of copper in ppb against counts per second in the experiments on 7800 mass spectrometer. Linear regression performed using SciDAVis

However, using collisional gas mode always results in sensitivity penalty due to the loss of ions in the collision process. Often, a reasonable decision must be made considering which mode fits best for the intended purpose. In order to ensure that the measurements are precise and correct, two certified reference materials (CRMs) were measured alongside the samples. TM28.4 Lake Ontario water reference material was analyzed to validate our analytical method. As seen in Figure 27 below, the measurement method was validated for 20 Elements (some elements in no gas as well as in Helium collisional gas mode).

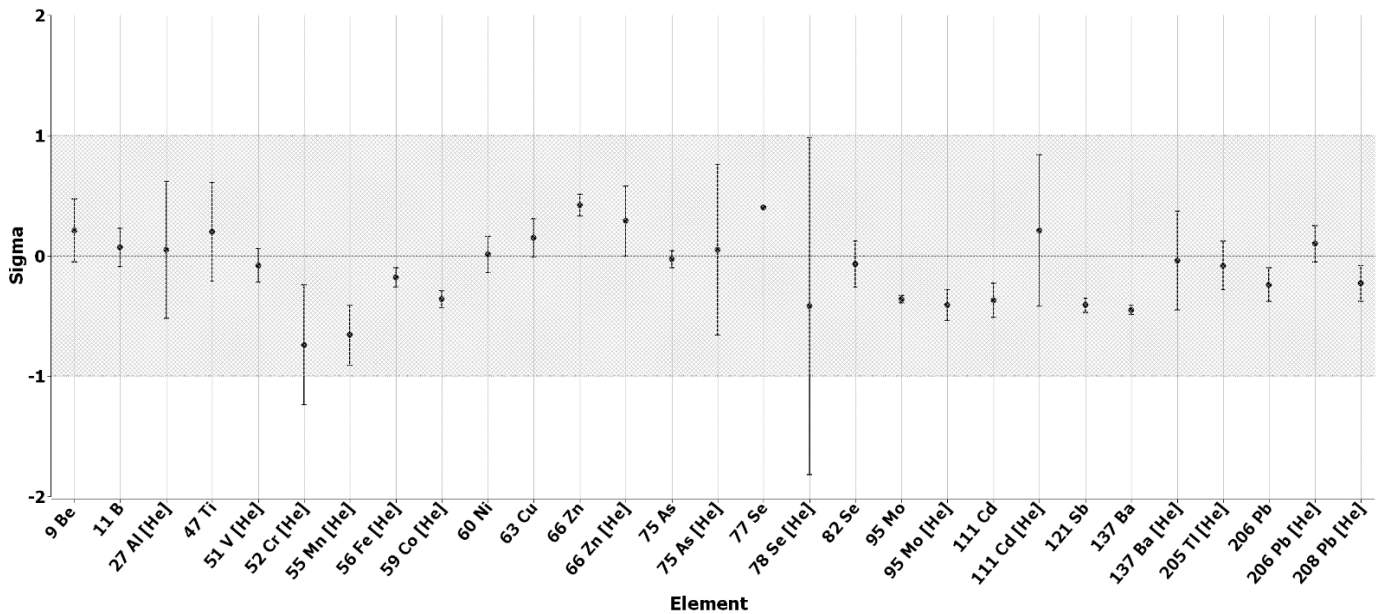


Figure 27: A quality assurance plot for the CRM measurement of Lake Ontario water. All depicted elements are certified as their mean values correspond to the mean value of the certified reference material with an uncertainty margin of $\pm 1\sigma$

Another certified reference material, concretely Seronorm™ (trace elements serum L-1), was also subjected to open-vessel digestion in order to validate the sample preparation chain. The results from this analysis are summarized in Figure 28 below in a quality assurance plot. Compared to measurement method validation only a small number of elements could be validated for the chain of sample preparation. Nonetheless, the most important elements Fe and Cu could be validated, which showed that the method was fit for purpose of assessing iron and copper contaminations in various samples, mainly in serum-like samples.

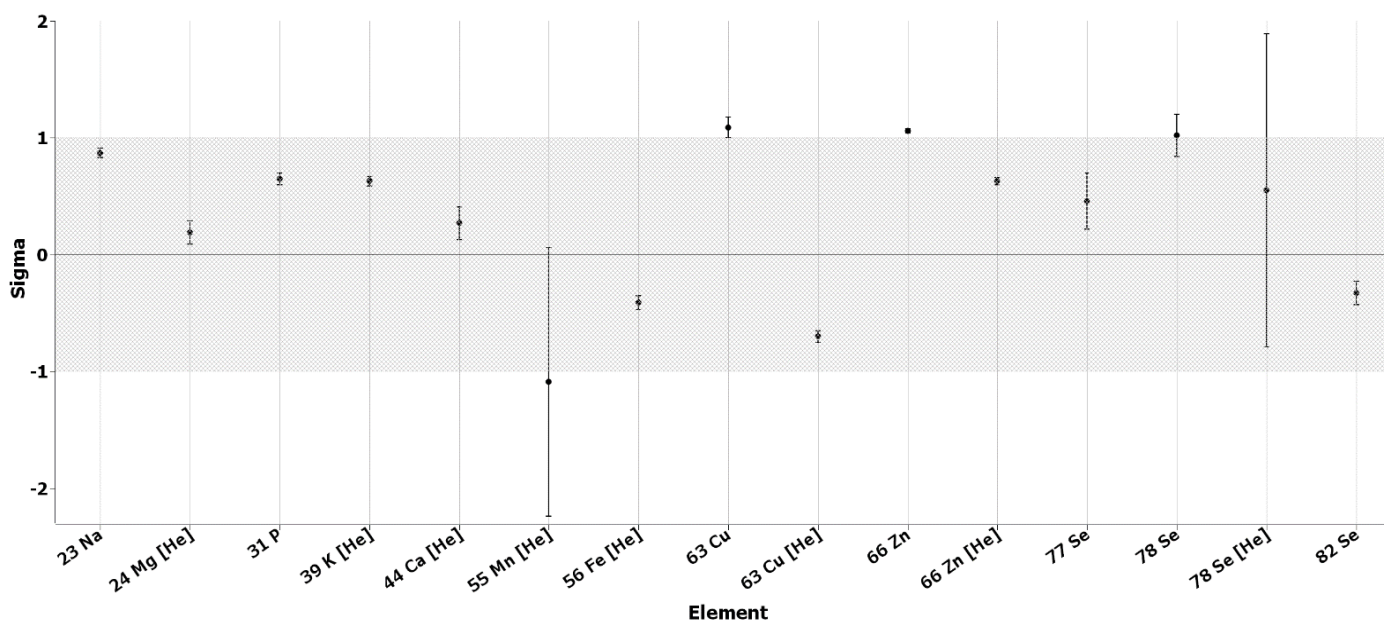


Figure 28: A quality assurance plot for the standard reference material measurement of Seronorm™. Most depicted elements are certified except for ⁶³Cu [no gas mode], ⁶⁶Zn [no gas mode] and ⁷⁸Se [no gas mode] which are almost certified (and can easily be corrected by using recovery factors). This is not an issue as these elements are certified in other measurement modi or via their sister isotopes.

The aim of the following measurements is to assess the metal contamination of cell culture media and components thereof, which could cause interferences with metallodrugs, but also cause inaccuracies in subsequent analytical measurements.

This assessment is of vital importance as free Thiosemicarbazones, which are the main subject of this master's thesis are strong chelators. Therefore, in order not to put the significance of main analyses in jeopardy these results become very important as will be discussed in later parts.

To avoid confusions, measurement results were converted to units of $\mu\text{mol}/\text{kg}$ as this is the main unit and average range of biological activity of (anticancer-) metallodrugs described in scientific publications for Thiosemicarbazones. This assessment becomes very important when put into the context of analysis of free thiosemicarbazones, which are able to pull copper from their environment and even from proteins like albumin (discussion in section 3.6 Main experiments – Incubation studies starting on page 65).

The results showed a slight reduction of the Fe and Cu background when preparing the media in a cleanroom. The main source of copper contamination seems to be sodium bicarbonate, which is commonly used in cell culture media to get a stable pH value. (see NaHCO_3 bar in Figure 29 and 30). This is a common issue in many commercially available inorganic salts. However, MEME and FBS also contribute similar concentrations to the Cu background, since NaHCO_3 is only added to the final medium in small amounts.

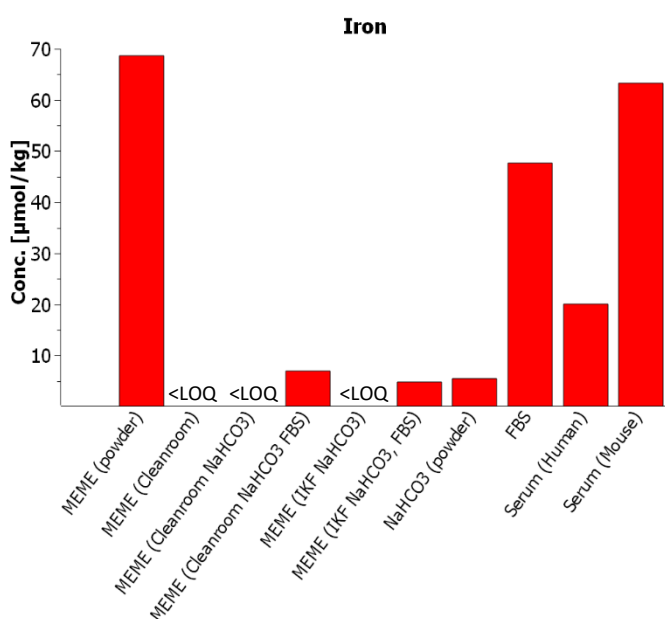


Figure 29: Results chart for the 10 analyzed samples showing the amount of Iron in the units of $\mu\text{mol}/\text{kg}$. This experiment was performed on the 7800 mass spectrometer

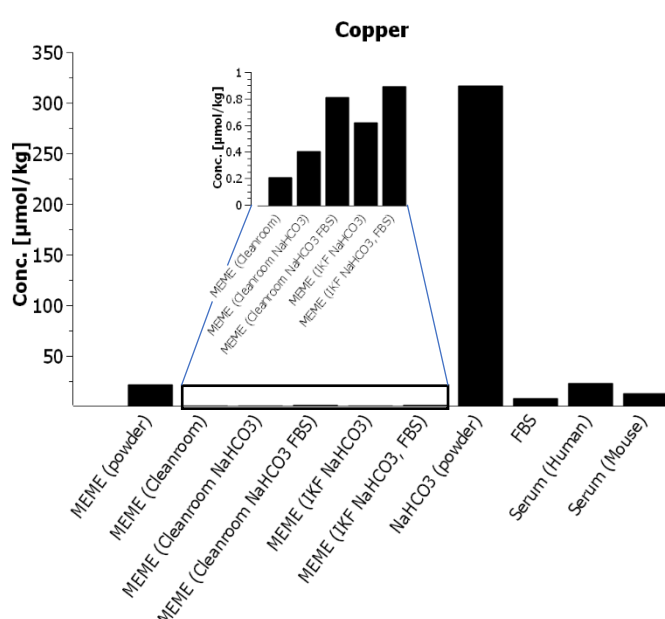


Figure 30: Results chart for the 10 analyzed samples showing the amount of Copper in the units of $\mu\text{mol}/\text{kg}$. This experiment was performed on the 7800 mass-spectrometer.

In the case of iron, the main source of contamination is FBS. After preparation of the full cell culture medium including FBS the concentration of iron was equal to about $7\mu\text{mol}/\text{kg}$.

A viable option for the reduction of the Cu background in NaHCO_3 could be the purchase reagents in higher grades of purity (e.g. Suprapur, which is readily available from Sigma Aldrich or Merck). Another alternative is to make the salt from its precursors, but this approach is not very feasible.

The full cell culture media (samples: MEME – Cleanroom, NaHCO₃, FBS and MEME – IKF, NaHCO₃, FBS) have a copper background of around 0.8µmol/kg and 0.9µmol/kg respectively. This seemingly low values can contribute much to e.g. formation of Cu-Thiosemicarbazones from free thiosemicarbazones as suggested previously – In this case the concentrations of iron and copper in full cell culture media may be high enough and may jeopardize experiments that target the precise analysis of the behavior of free TSCs

This issue is generally known and will be further underlined in the discussion of Incubation studies performed during this master's thesis (see section 3.6 Main experiments – Incubation studies starting on page 65). The important finding made here is to closely consider every possible contamination source. It is especially important when the topic of a given research are cell incubation studies with metallodrugs (and in the case of thiosemicarbazones - drugs whose activity is strongly modulated via complexation with various metals).

3.1.2 Contamination analysis using a flow-injection method

In this experiment, an alternative method was chosen for the quantification of contaminations in cell culture media and their components in order to cross validate the findings. This experiment was performed on the **Agilent 1260 HPLC setup** run in flow injection mode (no analytical column – Settings described in section 2.3.2 Liquid Chromatography system on page 32). The eluent was always 0,1% formic acid solution. The setup was coupled to **Agilent 8800 mass spectrometer** (settings described in section 2.3.1.2 Agilent 8800 mass spectrometer on page 30). The duration of one flow injection experiment was set to 1 minute as this was sufficient for complete elution. The samples were MEME solutions produced in the IKF or in cleanroom from its precursors. All cell culture media samples were additionally diluted in 1:1 ratio with the following solvents to test the solubility of Cu:

- | | | | |
|---------------------|--------------------------|---------------------|------------------------|
| 1) 0,1% Formic Acid | 3) 0,3% HNO ₃ | 2) Citric acid 10mM | 4) 1% HNO ₃ |
|---------------------|--------------------------|---------------------|------------------------|

For calibration, a single element (Cu) standard (Labkings) was used. The calibration points in a concentration range of 50-1000 µg/L (and Oppb ≅ Blank). were analyzed in each of the solvents. As can be seen in demonstrative figure 31 on the next page, good linearity was always obtained.

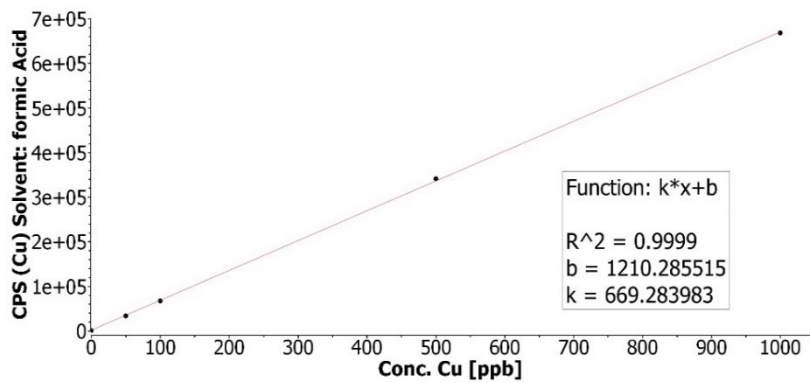


Figure 31: Calibration function of copper in solvent system: 0.1% Formic Acid

Several blanks (essentially each of the solvents without Cu-standard) were injected at the beginning to calculate limit of detection and limit of quantitation (see Table 7 below). Additionally, the CRM Seronorm™ was measured under the same conditions to ensure precision and accuracy of the measurement. Different sera (human, bovine) were used for comparison. These sera samples were not diluted in any way i.e. they were analyzed pure. The limits of detection were calculated from integrated areas of blank measurements at the beginning of the measurement series. Each integrated area value was plugged into each of the four analytical functions.

Table 7: Summarized values on Limits of detection and limits of quantitation in the investigated solvent systems

⁶³ Cu	0.1% Formic Acid	10mM Citrate	0,3% HNO3	1% HNO3
LOD [µg/kg = ppb]	1.531	0.012	0.081	0.492
LOQ [µg/kg = ppb]	3.461	1.832	2.689	3.463

The values of CRM Seronorm™ obtained in each of the solvent systems were in good agreement with the certified values. As can be seen from figure 32 below, a sharp elution signal was registered for Seronorm™ but also for human blood serum and FBS that were used as additional quality assurance materials with approximately known values.

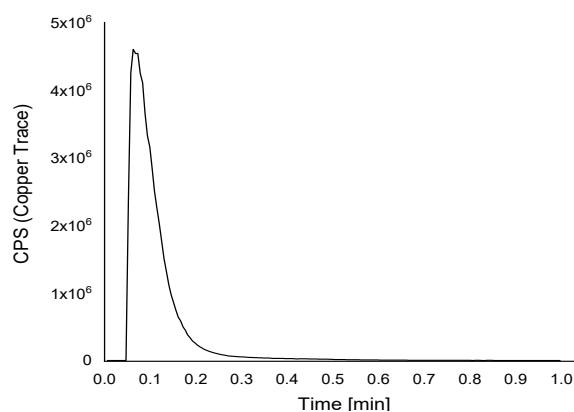


Figure 32: Elution profile of Seronorm™ in flow injection experiment performed on the 8800 Agilent mass spectrometer

Comparing the quantitation results of the CRM Seronorm™ in the flow injection experiment with the digestion method (see figure 33 below) it is clear that at least for serum-like analytes the two methods are equivalent in terms of precision and accuracy.

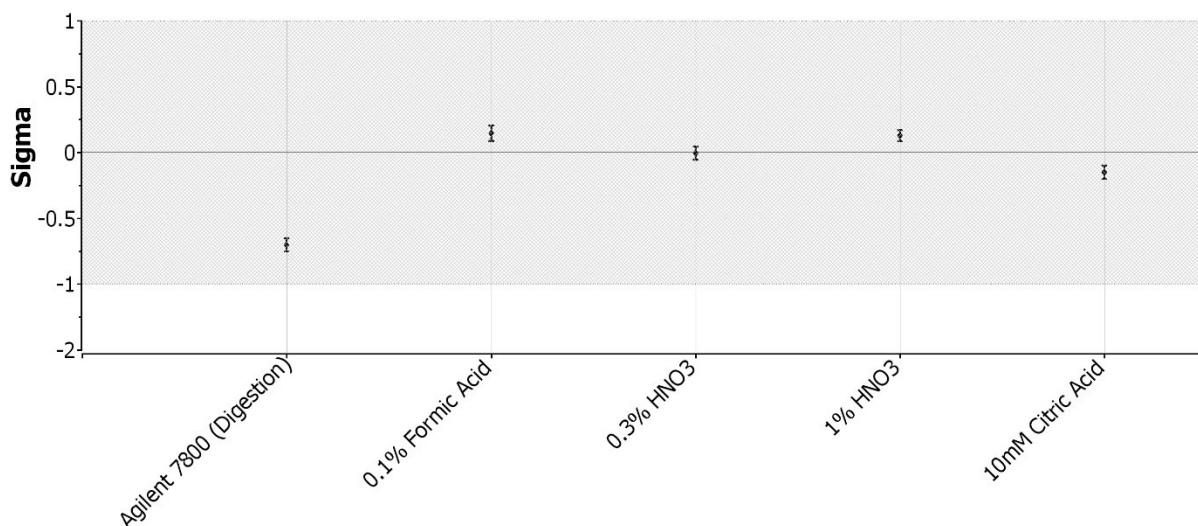


Figure 33: A quality assurance plot for the standard reference material measurement of Seronorm™. Comparison of the digestion method performed on the Agilent 7800 mass spectrometer against flow injection method performed on the Agilent 8800 mass spectrometer.

These findings can further be confirmed by comparing the results of human blood serum and FBS with the results from digestion method described earlier in section 3.1.1 contamination analysis using a digestion method on page 40 – see Table 8 below.

Table 8: Comparison table for digestion method (Agilent 7800) and flow-injection method (Agilent 8800). Values in [µg/kg = ppb]

	Digestion method		Flow-injection method	
	Fe	Cu	Fe	Cu
Human blood serum	22.62	26.56	24.47	30.54
FBS	50.03	8.33	55.23	12.65

As can be seen, there is a small discrepancy, however the results from both methods are well reproducible and a correction can be applied using a correction factor from the analysis of CRM Seronorm™ for better accuracy (mainly for the apparently slightly lesser precise digestion method).

Next, the same cell culture samples were investigated as described in section 2.5.2 Selection of viable solvent system for optimal measurement performance and background reduction (Cell culture media and Thiosemicarbazones in flow injection experiments) on page 34.

The copper signal for every sample was either below the limit of detection or extremely inconsistent in duplicate measurements (see Table 9 below).

Table 9: Results from the analysis of copper content in cell culture media (flow-injection method) Values in [$\mu\text{g}/\text{kg} = \text{ppb}$]

	0.1% Formic Acid	0.3% HNO ₃	1% HNO ₃	10mM citrate
MEME (Cleanroom)	< LOD	< LOD	< LOD	< LOD
MEME (Cleanroom, NaHCO ₃)	< LOD	< LOD	< LOD	< LOD
MEME (Cleanroom, NaHCO ₃ , FBS)	< LOD	< LOD	< LOD	0.05381
MEME (IKF, NaHCO ₃)	< LOD	< LOD	< LOD	< LOD
MEME (IKF, NaHCO ₃ , FBS)	< LOD	0.08267	< LOD	0.05905
NaHCO ₃ (Powder)	< LOD	< LOD	< LOD	< LOD

The same was true for the iron signal. In conclusion, it was found that complex samples such as cell culture media that consist of myriads of chemicals cannot easily be measured in flow injection mode analysis (for the chemical composition of Cell culture medium eagle – MEME see table 10 below).

Nevertheless, the method is suitable for many applications such as the assessment of copper content in serum-like samples, simple natural samples like lake or river waters and probably many more whose suitability, however, has to be confirmed with an appropriate certified reference material.

Table 10: An overview of the main contents of minimal essential medium eagle (MEME)

Amino acids			Vitamins	
L-Arginine	L-Leucine	L-Threonine	D-Biotin	D-Panthenic Acid
L-Asparagine	L-Lysine	L-Tryptophan	Choline Chloride	Pyridoxine
L-Aspartic Acid	L-Methionine	L-Tyrosine	Folic Acid	Riboflavine
L-Cysteine	L-Phenylalanine	L-Valine	Myo-Inositol	Thiamine
L-Glutamic Acid	L-Proline	Glycine	Niacinamide	Vitamin B12
L-Glutamine	L-Serin	L-Histidine	p-Amino Benzoic Acid	
Hydroxy-L-Proline	L-Isoleucine			

Inorganic salts	Other
Ca(NO ₃) ₂ • 4H ₂ O	D-Glucose
MgSO ₄	Glutathione
KCl	HEPES ⁹
NaHCO ₃	Phenol Red
NAaCl	
Na ₂ HPO ₄	

⁹ HEPES › (4-(2-hydroxyethyl)-1-piperazineethanesulfonic acid) – Buffering agent

3.2 Analysis of Thiosemicarbazones in flow injection analysis mode

All Thiosemicarbazones were tested prior to incubation studies in a flow injection analysis on the **8800 Agilent mass spectrometer** in the same manner as described in previous section 3.1.2 “Contamination analysis using a flow-injection method” in a concentration of 10 μ mol/L using a flow-injection method. The Thiosemicarbazones show normal elution pattern, albeit the peak shape is broader than it was the case in Seronorm™. Also, the background levels of copper after each TSC injection are harder to achieve (see figure 34 below). Therefore, a blank injection had to be performed after each thiosemicarbazone.

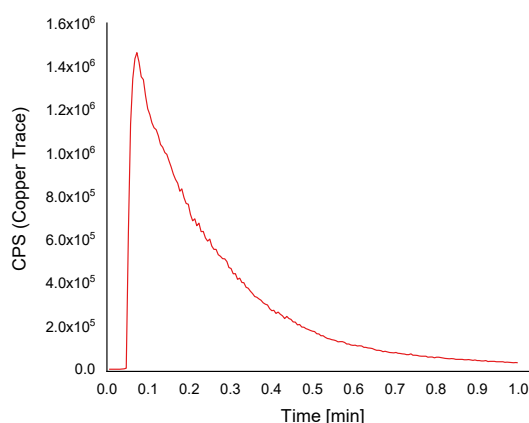


Figure 34: Elution profile of Triapine in flow injection experiment performed on the 8800 Agilent mass spectrometer. The peak is substantially broader than for example Seronorm™ peak in the same experiment

The copper-Thiosemicarbazones were produced such as the concentration of copper is equal to 1ppm. To calculate this concentration for each Cu-TSC a relative copper content was determined from the molar mass of the respective Cu-TSC, the molar mass of copper and the amount of copper atoms in each Cu-TSC which was always 1. For example, Cu-Triapine has a molar mass of 347.71 g/mol; the molar mass of one copper atom is 63g/mol. Therefore, the relative mass% of copper in Cu-Triapine is equal to $63/347.71 = 0.1812 = 18.12 \text{ mass\% Cu}$. In order to produce a Cu-Triapine solution with a copper concentration of 1ppm = 1mg/L a simple equation $0.1812 \cdot x = 1$ will be solved. The concentration of Cu-Triapine that needs to be produced is therefore $x = 5.52 \text{ mg/L}$. This calculation was done for all Cu-TSCs and for free TSCs roughly the same (molar-) concentrated solutions were prepared as their copper counterparts. Using the calibration function for copper in solvent system 0.1% formic acid, it was possible to quantify the copper content in all copper Thiosemicarbazones¹⁰

¹⁰ In order to analyze Cu-COTI2, special measures had to be employed to facilitate its dissolution – 1100 μ L DMF for each mg of COTI2 have to be added. The suspension needs furthermore to be put into a laboratory shaker at 45°C for extended period of time.

This experiment showed that there are no major issues with the internals of the **1260 Agilent HPLC** setup or **8800 Agilent mass spectrometer** setup retaining the Thiosemicarbazones in any significant way. The quantified copper was also in good agreement with the calculated and prepared concentration of copper complexed to TSCs. Hence, the setup can be used for more demanding tasks as intended – Size exclusion HPLC separations and analysis in incubation studies (Results described in section 3.6 Main experiments – Incubation studies starting on page 65).

3.3 Analytical column choice for main experiments

For the incubation studies 4 different analytical columns were available. The purpose of these experiments was to identify a single analytical column capable of separating the most components from human blood plasma in a justifiable time span of analysis.

-) Acquity UPLC Protein BEH, 4.8mm x 300mm, 1.7 μ m, 200Å - **AcqUHPLC_200Å/300mm**
-) Acquity UPLC Protein BEH, 4.6mm x 150mm, 1.7 μ m, 200Å - **AcqUHPLC_200Å/150mm**
-) Acquity UPLC Protein BEH, 4.6mm x 150mm, 1.7 μ m, 125Å - **AcqUHPLC_125Å/150mm**
-) ThermoScientific MAbPac SEC-1, 4mm x 300mm, 5 μ m, 450Å - **MAbPac_450Å/300mm**

As for the results, the separatory performance of the **AcqUHPLC_125Å/150mm** column can be seen as rather basic with two distinct signal peaks in the sulfur trace of the chromatogram (See figure 35). This trace corresponds generally to proteins, as most of the large proteins contain either methionine or cysteine or both to some extent. The two signals at around 3,4min and 3,9min can be found in all three traces (S, Fe and Cu). Analytes eluting in the early stages of the separation are generally large proteins. According to the manufacturer, the effective separatory range of this column for proteins lies in the range 1 – 80kDa. In our case a rather large Cu-containing Protein, namely Ceruloplasmin with a molecular weight of around 150kDa[73] is assumed to elute at 3,4min followed by Albumin (molecular weight 66kDa)[74] at 3,9min. This can be confirmed by examining the copper trace (see figure 37 on the next page) – Ceruloplasmin is a copper dependent protein and Albumin generally serves as all-round transport protein, which under general circumstances contains copper among other metals. Looking into the iron trace (see figure 36 on the next page), also the two exact same signals can be observed. Ceruloplasmin (3,4min) does not contain iron, however it facilitates redox reactions of iron and therefore, some iron may be associated with Ceruloplasmin.[75]

Another satisfiable explanation is the formation of an albumin dimer. Albumin dimer has a combined molecular weight of around 130kDa.[74]

Such analyte can here no longer be separated from Ceruloplasmin. Moreover, the Albumin dimer is expected to be superimposed over ceruloplasmin in all our separation experiments due to mass similarity. The last signal to interpret from this experiment is located in the copper and iron trace at around 6,1min and does not show up in the sulfur trace. In this range small species are expected, such as metal-peptide, metal-aminoacid conjugates and other small molecular species. In the case of iron, also Fe-Hem might be the predominant.

The presence of Fe-Hem in human serum is a common occurrence, as erythrocytes may burst during the process of serum extraction from blood and thereby releasing Fe-Hem from hemoglobin. This process is known as Hemolysis. Even though the separatory performance of this column is not the most optimal for our purpose, it was used several times during the incubation studies after severe issues occurred regarding the elution of thiosemicarbazones.

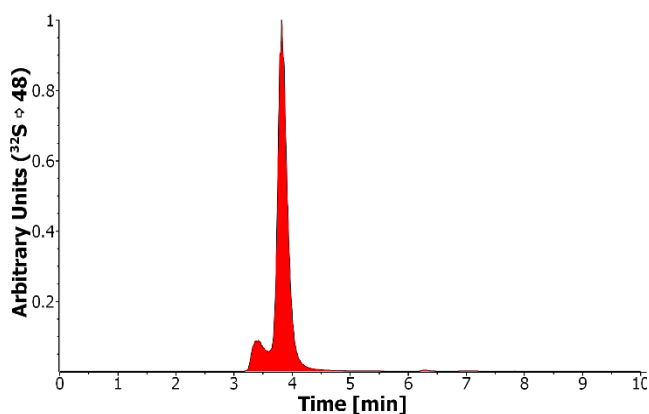


Figure 35: The sulfur trace of the separatory experiment with human blood serum on the AcqUHPLC_125Å/150mm analytical

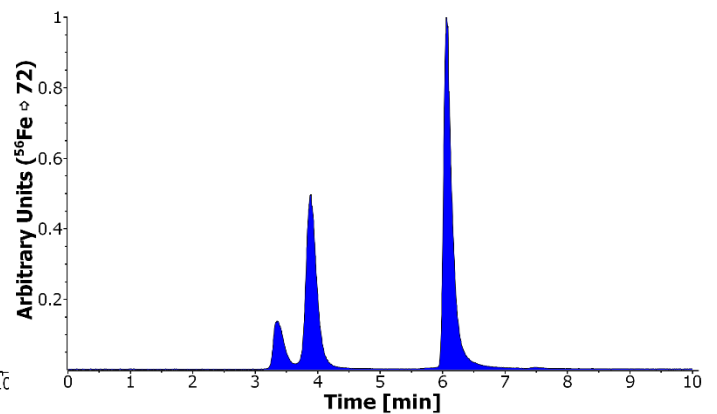


Figure 36: The iron trace of the separatory experiment with human blood serum on the AcqUHPLC_125Å/150mm analytical column.

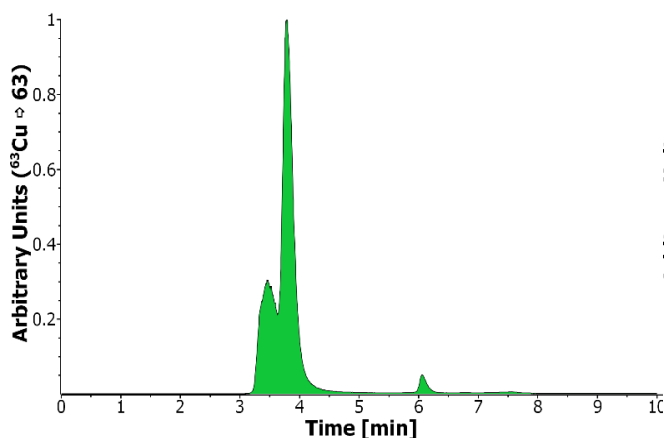


Figure 37: The copper trace of the separatory experiment with human blood serum on the AcqUHPLC_125Å/150mm analytical column.

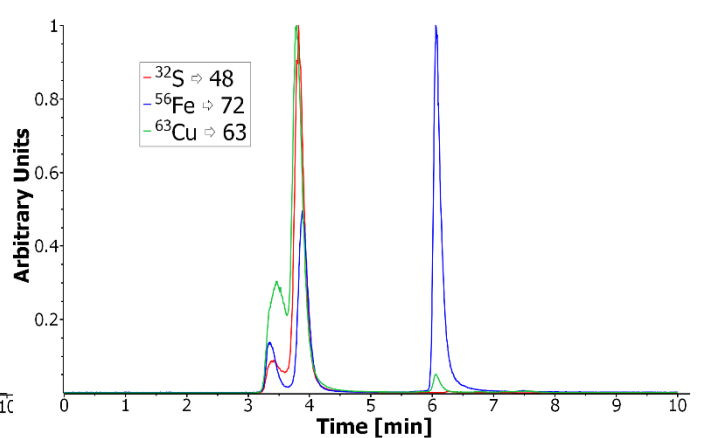


Figure 38: The combined trace of the separatory experiment with human blood serum on the AcqUHPLC_125Å/150mm analytical column.

The interpretation of signal peaks analyzed with the **MABPac_450Å/300mm** column appears a little difficult at first glance. In the combined sulfur, iron and copper traces (see figure 42) it is visible, that sulfur signal only overlaps with one copper signal at around 11.5min. This signal is most probably attributable to albumin. Half a minute earlier at around 11min a large copper peak is accompanied with a high background of sulfur signal. This is most likely a signal from Ceruloplasmin as this large protein is expected to elute before Albumin. Interestingly, a very large signal in the iron trace occurs at around 12.1min without a corresponding signal in the sulfur trace (only a slight overlap can be seen). The overall performance of this column is not satisfactory. This is not surprising as this analytical column is intended for separations of proteins with a molecular weight in the range of 10 – 1 000kDa. The testing of this column was solely based on the assumption, that an extended physical length would make up for its ineligibility for our purpose. This was clearly not the case.

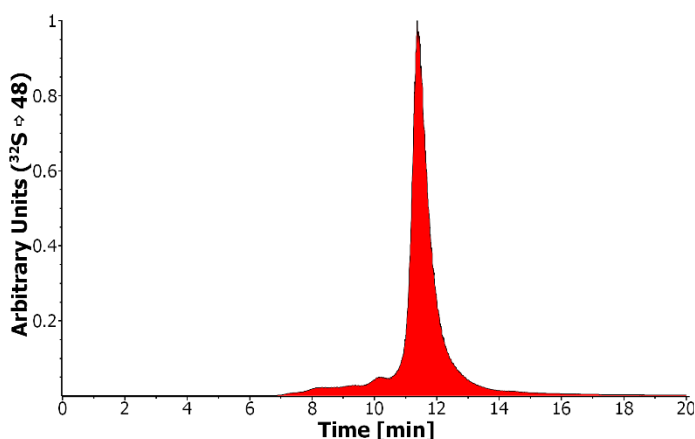


Figure 39: The sulfur trace of the separatory experiment with human blood serum on the MABPac_450Å/300mm analytical column.

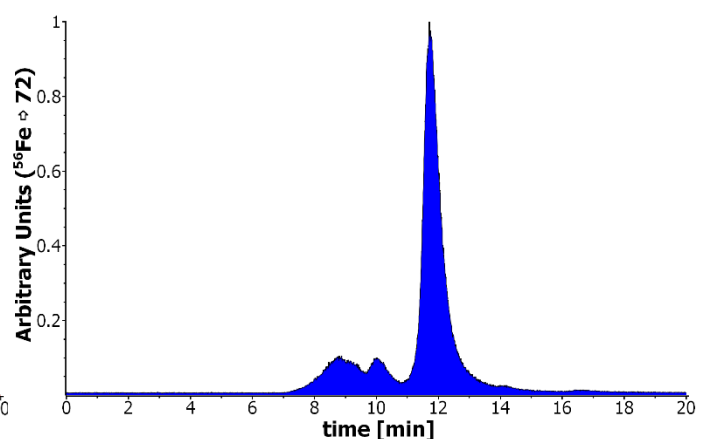


Figure 40: The iron trace of the separatory experiment with human blood serum on the MABPac_450Å/300mm analytical column.

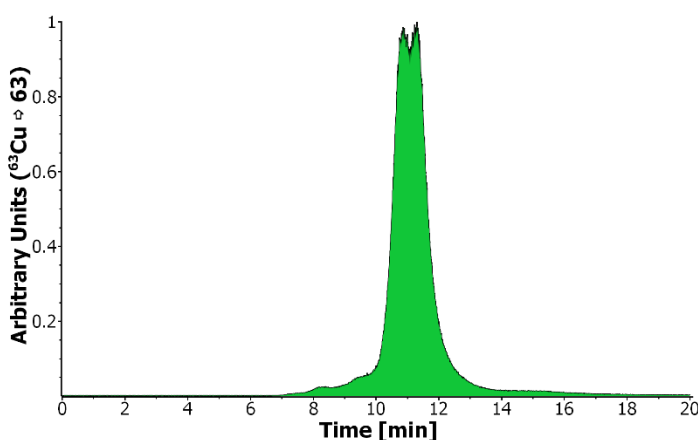


Figure 41: The copper trace of the separatory experiment with human blood serum on the MABPac_450Å/300mm analytical column.

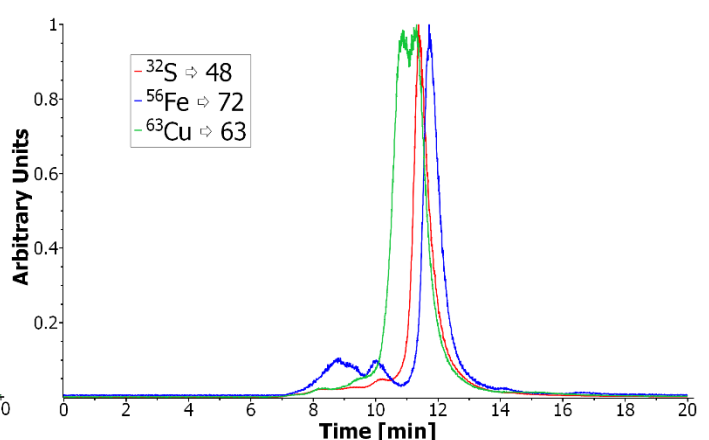


Figure 42: The combined trace of the separatory experiment with human blood serum on the MABPac_450Å/300mm analytical column.

The **AcqUHPLC_200Å/300mm** analytical column in our experimental series turned out to be the most satisfactory choice from the available columns. According to the manufacturer, this column is intended for protein separations which are in the molecular weight range of 10 – 500kDa. This analytical column was able to resolve Albumin and Ceruloplasmin, which can be seen in the copper trace as two signal peaks at around 7min (Ceruloplasmin) and 7.8min (Albumin) – see figure 45. Unfortunately, other heavier copper protein species are still not resolved, which might be of significant interest such as just recently explored and scientifically described α_2 -Macroglobulin (in some publications mentioned as Transcuprein). α_2 -Macroglobulin is a copper harboring protein which was historically overlooked due to difficulties in accurately measuring sparsely abundant copper proteins in human samples, but also due to difficulties in separatory procedures.

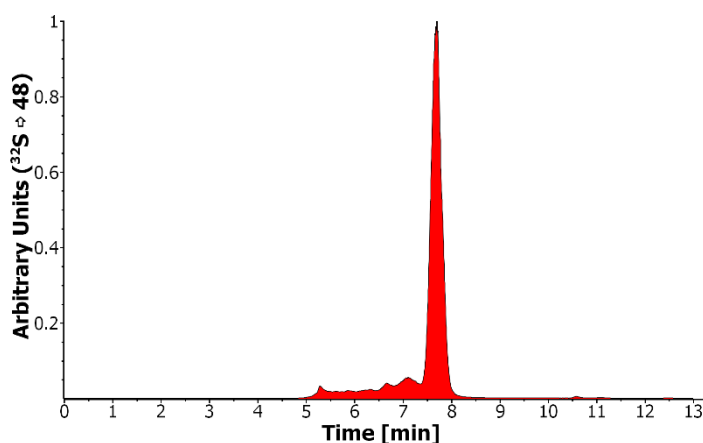


Figure 43: The sulfur trace of the separatory experiment with human blood serum on the AcqUHPLC_200Å/300mm analytical column.

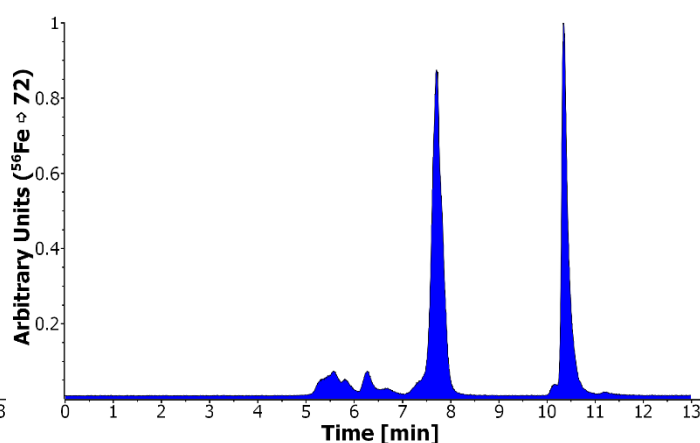


Figure 44: The iron trace of the separatory experiment with human blood serum on the AcqUHPLC_200Å/300mm analytical column.

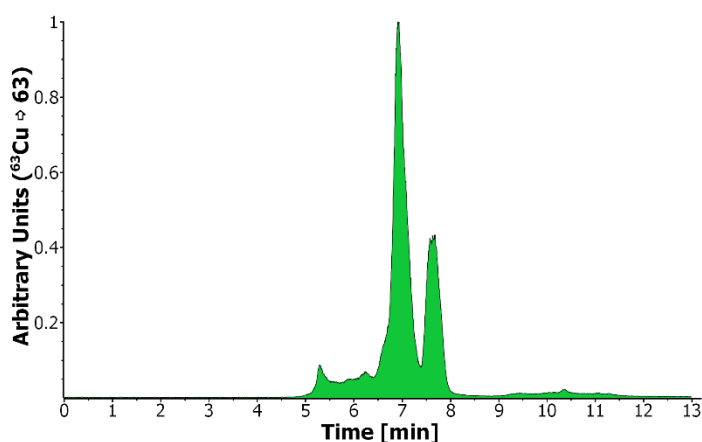


Figure 45: The copper trace of the separatory experiment with human blood serum on the AcqUHPLC_200Å/300mm analytical column.

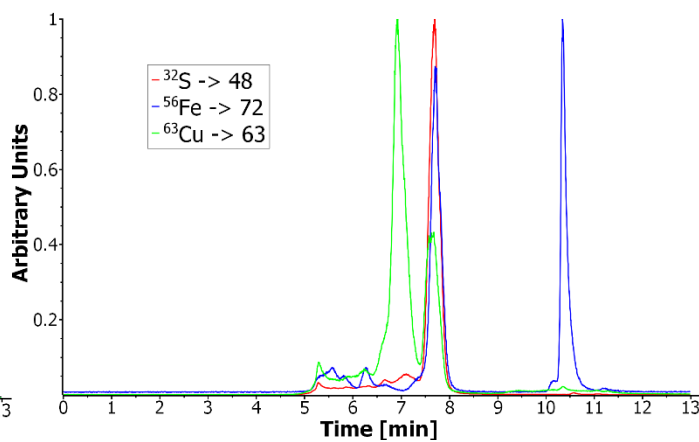


Figure 46: The combined trace of the separatory experiment with human blood serum on the AcqUHPLC_200Å/300mm analytical column.

The **AcqUHPLC_200Å/150mm** column was tested, as this column has the same porous material as AcqUHPLC_200Å/300mm it promised an easier handling and shorter method times. Unfortunately, this analytical column was already some time in use and showed therefore very high background signals of iron and copper even after extensive washings with 50mM Ammonium acetate solution, pure water, 20:80 MetOH:Water solution and Acetonitrile. The Iron background noise was in fact high as to severely interfere with all measurements (see figure 48 and 50). The copper background of the column did not show qualitatively any significance in regard to separatory performance; however, it was still around an order of magnitude higher than other analytical columns tested here – see figure 49. The general identification of the showed peaks follows the same logic as it was the case from other analytical columns tested – In the sulfur trace a single prominent signal at around 4min can be seen corresponding to albumin. Other sulfur signals can be seen in the range from 2.5min to 3.5min which have their counterparts in the copper and possibly iron traces. The overall qualitative separatory performance in comparison to AcqUHPLC_200Å/300mm column is, however, not as good and the relatively high background noise prevents this column from our further consideration.

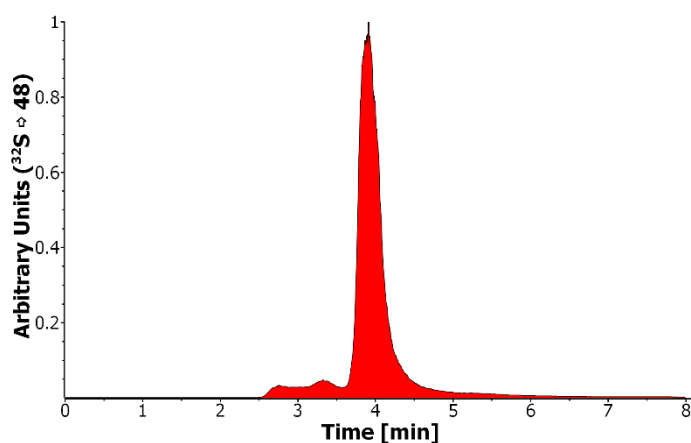


Figure 47: The sulfur trace of the separatory experiment with human blood serum on the AcqUHPLC_200Å/150mm analytical column.

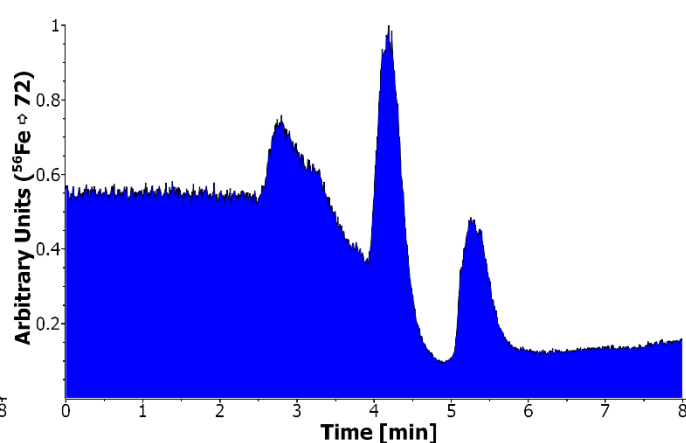


Figure 48: The iron trace of the separatory experiment with human blood serum on the AcqUHPLC_200Å/150mm analytical column.

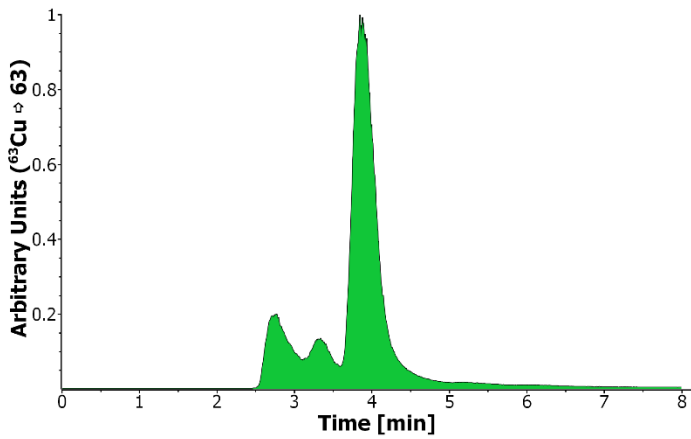


Figure 49: The copper trace of the separatory experiment with human blood serum on the AcqUHPLC_200Å/150mm analytical column.

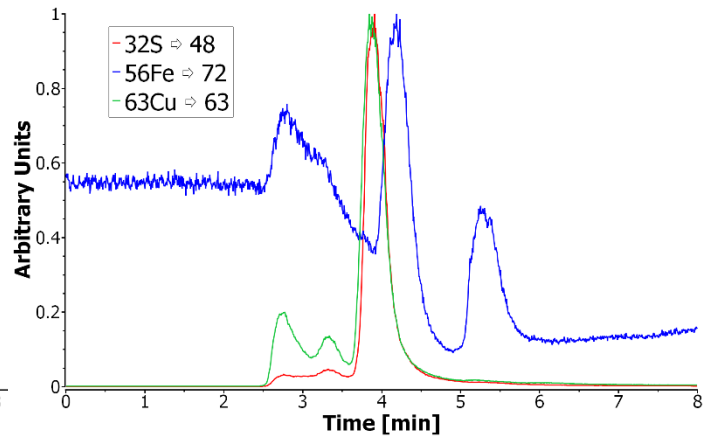


Figure 50: The combined trace of the separatory experiment with human blood serum on the AcqUHPLC_200Å/150mm analytical column.

To round off the comparison of all the tested analytical columns a graphic illustration was created to assess the background signals of blank measurement (figures 51 and 52 below). As can be seen the MAbPac_450Å/300mm column showed the lowest background in the copper trace as well as in the iron trace. This particular column is entirely made from an inert material PEEK (Polyether-ether-ketone) and does not exhibit any metal leaching, even with acidic effluents like 3% nitric acid. The columns AcqUHPLC_200Å/300mm and AcqUHPLC_125Å/150mm both exhibit comparable blank background noise levels – in the copper and the iron trace around maximal 1000 CPS. The worst performance was exhibited by the analytical column AcqUHPLC_200Å/150mm – its copper background noise was around an order of magnitude higher than other tested columns and at least four(!) orders of magnitude higher regarding the iron blank noise. This is most likely due to its long previous use.

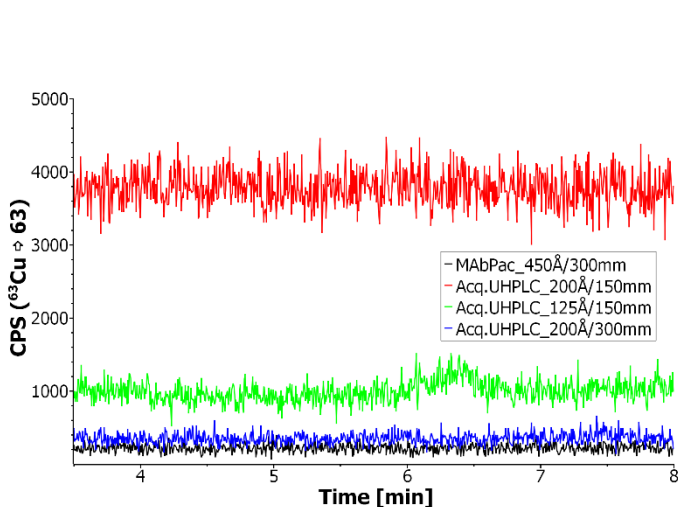


Figure 51: Comparison of the background signal of copper for all tested analytical columns

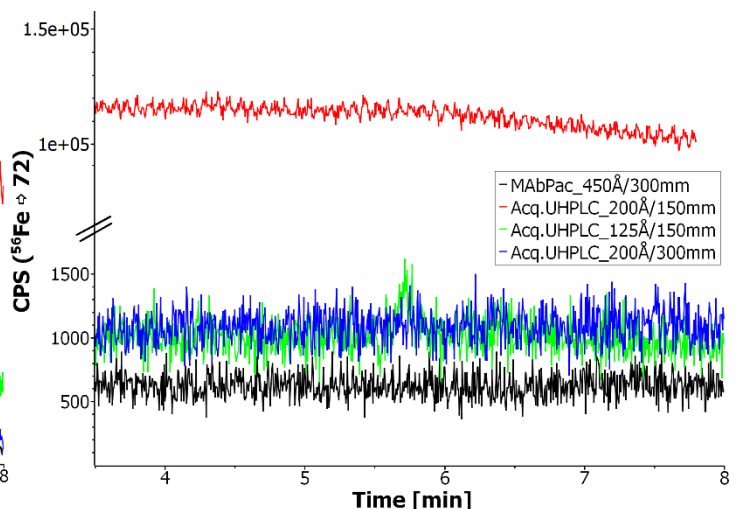


Figure 52: Comparison of the background signal of iron for all tested analytical columns

After identifying the best suitable analytical column, a sample mixture (provided by Dr. Christian Kowol) of major human proteins Albumin and Myoglobin along GSSG and Methionine was analyzed. This sample was introduced to the HPLC equipped with the most powerful **AcqUHPLC_200Å/300mm** analytical column to additionally demonstrate its capabilities on a simple mixture. As can be seen in Figures 53 – 56 all components were separated as good as to the baseline. The identification of peaks is straight forward in this case- There are 4 analytes and the separation occurs according to the molecular size. Hence, Albumin dimer elutes first following by Albumin, Myoglobin, GSSG and Methionine (being the smallest molecule)

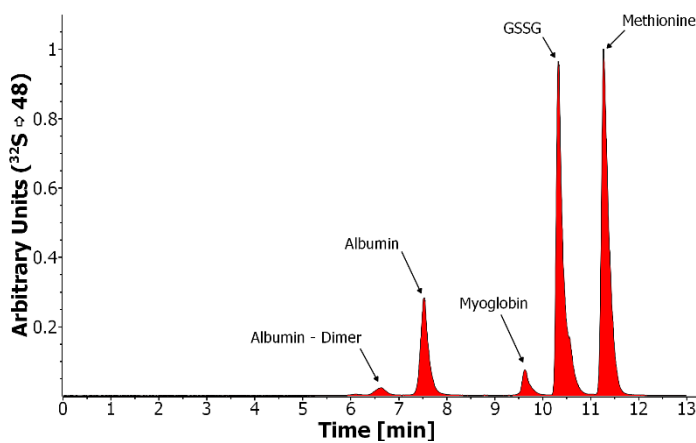


Figure 53: Additional experiment sulfur trace: separatory performance of the selected AcqUHPLC_200Å/300mm on a mix of protein standards

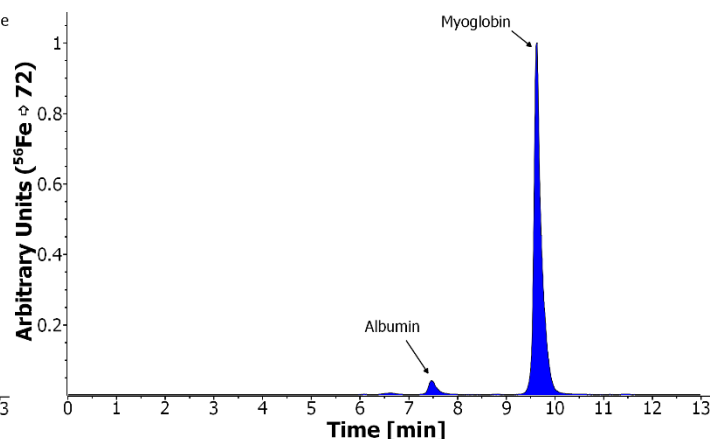


Figure 54: Additional experiment iron trace: separatory performance of the selected AcqUHPLC_200Å/300mm on a mix of protein standards

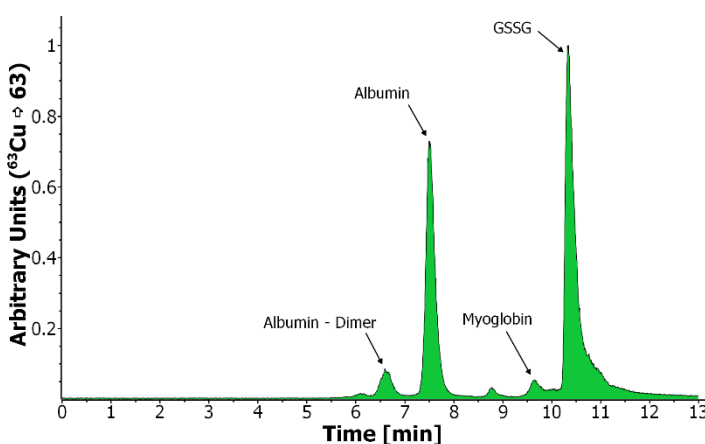


Figure 55: Additional experiment copper trace: separatory performance of the selected AcqUHPLC_200Å/300mm on a mix of protein standards

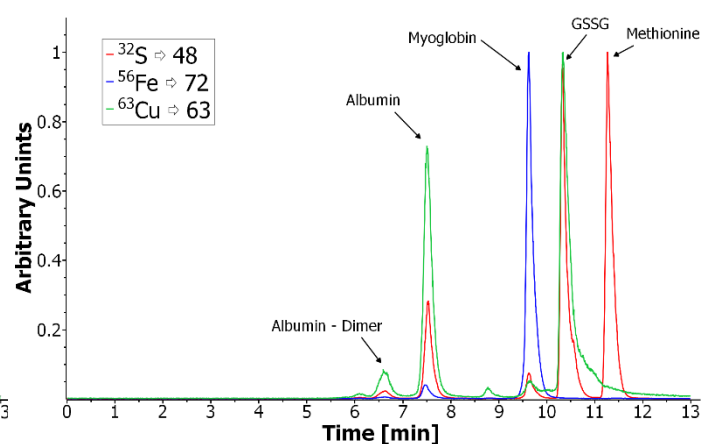


Figure 56: Additional experiment combined traces: separatory performance of the selected AcqUHPLC_200Å/300mm on a mix of protein standards

3.4 Analysis of human blood protein standards

In order to identify proteins in the human blood plasma definitely, ten protein standards were tested before the incubation studies were commenced. The protein standards were:

- | | |
|---------------------------------------|---|
| 1) Albumin 100 μ M | 6) α 1-Acid glycoprotein 100 μ M |
| 2) Fibrinogen 100 μ M | 7) IgG 100 μ M |
| 3) Transferrin 100 μ M | 8) IgA 10 μ M |
| 4) α 1-Antitrypsin 100 μ M | 9) IgM 1,1 μ M |
| 5) Ceruloplasmin 40 μ M | 10) Haptoglobin 30 μ M |

All standards were tested using SEC – HPLC (as described in section 3.3.2 Liquid Chromatography system on page 32). The HPLC was directly interfaced with **Agilent 8800 mass spectrometer** (the parameters were set as described in section 2.3.1.2 Agilent 8800 mass spectrometer on page 30).¹¹ As all proteins contain sulfur to some extent (Aminoacids Cysteine and Methionine) it is feasible to follow their elution on the sulfur trace of the chromatogram. From the results (see figure 57 below – normalized sulfur trace chromatograms, arbitrary CPS) we can observe that Albumin (the major serum protein) coelutes at least with 3 other proteins, namely Transferrin, α 1-Acid-Glycoprotein and α 1-Antitrypsin.

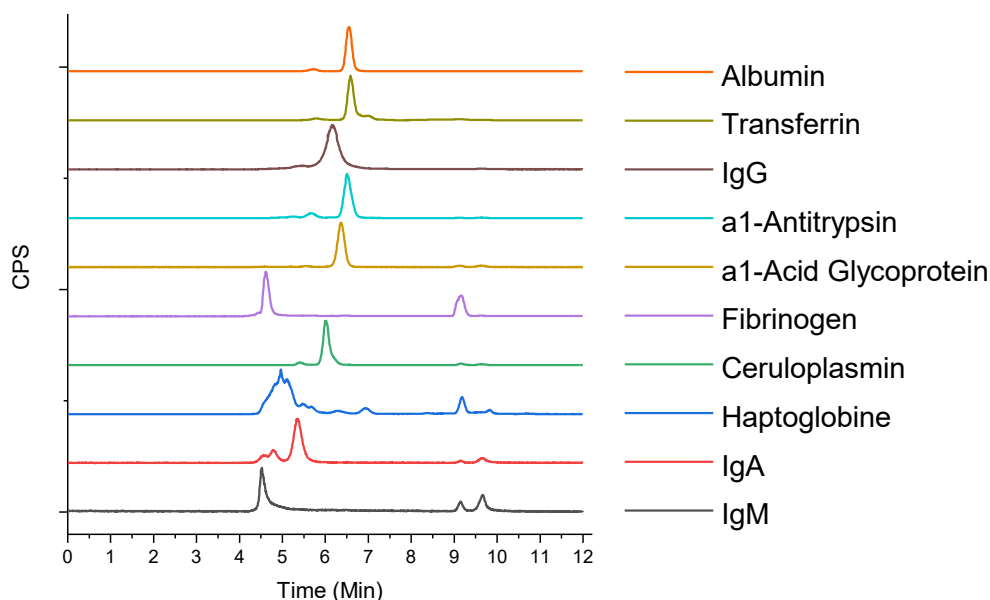


Figure 57: Stacked chromatograms (Sulfur traces) of 10 of the investigated protein standards

¹¹ For the analysis of protein standards, a new guard column was installed to the analytical column because injections with thiosemicarbazones proved to alter the elution behavior of all human blood serum components. For this reason, there is a retention shift of about 1 minute for all analytes in the incubation studies.

Comparing the elution patterns of the 10 protein standards and the chromatogram of human blood serum in the range of 4min to 7min it becomes apparent that many signals overlap (see figure 58 below). It is also apparent that albumin has a very broad signal, owing to its abundance. Albumin is a protein with a mass of 66 kDa[74] and elutes in this case from 6.2min to almost 7min.

The second largest signal corresponds to Ceruloplasmin (~150 kDa)[73] together with IgG (~160kDa)[76]. IgA with its mass of ~170kDa[76] elutes at around 5.5min. The last prominent feature of the human blood serum chromatogram (sulfur trace) is a peak at 4.5min that corresponds to pentameric IgM (up to around 900 kDa)[77] and Fibrinogen (~340 kDa)[76]. As can be seen there is a correlation between elution time and mass of a protein, but it is not a strict linear correlation. The main parameter determining the elution time in size exclusion chromatography is the hydrodynamic size or radius of a protein (as mentioned in the introductory section 1.3 Size exclusion High-performance liquid chromatography starting page 18).

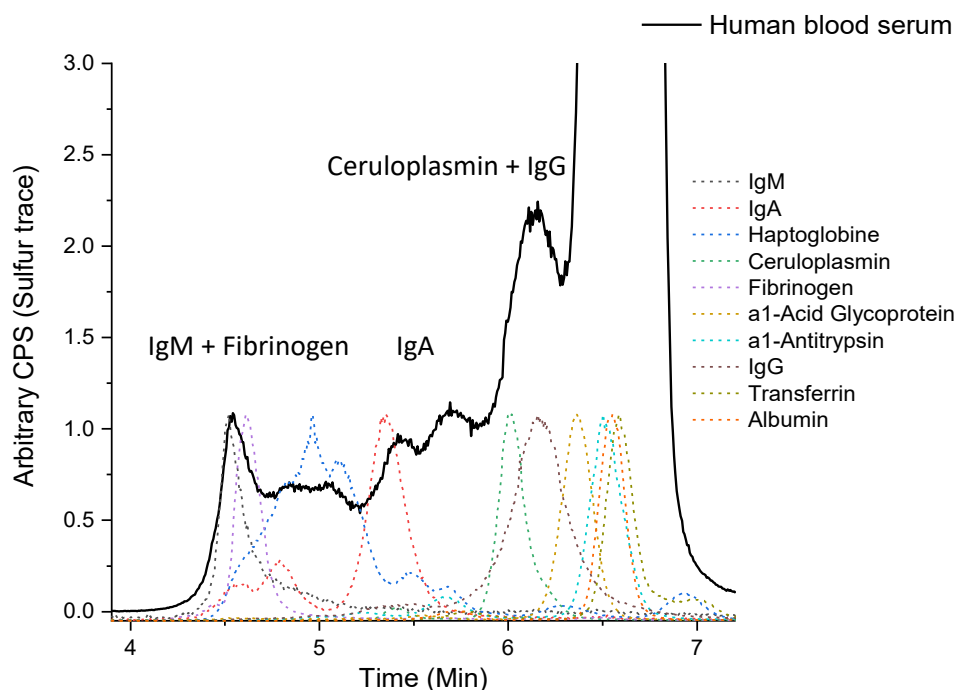


Figure 58: An overlay plot of the human blood serum chromatogram (sulfur trace) with 10 of the investigated protein standards. As can be seen there are unfortunately areas with significant overlaps

In this experiment three other traces were recorded mass-spectrometrically, namely Iron, copper and zinc. Those traces provide additional (in this case redundant) analytical information and will be presented with a short comment in the next few lines.

Figure 59 below shows the normalized copper traces of all standard's chromatograms. Although each of the 10 Standards seem to have at least some copper associated with it, only albumin and ceruloplasmin are human blood plasma proteins that significantly contribute to the overall copper content in human blood plasma.

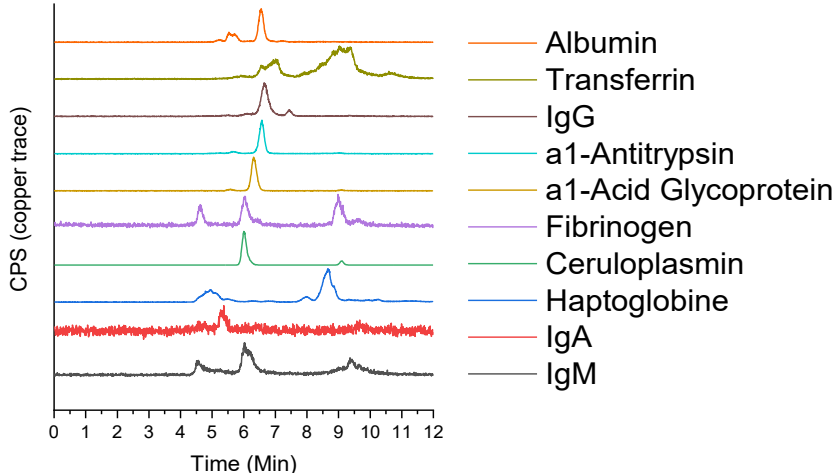


Figure 59: Stacked chromatograms (copper traces) of 10 of the investigated protein standards

This fact can be seen in the overlay chromatogram of the two aforementioned proteins with human blood plasma chromatogram (copper trace normalized, Arbitrary CPS). In the high molecular region (between 4.5min to 5min), only few small peaks in the human blood plasma chromatogram cannot be explained by the signal of either albumin or ceruloplasmin.

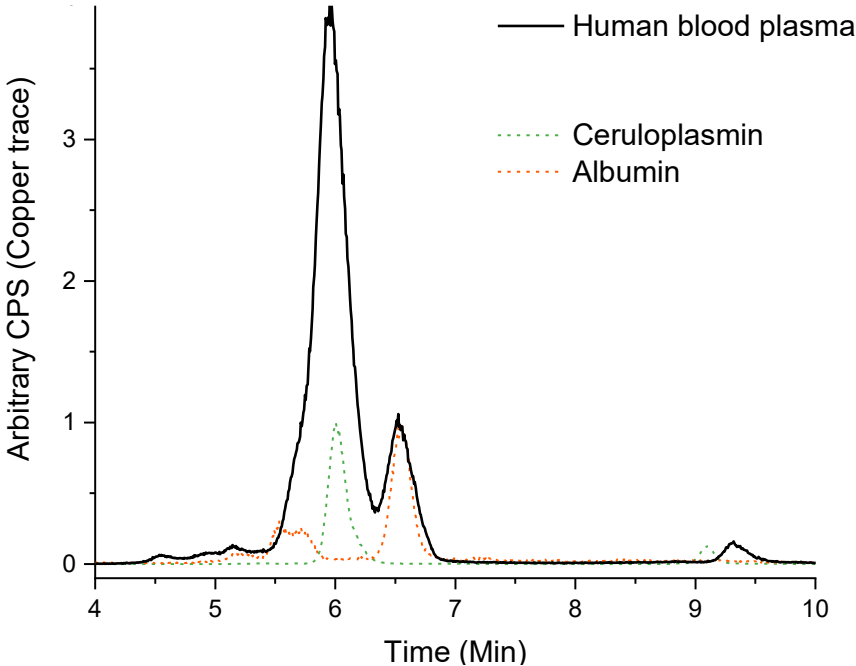


Figure 60: An overlay plot of the human blood serum chromatogram (copper trace) with 10 of the investigated protein standards. Only 2 of the proteins are significant in the copper trace. Therefore, all the others will be omitted here.

Next, we look into the iron traces of the protein standards. As can be seen from the normalized chromatograms in figure 61 below, the signals of most standards are near the noise level of the measurement. The most significant proteins are Albumin (for its general metal binding capability), Transferrin (as for its iron transport function) and Fibrinogen. The Ceruloplasmin standard may contain some traces of low molecular iron species – that can be seen eluting between 9min and 11min. The reason for this occurrence is due to the fact that ceruloplasmin plays a crucial role in mediating the iron transfer between stable iron pools in human blood and receiving cells.[75] The protein by itself, however, does not contain iron atoms for functionality, thus no signal can be seen at around 6 minutes.

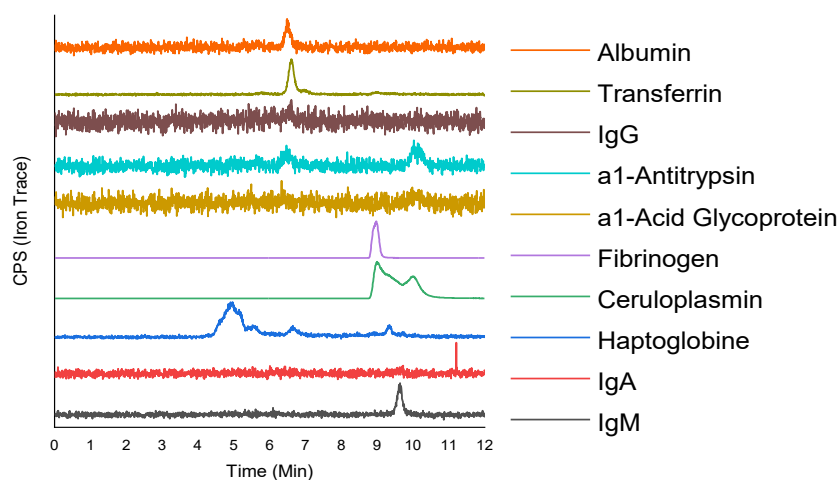


Figure 61: Stacked chromatograms (Iron traces) of 10 of the investigated protein standards

The last significant contributor is Haptoglobin, which elutes as a broader peak at around 5min. Haptoglobin is a transport protein commonly found in human blood serum. It functions as inflammation mediator with an iron modulating and transporting function.[78] As can be seen in its iron trace chromatogram haptoglobin forms some aggregates with nonuniform mass – the most abundant signal appears at around 5min, and a lesser abundant aggregates at around 6.8min and 9.4min. The overlaid chromatograms of protein standards and human blood plasma can be found in Figure 62 on the next page for better understanding.

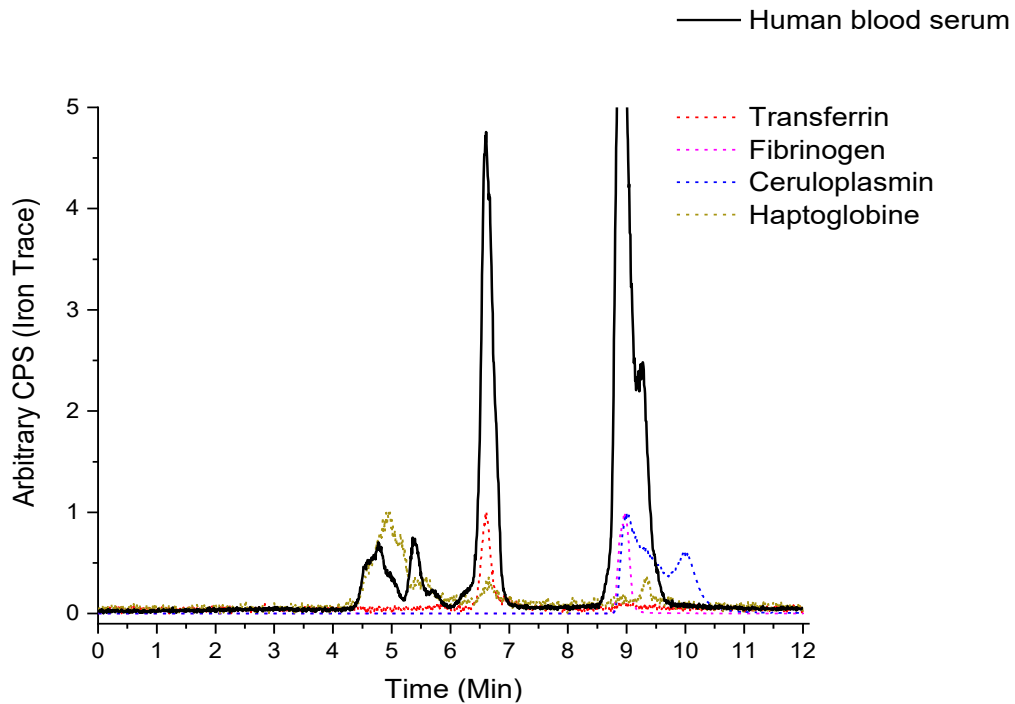


Figure 62: An overlay plot of the human blood serum chromatogram (Iron trace) with 10 of the investigated protein standards. Only 4 of the proteins are significant in the Iron trace. Therefore, all the others will be omitted from this plot

Finally, Zinc traces can be discussed. Zinc is here the least significant element in my considerations and as can be seen in figures 63 and 64, most standards do not show any zinc in their traces, or the signals are extremely near the noise level of measurements.

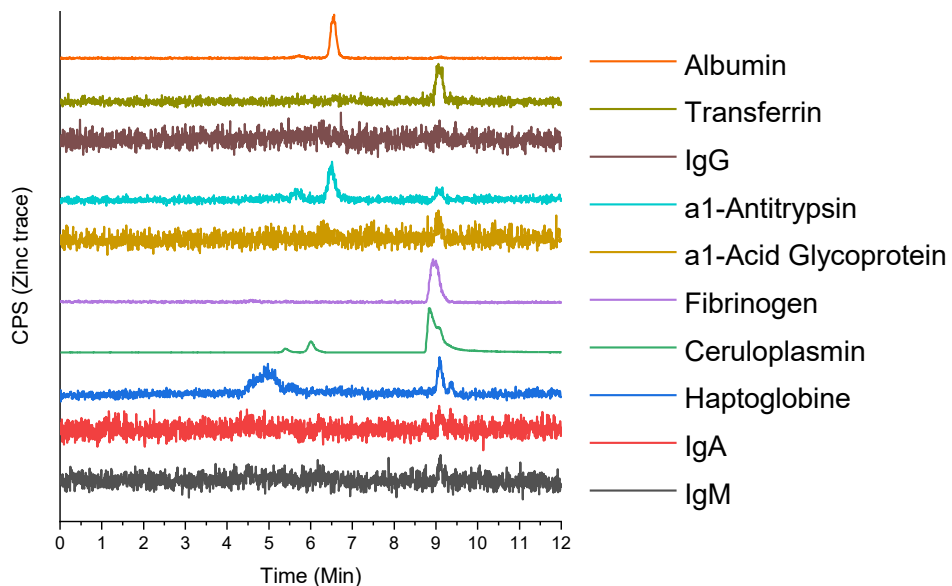


Figure 63: Stacked chromatograms (Zinc traces) of 10 of the investigated protein standards

From the overlay chromatograms of standards with human blood plasma it is apparent that few proteins are of some minor significance. Those are namely, Albumin, α 1-Antitrypsin, Ceruloplasmin and haptoglobin.

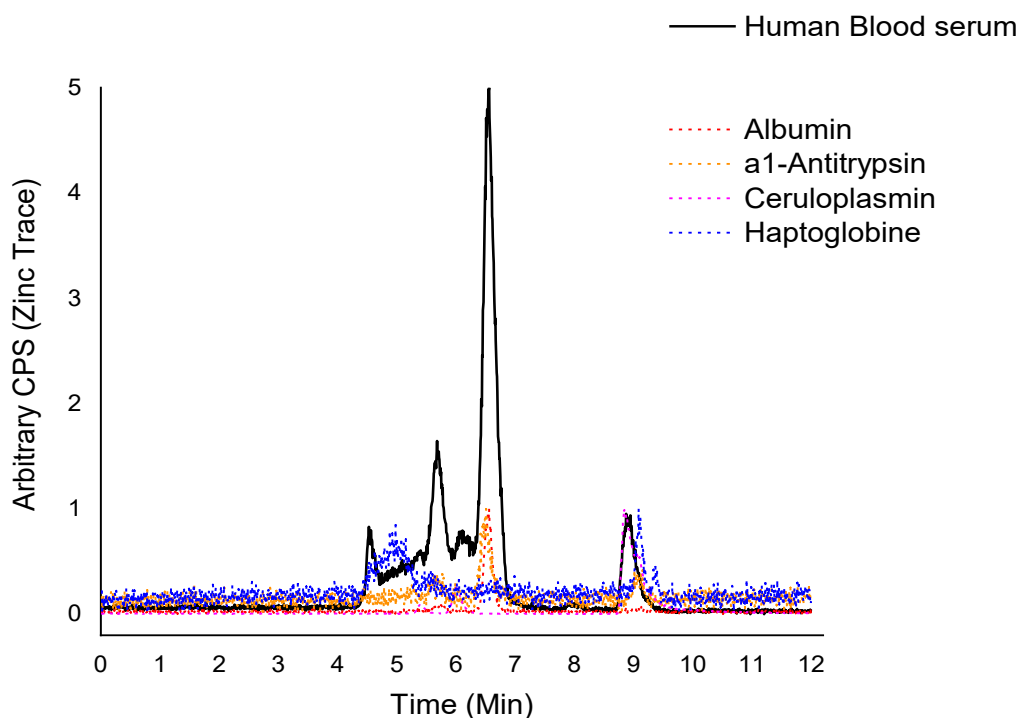


Figure 64: An overlay plot of the human blood serum chromatogram (Zinc trace) with 4 significant protein standards, namely Albumin, Ceruloplasmin, Hatoglobine and a1-Antitrypsin. The signal to noise ration of the peaks in the zinc trace is rather low.

However, the signal to noise ratio of the zinc trace of human blood plasma is very low by itself, so no deep discussion is necessary for further intended measurements – incubation studies (description in section 3.6 Main experiments starting on page 65)

3.5 Multilinear regression – protein standards

As far as the most major components of human blood serum are tested in this experiment series in their pure form, it should be possible to combine all chromatograms in such a way that a chromatogram of human blood serum can be reconstructed. For this purpose, the method of multilinear regression (MLR) was chosen. MLR is usually used for multidimensional datasets, such as spectrometric data of many analytes and mixtures of analytes. In this case MLR is applied to chromatographic traces (S, Fe, Cu, Zn) which are in theory also a type of multidimensional fingerprint. Therefore, a simple model was assumed, where T is a target matrix (the chromatogram of human blood serum); S is the chromatogram-matrix (spectra-matrix) of the 10 protein standards; C is the unknown concentration-matrix and E is an error-matrix

$$T = S \times C + E$$

In order to calculate the unknown concentration-matrix, we ignore the Error-matrix E for the moment and convert the spectra-matrix into a quadratic Matrix by multiplying both sides with transposed spectra-matrix S^T

$$T \times S^T = (S \times S^T) \times C$$

Next, the quadratic Spectra-matrix can be divided on both sides by itself.

$$T \times S^T \times (S \times S^T)^{-1} = C$$

Doing this matrix operations, concentration coefficients can be calculated that describe a linear contribution of every protein standard to the target chromatogram – in this case Human blood serum. The results do not look very promising at first glance (See figure 65 below).

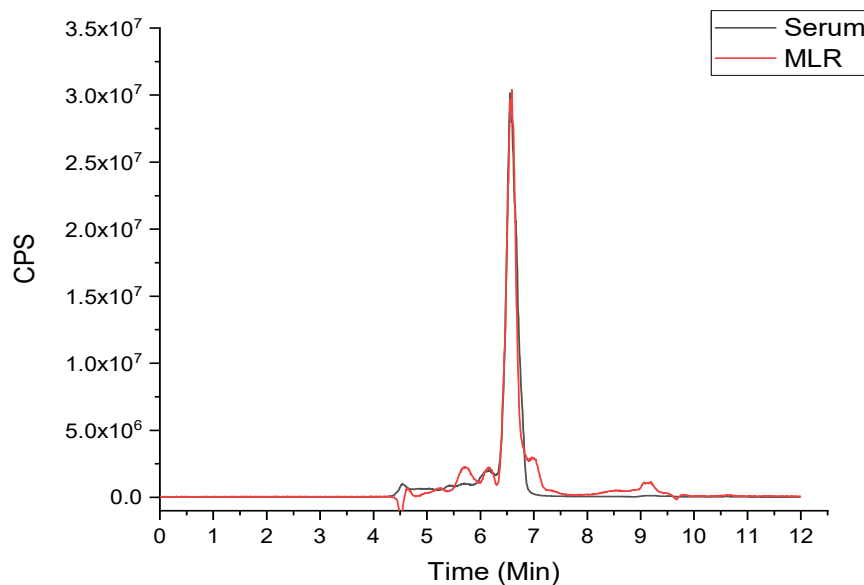


Figure 65: Sulfur trace of human blood serum (black line) and calculated sulfur trace from pure analyzed proteins by means of multilinear regression (red line). This initial calculation shows large errors, and even negative contributions from some protein standards.

There are obviously many spots where the MLR method cannot find any linear combination of chromatograms such as the human blood serum chromatogram can be constructed. There are even negative contributions from some chromatograms, which does not make sense. However, upon further investigation a major interference could be made out. This interference was concretely Transferrin with its many signals corresponding to some unusual conglomerates and adducts, that resulted in strange elution behavior. After removing Transferrin chromatogram, much better MLR results were obtained (See figure 66 on the next page).

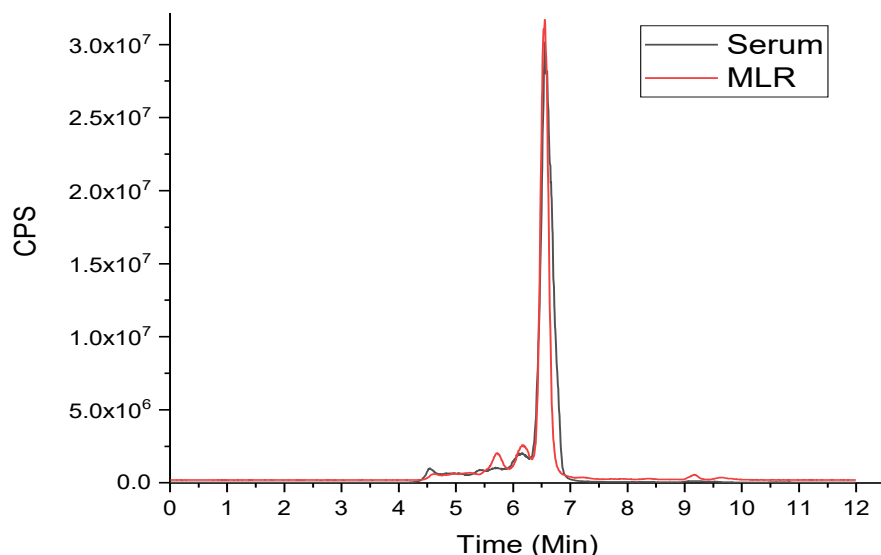


Figure 66: Sulfur trace of human blood serum (black line) and calculated sulfur trace from pure analyzed proteins by means of multilinear regression (red line). This second calculation performed statistically better than the initial calculation

To assess the error in the multilinear regression performed with 9 serum protein standards and human blood serum, the error matrix E is calculated as:

$$T - (S \times C) = E$$

As for the low error the error matrix was further converted to depict the relative error in order to show where is the most severe deviation from human blood serum. As can be seen the largest deviation occurs at the elution time of Albumin. This is due to a broader Albumin signal in human blood serum but also due to absence of transferrin from the calculation which elutes during the descending stage of albumin elution (partly coelution). Therefore, it is impossible to cover the human blood serum signal at 6.5 – 7 min correctly via MLR. The relative error (see figure 67 below) of other regions of the sulfur chromatogram are rather low, which is fortunate, as this may allow for correct assignment of concentrations of the proteins tested.

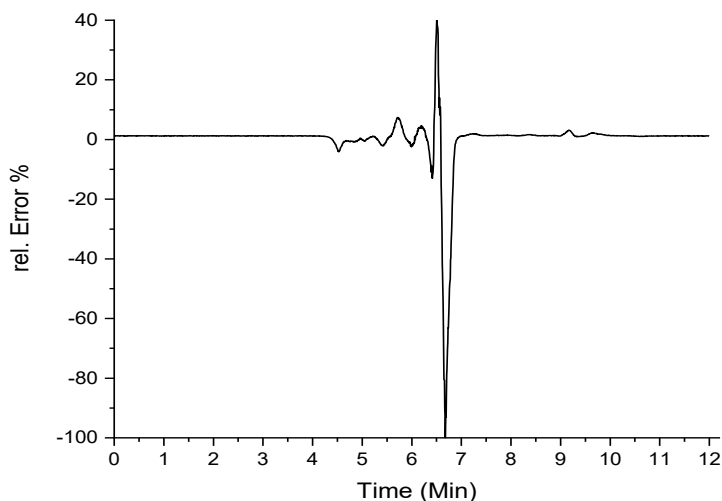


Figure 67: The error plot constructed from the error matrix. This plot depicts, where is the highest relative error in the calculation (Multilinear regression)

The calculated concentration-matrix can now be used to estimate the concentrations of the analyzed proteins in the human serum. To do this, the Concentrations in the concentration matrix have to be multiplied with the concentrations that were used to perform the chromatographic analyses. A summary on the results can be found in Table 11 below. As there is no means to quantitatively and precisely determine the concentration of each protein in the human blood serum at this point, only reference values from other sources can be presented.

Table 11: An overview table on the theoretical and calculated (MLR) protein concentrations in human blood plasma.

Protein	Molar Mass (Da)	Concentration in Analysis (µM)	Concentration in Analysis (mg/L)	Concentration-Matrix (Factors)	Calculated Concentration (mg/L)	Reference concentration (mg/L)
IgM	970 000 ^[77]	1.1	1 067	0.3535	377	n.A
IgA	170 000 ^[76]	10	1 700	0.1394	237	700 – 4 000 ^[80]
Haptoglobin	n.A	30	n.A	0.3150	n.A	n.A
Ceruloplasmin	150 000 ^[73]	40	6 000	-0.1224	n.A	200 – 600 ^[81]
Fibrinogen	340 000 ^[76]	100	34 000	0.0802	2 727	1 600 – 4 000 ^[82]
α1-acid glycoprotein	43 000	100	4 300	0.0897	386	n.A
α1-Antitrypsin	52 000	100	5 200	0.5451	2 834	1 000 – 3 000 ^[83]
IgG	160 000 ^[76]	100	16 000	1.3221	21 154	7 000 – 16 000 ^[80]
Albumin	66 440 ^[74]	100	6 644	5.1740	34 376	35 000 – 52 000 ^[84]
Transferrin	79 600	100	7 960	Removed prior to calculation	n.A	2 000 – 3 600 ^[85]

Comparison of the reference values to the calculated values reveals that at least some major proteins like Albumin, Fibrinogen, IgG, IgA and α1-Antitrypsin can be calculated to a precision level of the correct concentration range. The only proteins for which no value could be calculated were Transferrin (due to reasons discussed earlier) and ceruloplasmin probably due its low concentration and low sulfur content. To conclude, MLR is of course not the most optimal approach to this particular problem as there is much greater variance in a type of data like chromatograms than e.g. in spectral data (spectrometry is the main field of use of MLR). There are many more problems like complex aggregate and oligomer forming of proteins in human blood plasma which cannot be accounted for with simple protein standards. A large contribution of inaccuracy probably also stems from different microenvironments of proteins in native human blood plasma and single protein standards like those used in the experiment series. Nevertheless, the performance of the MLR method in this case - the calculation of unknown protein concentrations in human blood plasma is still impressive. An improvement might be achieved by analyzing more protein standards that are commonly found in the human blood plasma in great abundancies (such as Transthyretin, α1-Proteinase inhibitor...).

3.6 Main experiments – Incubation studies

3.6.1 Baseline measurements (Buffered human blood plasma)

The incubation experiment series were started by establishing baseline measurements. First, blank buffered human blood serum was analyzed in “incubation” conditions i.e. a sample of it without any agent was chromatographically separated using **AcqUHPLC_200Å/300mm** in the **Agilent 1260 HPLC system** (parameters are given in section 2.3.2 Liquid Chromatography system on page 32) coupled to **Agilent 8800 mass spectrometer** (parameters are given in section 2.3.1.2 Agilent 8800 mass spectrometer on page 30 and the overall description of incubation studies is given in section 2.5.5 Description of main experiments - incubation studies on page 36). These measurements shall show that no significant changes occur during a long-term incubation analysis, which is the most crucial requirement for subsequent measurements on Thiosemicarbazones and their copper complexes.

As can be seen in Figure 68 below the sulfur traces show some apparent variance, mainly in the large signal of albumin. Upon integrating the sulfur signals over a time of 4min to 8min there is, however, little to no relative change. The peak shape of some signals (mainly albumin) may not be fully reproducible, but its integration value is consistent (see table 12 on the next page) and, therefore, satisfactory for this purpose.

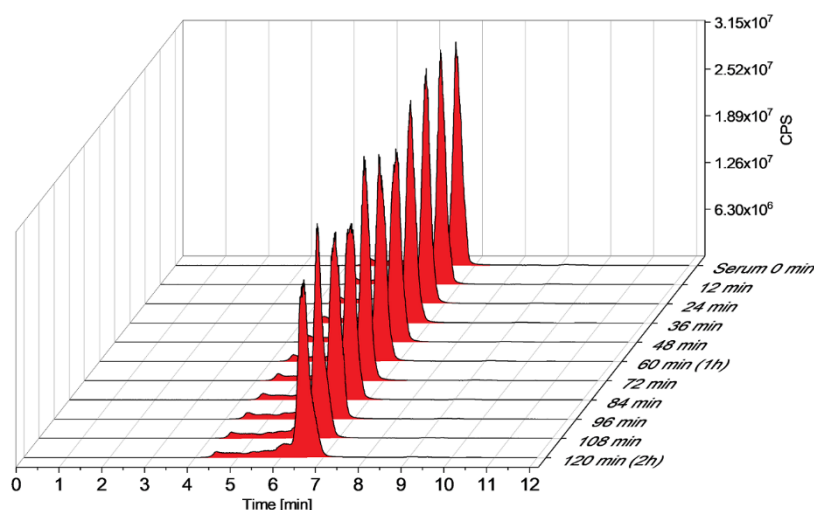


Figure 68: Sulfur trace of the blank incubation (no TSC agent) of human blood serum. Integrated values are highlighted blue

Additionally, the integrated areas were further normalized to allow for better comparison between all samples. The normalization was performed such as the first integrated value (Serum 0 min) is the base value and all other integration values were divided by that base value. This means that the first measurement result is always assigned the value 1 and all subsequent measurements represent a proportionate change. This method turns out to be an optimal comparison mainly in the subsequent incubation studies.

Table 12: The integration data from sulfur traces integrated over the elution time between 4min and 8min

Time	Area	Area (norm.)		
0 min (Base value)	54419629	1.000		
12 min	54695724	1.005		
24 min	55160174	1.014	<hr/>	<hr/>
36 min	55881850	1.027	Std. Deviation %	1.548 %
48 min	56379662	1.036	<hr/>	<hr/>
60 min	56252375	1.034	Variance %	2.395 %
72 min	56783212	1.043		
84 min	56596451	1.040		
96 min	56879190	1.045		
108 min	56055641	1.030		
120 min	56495864	1.038		

The iron trace of human blood serum measurement without any TSC agent over time shows rather large variance. This is especially apparent as not only peak heights/areas change but also peak shapes (See figure 69 below).

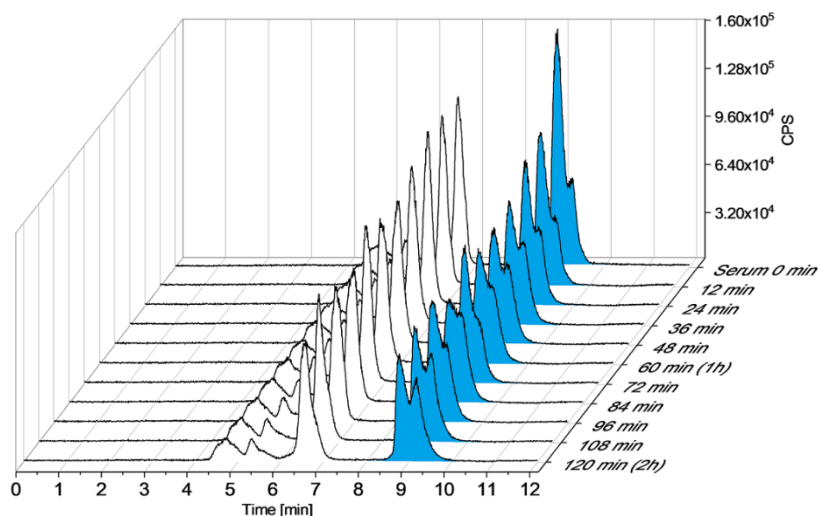


Figure 69: Iron trace of the blank incubation (no TSC agent) of human blood serum. Integrated values are highlighted blue

As for the integration a signal window between 8min and 11min was chosen as there were no changes in high molecular region either in blank buffered human blood serum nor in subsequent thiosemicarbazones incubation studies. As for the blank results of the iron trace, low molecular species integration shows a data variance of 97% (see table 13). However, this variance stems solely from a clear downwards trend of the signal. This behavior is very surprising as it was not seen in the blank incubation study of unbuffered human blood serum. Therefore, it can be hypothesized that the phosphate buffer might facilitate some reactions with the low molecular iron pool – however, the analytical setup does not allow for correlation with any other signal. This is very unfortunate, and it renders the method less versatile. A way to prevent such large variance in future experiments is to omit the buffering of the human blood serum.

Table 13: The integration data from iron traces integrated over the elution time between 8min and 11min

Time	Area	Area (norm.)		
0 min (Base value)	341377.0	1.000		
12 min	252607.0	0.740		
24 min	244498.2	0.716	Std. Deviation %	9.55 %
36 min	234999.0	0.688		
48 min	234703.9	0.688	Variance %	96.94 %
60 min	230997.8	0.677		
72 min	230332.8	0.675		
84 min	234954.5	0.688		
96 min	238116.8	0.698		
108 min	237297.3	0.695		
120 min	223650.3	0.655		

The Copper traces of human blood serum measurement without any TSC agent look consistent at first glance. Small changes in peak shape of albumin can be made out but overall, the chromatograms look very reproducible (see figure 70 below).

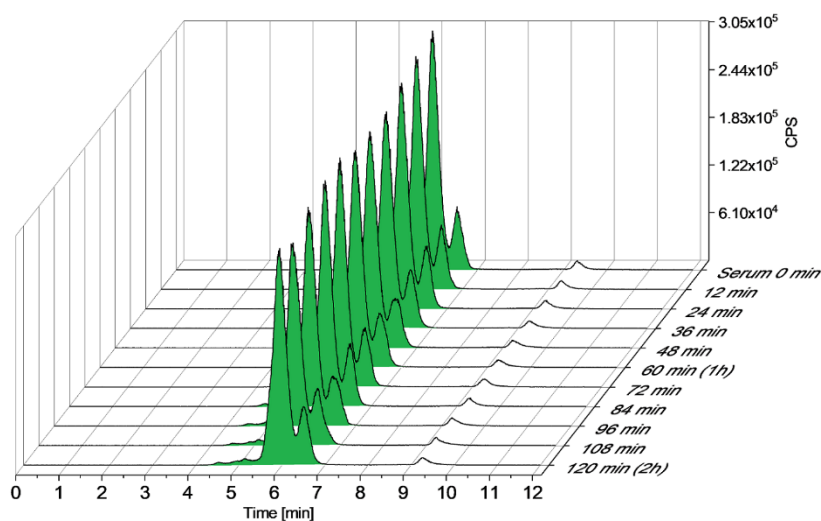


Figure 70: Copper trace of the blank incubation (no TSC agent) of human blood serum. Integrated values are highlighted green

This can be confirmed upon integration of the high molecular region from 4min to 8min. As there is no baseline separation of albumin and ceruloplasmin it is more convenient to integrate those two prominent signals together.

Table 14 below summarizes the integration data. The calculated variance of the integrated areas is <1%. However, the range of normalized values is about 0.02 = 2%. Therefore, even when the copper signal seems to be stable on average the results of TSCs incubations will have to be evaluated carefully on case-to-case basis.

Table 14: The integration data from copper traces integrated over the elution time between 4min and 8min

Time	Area	Area (norm.)		
0 min (Base value)	789241	1.000		
12 min	788180	0.999		
24 min	788109	0.999	Std. Deviation %	0.65 %
36 min	792196	1.004		
48 min	792410	1.004	Variance %	0.81 %
60 min	796388	1.009		
72 min	795545	1.008		
84 min	800697	1.015		
96 min	804839	1.020		
108 min	793210	1.005		
120 min	796813	1.010		

The zinc trace has unfortunately the highest variance among all analytes that were measured with our setup (see figure 71 below). As for very low signal to noise ratio it was decided to integrate the whole visible trace from 4min to 11min.

As can be seen from the integrated areas, there is a clear downwards trend of the signal intensity. Therefore, it will probably be impossible to account for this behavior and filter out any significant changes from the integration data.

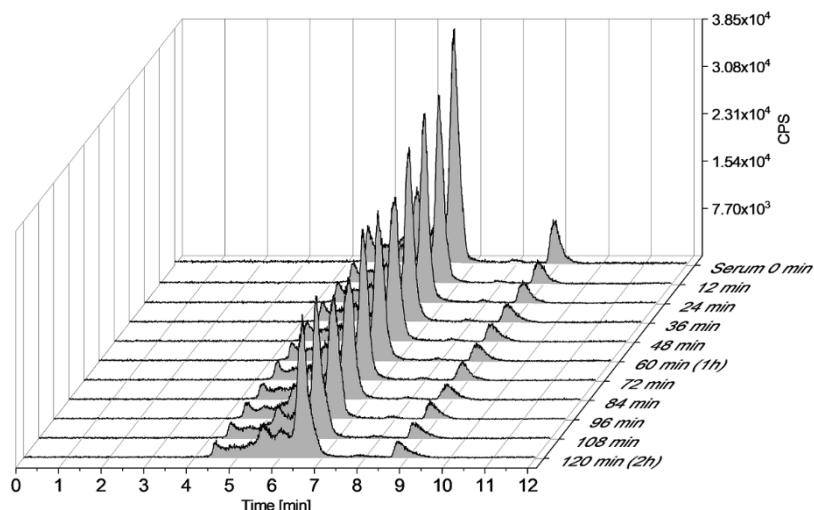


Figure 71: Zinc trace of the blank incubation (no TSC agent) of human blood serum. Integrated values are highlighted grey

Table 15 below summarizes the integration data. The calculated variance of the integrated areas is unfortunately over 130% making this trace mostly unusable.

Table 15: The integration data from zinc traces integrated over the elution time between 4min and 11min

Time	Area	Area (norm.)		
0 min (Base value)	123621.51	1.000		
12 min	82267.94	0.665		
24 min	87321.24	0.706	Std. Deviation %	11.46 %
36 min	83891.52	0.679		
48 min	83018.74	0.672	Variance %	131.45 %
60 min	78953.82	0.639		
72 min	73187.88	0.592		
84 min	74190.86	0.600		
96 min	76241.45	0.617		
108 min	73570.66	0.595		
120 min	79213.35	0.641		

To conclude the baseline measurements, the main focus shall be laid on the sulfur and copper trace for finding significant changes/reactions in the incubation studies with Thiosemi-carbazones and their copper complexes. For the iron and zinc trace an attempt for interpretation can be given but these have to be treated with high caution in order not to misinterpret their behavior.

3.6.2 Incubation experiments of Thiosemicarbazones with buffered human blood serum

The incubation experiments were performed as described in section 2.5.5 Description of main experiments - incubation studies on page 36 with 5 free TSCs and 5 respective Cu-TSCs. The settings of the two instruments, the **Agilent 8800 mass spectrometer** and **Agilent 1260 Bioinert HPLC** are described in sections 2.3.1.2 Agilent 8800 mass spectrometer (page 30) and Section 2.3.2 Liquid Chromatography system (page 32) respectively.

During the experiments, guard columns had to be swapped 2 times due to accelerated separatory performance deterioration caused by TSCs and Cu-TSCs. Due to these changes, there are some minor elution time shifts throughout the experiments which, however, do not impede the quality of the measurements in a significant manner.

As for the actual measurements, free thiosemicarbazones in the lowest concentration 1 μ M were analyzed first to limit the damage to the guard column. Then, the concentration was increased to 10 μ M and 100 μ M. The most damaging Cu-TSCs were analyzed last in a concentration of 10 μ M. In order to make all samples comparable a special normalization strategy (as described in previous section) was implemented on the respective chromatographic traces.

Triapine (3AP) is a prime prototype of a partly successful drug. Although failed in clinical trials II, it is of utmost interest in current research to modify this molecule such as fast metabolization and inactivation can be prohibited in patients. In my incubation study, free 3AP showed a prominent complexation reaction with Albumin bound copper. Concretely, looking into the copper trace of chromatograms the copper-albumin signal (elution between 7min and 8min) decreases over a time period of about 36min before reaching an equilibrium (see figure 73 on next page). This behavior is clearly visible in incubation studies with a concentration of the free agent of 10 μ M and 100 μ M. 1 μ M was found to be insufficient to cause significant changes.

The sulfur traces of free Triapine incubation study (see figure 72 on the next page) show no apparent changes aside from small variance in albumin signal, which over time remains stable on average. Also, the integration of sulfur signals from 5min to 9min remains the same. This finding only makes sense as TSCs in general do not cause any degradation or alteration of proteins.

The analysis of the iron and zinc traces is probably not feasible because it was shown that iron and zinc signals both diminish in given regions even without adding a TSC agent to buffered blood serum. For the sake of completeness, the results will always be presented in a short manner (See figures 74 and 75 below) as there might be some significance upon case to case-based inspection that should not be deliberately hidden away from the results.

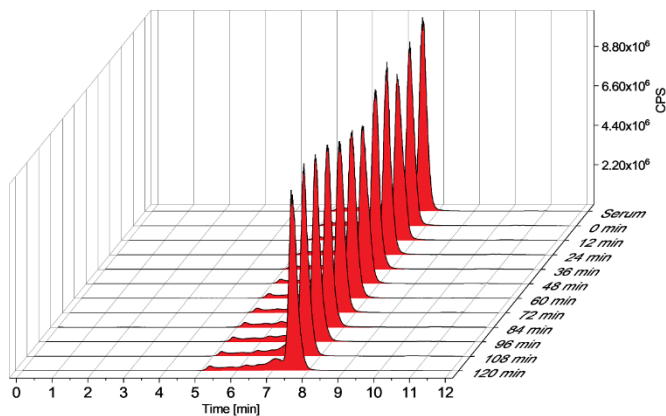


Figure 72: Chromatograms from 10 μ M Triapine incubation Study (sulfur traces)

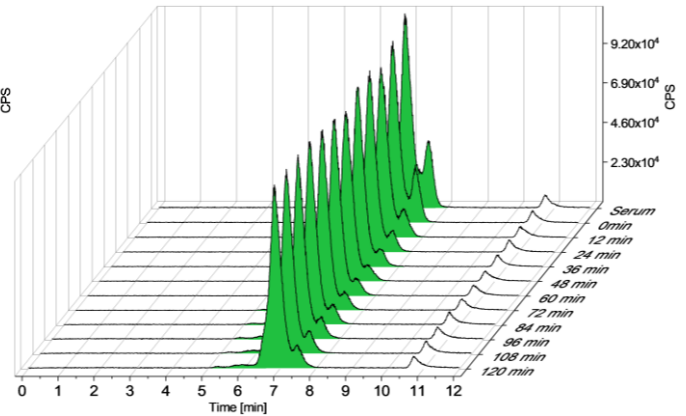


Figure 73: Chromatograms from 10 μ M Triapine incubation Study (copper traces)

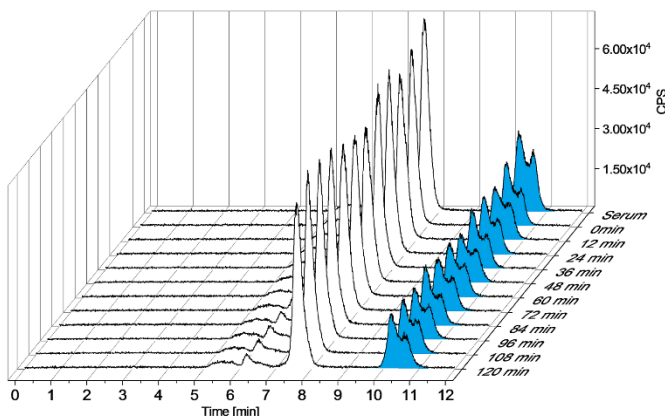


Figure 74: Chromatograms from 10 μ M Triapine incubation Study (iron traces)

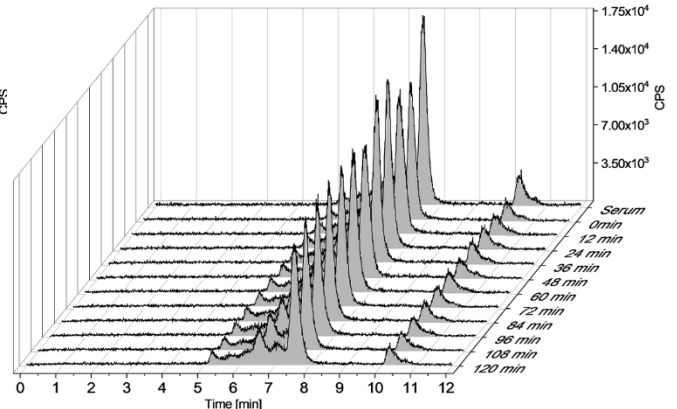


Figure 75: Chromatograms from 10 μ M Triapine incubation Study (zinc traces)

In order to simplify the complex graphs and extract all important informations an integration method was chosen that encompasses all the relevant changes. The sulfur trace was in all incubation studies indifferent and therefore, no further data treatment is necessary.

For copper trace, the changes took place in the region of albumin. However, albumin and ceruloplasmin overlap and in the course of the incubation studies the separatory performance of the HPLC setup was partly impeded by the Thiosemicarbazones themselves. Therefore, an integration and normalization of the whole signal from 5min to 8min was performed (as described in previous section on page 68 - see figure 76 below). A very distinct feature that sets most free thiosemicarbazones from their copper counterparts is that free TSCs cause the albumin copper signal to diminish over time while copper TSCs probably bind to albumin and increase its signal (see figure 76 below – black line). This finding is very interesting. Additionally, as can be seen in figure 76 all incubation studies on Triapine ended in a state of equilibrium i.e. the copper integrations of free Triapine reached an equilibrium after about 24min-36min regardless of the employed agent concentration. The Copper-Triapine reached an equilibrium (signal plateau) after about 72min-84min. This opposing behavior cannot be easily explained – It is however, to be expected that the two agents, Cu-TSC and free TSC share the same reaction mechanism which will be later further discussed in case of Dp44mT agent where it is more apparent.

Nevertheless, for the incubation study of Triapine (and more importantly for the duration of the study) it can only be said that the two agents free Triapine and Cu-Triapine react in opposition to each other on albumin. This means that free Triapine reduces the copper albumin signal and Cu-Triapine increases this signal.

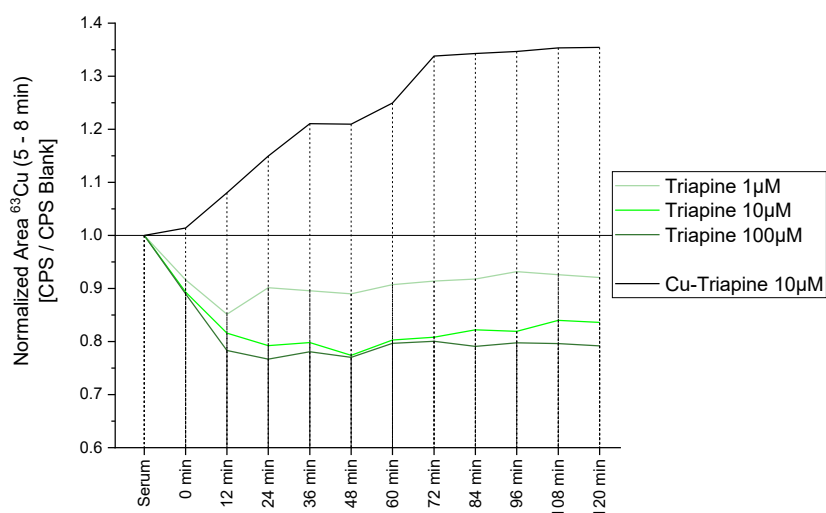


Figure 76: A comparison plot: Integration of signals in an elution time of 5-8min in the copper traces of Triapine agents.

For the iron trace an integration of all signals between 9min and 11min was performed as there are no distinct peaks (as previously explained in section 3.6.1 Baseline measurements (Buffered human blood plasma) on page 67; see figure 77 below - this is the low molecular region i.e. small iron adducts like Hem etc.). Unfortunately, no distinct behavior of Triapine or Cu-Triapine can be made out. In this case both forms (free Triapine and Cu-Triapine) seem not to have any influence on the low molecular iron pool.

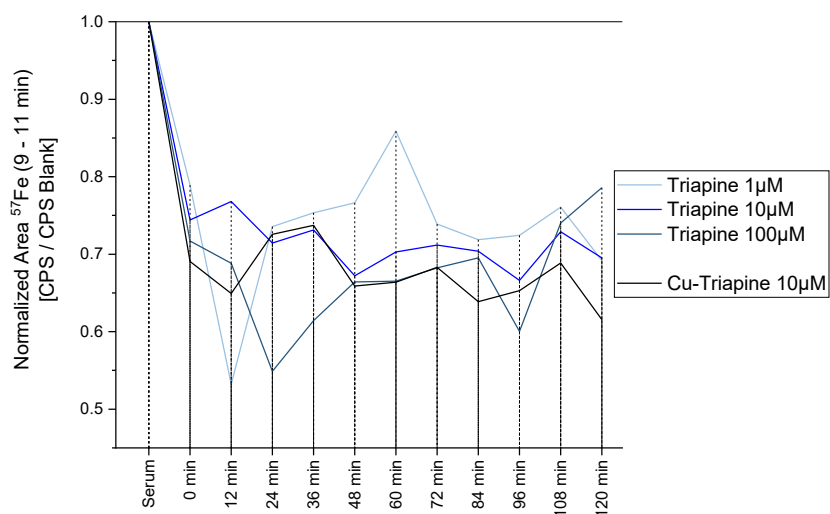


Figure 77: A comparison plot: Integration of signals in an elution time of 9-11min in the iron traces of Triapine agents.

Lastly, all signals in the zinc trace were integrated and normalized i.e. every signal between 5min and 11min (as previously explained in section 3.6.1 Baseline measurements (Buffered human blood plasma) on page 69; see figure 78 below). The variance of the measurement is however very large and there is an apparent downwards trend of the signal as it was the case in blank buffered human blood serum incubation. Cu-Triapine might possibly exert some unexpected behavior, however there is no indication of where is the additional zinc coming from – The whole signal in the zinc trace was in this case integrated so the only logical explanation of the signal raising to 110% at one point is to attribute the course of signal to measurement variance.

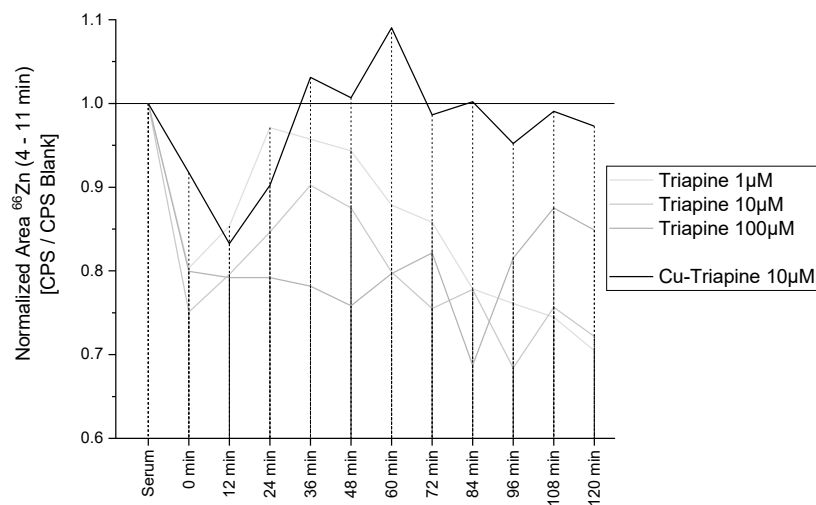


Figure 78: A comparison plot: Integration of signals in an elution time of 5-11min in the zinc traces of Triapine agents.

Me₂NNMe₂. In the case of Me₂NNMe₂ incubation with buffered human blood serum, similar results were obtained in the copper trace (see figure 79 below). The rate of diminishing of the copper-Albumin signal in the copper trace occurs at around the same pace as in incubation with Triapine. Me₂NNMe₂ in 10μM concentration, however, completely complexed Albumin copper in about 48minutes, whereas Triapine copper complexation from Albumin was not complete in the same concertation experiment. This cannot be easily seen in the integration figures. Therefore, when discussing some features of the copper traces the two plots (raw copper traces in the incubation study and integration plots) have to be considered together. The integration values (see figure 80 below) show qualitatively the same behavior as it was the case with Triapine. The attainment of the equilibrium (signal plateau) happens at 12-24min in the case of free Me₂NNMe₂ regardless of the incubation concentration. In case of Cu-Me₂NNMe₂ the equilibrium is attained after around 36min after incubation start.

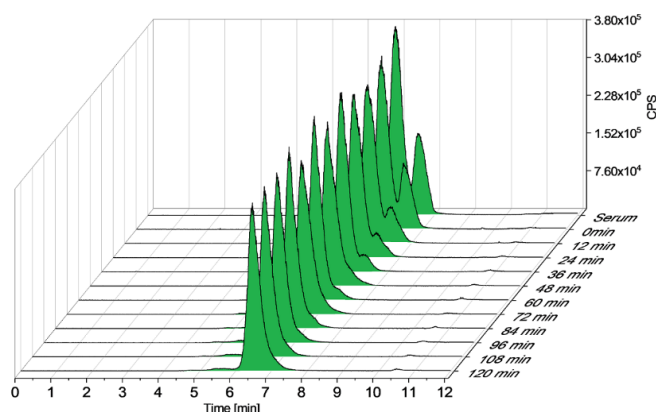


Figure 79: Me₂NNMe₂ Copper traces in the incubation study

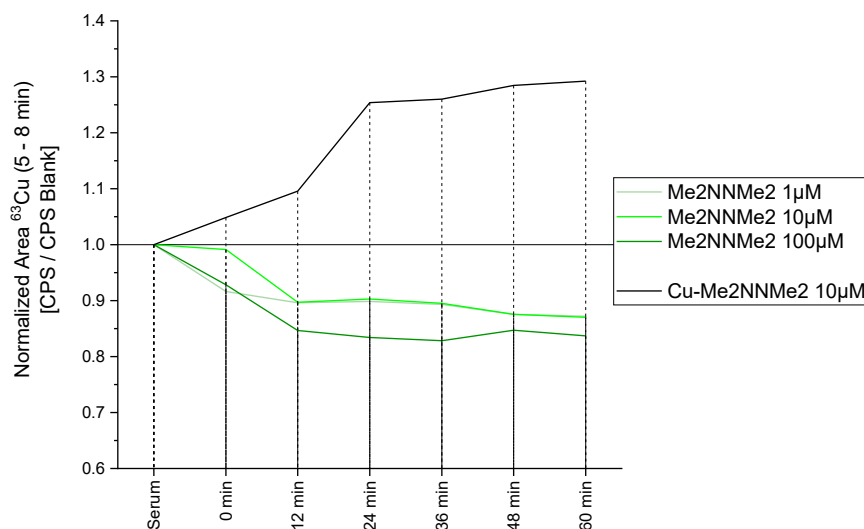


Figure 80: A comparison plot: Integration of signals in an elution time of 5-8min in the copper traces of Me₂NNMe₂ agents

Therefore, it can be concluded that the kinetics of Me₂NNMe₂ is apparently slightly faster than the kinetics of Triapine. This can possibly be correlated to Me₂NNMe₂ being a more potent cytotoxic agent, however a causal conclusion cannot be made.

As for the iron integration the free Me₂NNMe₂ agent in all concentrations showed a downwards trend of the low molecular iron pool (not significant as blank human blood serum showed the same feature). However, copper-Me₂NNMe₂ showed an increase of the iron integration signal after initial decrease (see figure 81 below). As it turns out, this seems to happen across some of the investigated Cu-TSCs as will further be discussed in later parts of this chapter. Unfortunately, many incubation studies were stopped before such changes were finished. This is due to peak features that were not recognizable from the raw data. It is for these rather complicated evaluation methods that allow for recognition of subtle changes. This increase of the low molecular iron pool signal will further be discussed in other TSC agents in the next parts of this chapter. The discussion about zinc integration and comparison of free Me₂NNMe₂ and Cu-Me₂NNMe₂ in the zinc traces will be omitted here because of its very low significance.

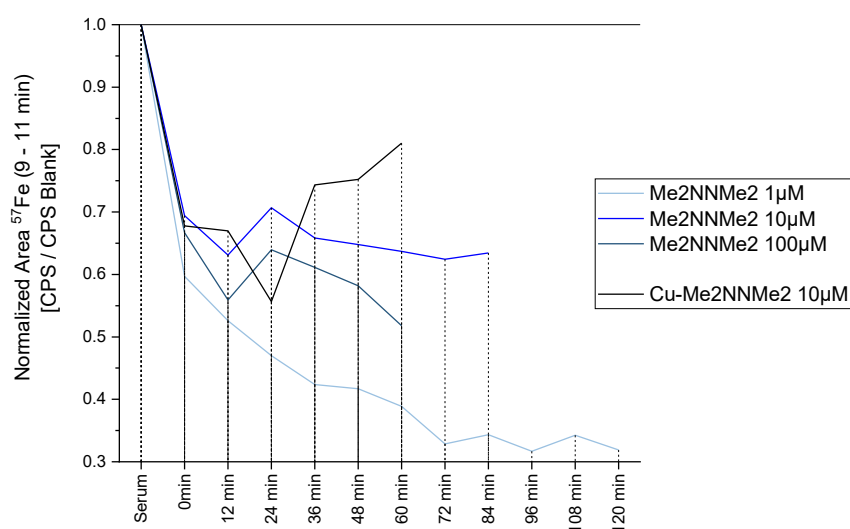


Figure 81: A comparison plot: Integration of signals in an elution time of 9-11min in the copper traces of Me₂NNMe₂ agents.

Dp44mT is one of the most potent cytotoxic agents in the current Thiosemicarbazone-class anticancer drug research. As can be seen from the results the albumin copper signal disappeared quantitatively as soon as after 36min (10 μ M concentration – see figure 82 below). The used 10 μ M incubation concentration of Dp44mT should be sufficient to complex additional copper from other compartments such as from ceruloplasmin. The signal for ceruloplasmin occurs as large peak at around 7,2 minutes but the copper signal from ceruloplasmin does not seem to alter over time. This behavior was previously seen with the “less” aggressive Me₂NNMe₂ and Triapine. These facts allow for several cautious conclusions at this point.

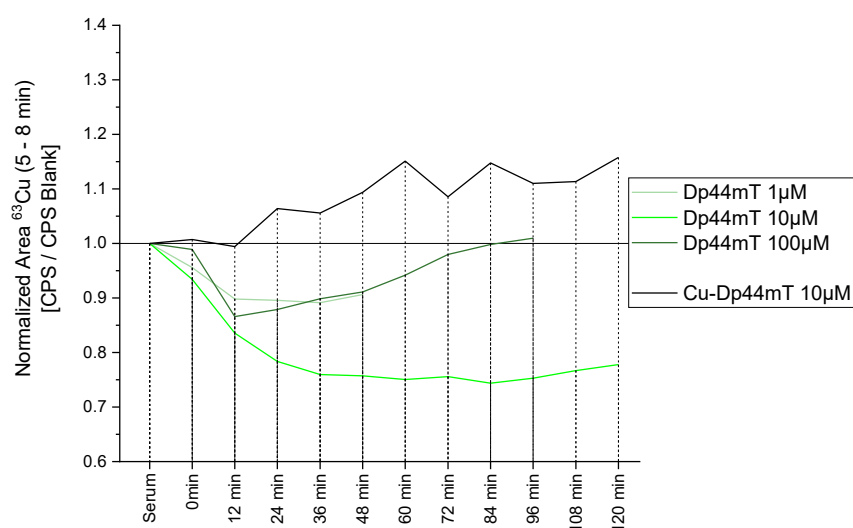


Figure 82: A comparison plot: Integration of signals in an elution time of 5-8min in the copper traces of Dp44mT agents.

First of all, Ceruloplasmin is a protein which serves as means of transport and storage of specifically copper.[75] In humans, but also in other living organisms, copper needs to be tightly regulated because it is, as iron and few other essential metals a potent redox reactive agent. Copper can easily cycle between +I and +II states. Therefore, copper is strongly bound to ceruloplasmin and any cellular and biological copper transactions take place via complicated exchange mechanisms. For this reason, it can be suggested that loosely bound copper in albumin can easily be complexed by some Thiosemicarbazones most likely via cation exchange reaction. This seem not to be the case with ceruloplasmin, and it can be assumed with caution that (at least our tested) thiosemicarbazones lack the mechanistic means of copper extraction from ceruloplasmin.

Secondly, it can be suggested that there might be an equilibrium where the copper-TSCs attach themselves to albumin even when the copper originally stemmed from albumin. This is not very well visible in case of most TSCs tested here but it is identifiable in the case of DpC – the free agent in 100 μ M concentration attains the initial copper albumin level as in blank human blood serum after about 72min. The process is slower for the agent in 1 μ M and 10 μ M concentrations and although not fully verified as the experiment was ended earlier, there is a perceivable upwards trend in the copper albumin signal. Additionally, although not confirmed this attainment of initial conditions is presumed in other TSCs as well.

As for the iron integration of low molecular iron pool a prominent reaction can be seen in Cu-Dp44mT agent where initial conditions are attained after about 240min (4h) – see figure 83. in case of the free agent no such behavior can be made out in the narrow time frame of the measurement.

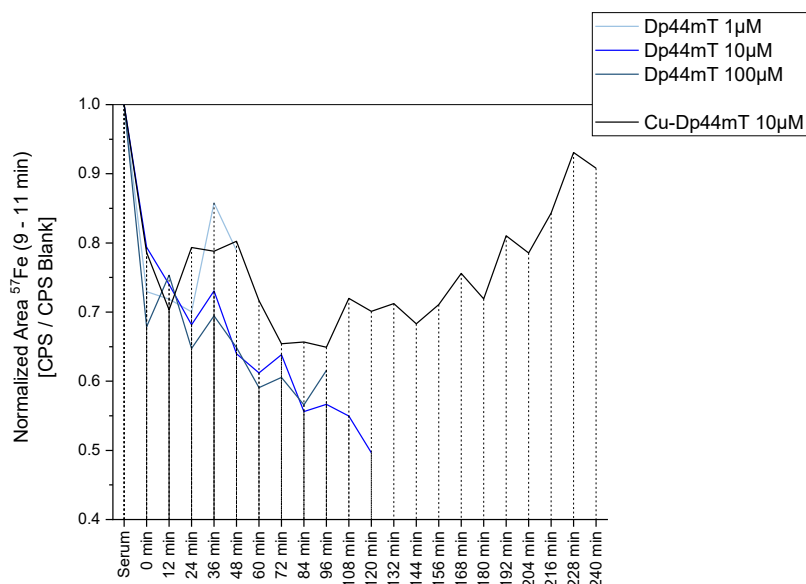


Figure 83: A comparison plot: Integration of signals in an elution time of 9-11min in the copper traces of Dp44mT agents.

DpC: The results for DpC were quite unexpected after a constantly appearing streak of experiments on other Thiosemicarbazones. As can be seen from figure 84 the complexation reaction of DpC with and copper from albumin is somewhat slower than the other TSCs. The striking feature, however, is that copper-DpC does not seem to bind to albumin as other previous TSCs. This agent reduces the copper albumin signal, which can possibly be explained by insufficient copper tagging of the agent at the synthesis step. Additionally, there is a small unremarkable upwards trend, mainly in the case of DpC in a 100 μ M concentration. If this is the case, it would indicate that there is in fact an equilibrium between Albumin-bound and unbound TSC. This is, however, just not visible in the narrow time scale of this incubation study.

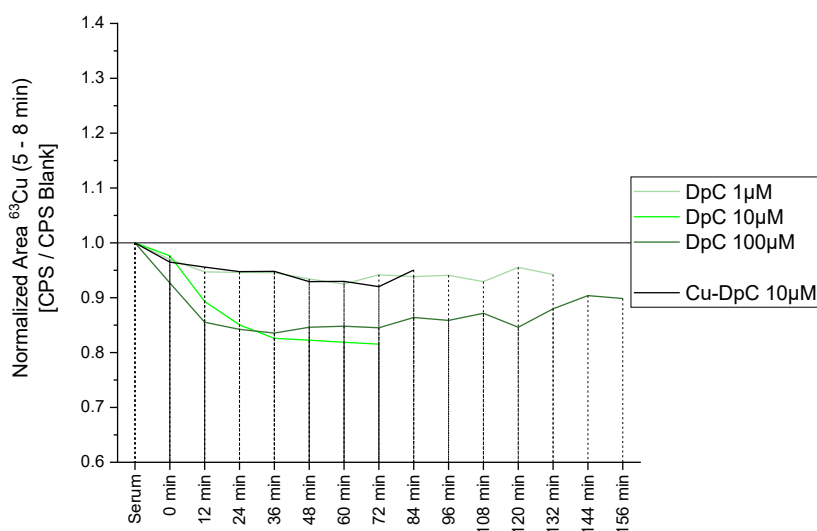


Figure 84: A comparison plot: Integration of signals in an elution time of 5-8min in the copper traces of DpC agents.

The evaluation of iron integration values reveals an apparent process where DpC in high concentration of 100 μ M initially reduces the iron signal in the low molecular region, which then after about 96min begins to increase. This might be the case for all employed concentrations of the agent, there, however, is the rate of the reaction slow enough that it does not show up in this narrow analysis window. This reaction is more prominent in the case of Cu-DpC (see figure 85 below)

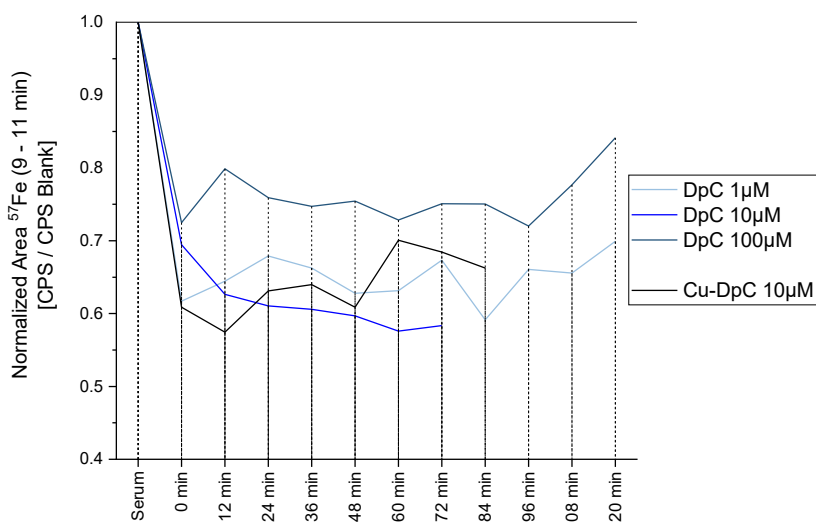


Figure 85: A comparison plot: Integration of signals in an elution time of 9-11min in the iron traces of DpC agents.

COTI2 Figure 86 below depicts the copper trace of the experiment on incubation of COTI2 with human blood serum. As can be seen the previous decrease in the copper signal for albumin does not take place. A generally altered behavior of COTI2 was already suggested by some authors – according to several publications, COTI2 may exert its anticancer cytotoxic function by some other (additional) molecular mechanism than the “classic” thiosemicarbazones[79] analyzed in the scope of this research thesis. In contrast to others, COTI2 has a bulky pyridinylpiperazine moiety attached to its terminal thiosemicarbazone amin.

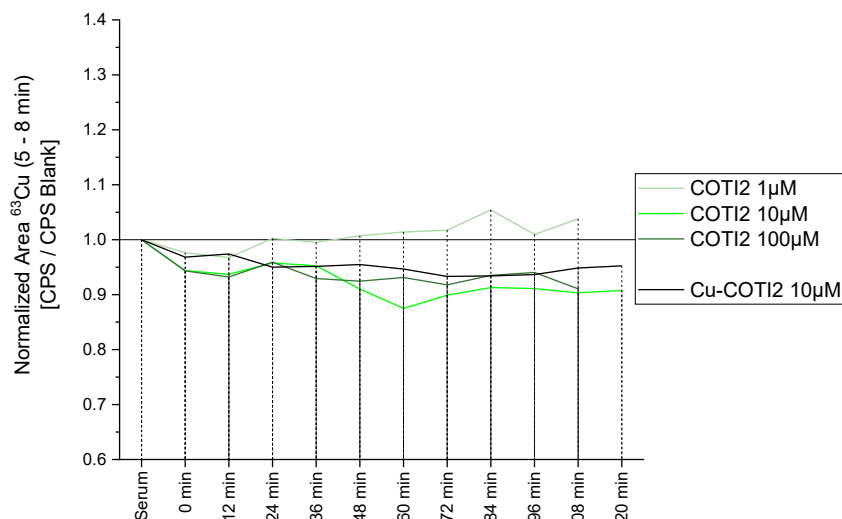


Figure 86: A comparison plot: Integration of signals in an elution time of 5-8min in the copper traces of COTI2 agents.

The Iron integrations of the incubation experiment series of COTI2 can be seen in figure 87 below. There, no clear upwards trends can be made out.

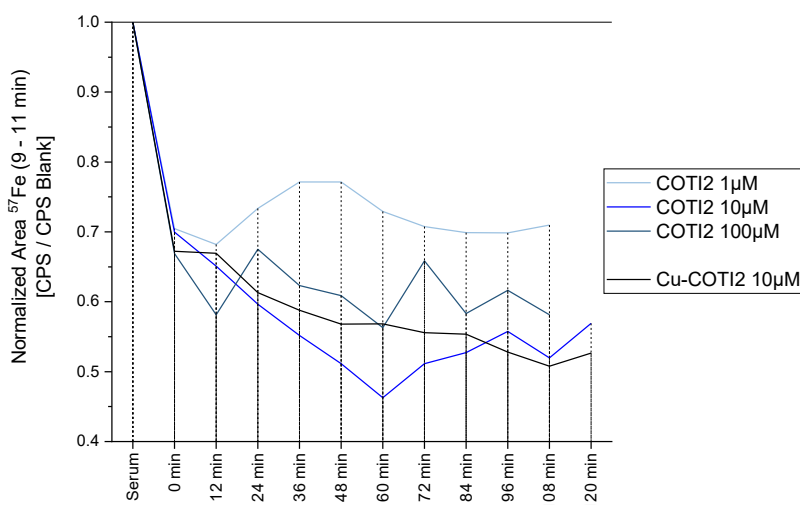


Figure 87: A comparison plot: Integration of signals in an elution time of 9-11min in the Iron traces of COTI2 agents.

To sum up the comparison of all thiosemicarbazones tested in the resulting concentration of 10 μ M, graphs showing a relative change of the integrated areas in the copper, iron and zinc traces of all chromatograms were constructed (see figures 88 – 93 in proceeding parts).

Copper Integration (5-8min) All free TSC agents except for COTI2 complexed the copper from albumin and reached an equilibrium or end of the reaction process¹² after about 48-60min (reaction plateau) – see figure 88. After that no noticeable signal reduction of any analyte was found. On contrary, an apparent opposite process might have taken place where the newly formed copper bound thiosemicarbazones attach themselves to Albumin as a whole (See figure 88) increasing the signal.

The latter process might be plausible for most of the investigated Thiosemicarbazones when considering the behavior of their Copper counterparts (see figure 89). As can be seen Cu-TSCs probably attach to albumin increasing its copper signal. This is true for Cu-Triapine, Cu-Me2NNMe2 and Cu-Dp44mT.

These findings suggest that free Thiosemicarbazones most likely only complex copper that is loosely bound to albumin. Additionally, this process is slightly faster than the binding reaction of Cu-TSCs to Albumin. This theory can explain why there is a reduction of copper albumin signal before an increasing trend of the signal takes place – See figure 88.

The apparent decreasing copper albumin signal caused by Cu-COTI2 and Cu-DpC may be due to some other unknown molecular mechanism or due to higher than usual variance in the measurement and therefore has to be considered carefully.

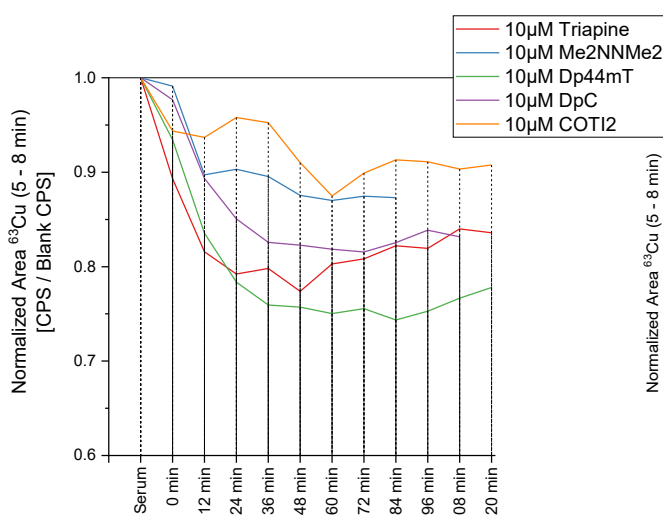


Figure 88: A copper integration comparison plot of all tested TSCs in 10 μ M concentration.

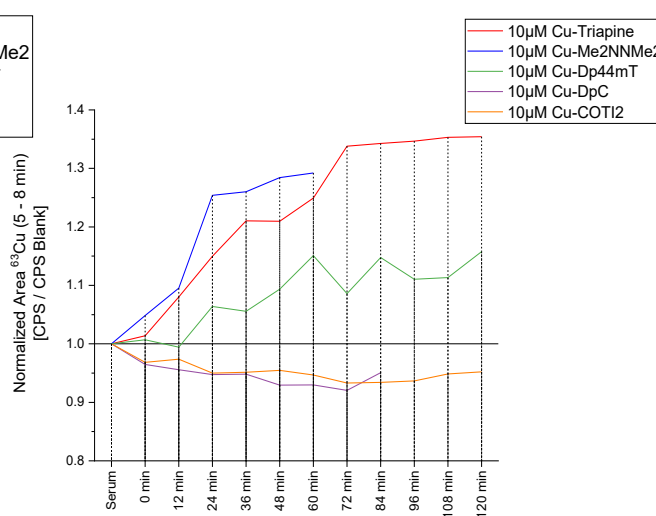


Figure 89: A copper integration comparison plot of all tested Cu-TSCs in 10 μ M concentration.

¹² COTI2 showed no significant/profound change in the copper albumin signal. The change that is observable in the copper area integration stems from higher than usual variance of analysis.

Iron Integration (9-11min). The Iron evaluation of all free TSCs (see figure 90) and all Cu-TSCs (see figure 91) show some interesting but unspecific features. The integrated signal of the low molecular iron pool diminishes even in the blank human blood serum in “incubation” conditions. Therefore, all integrated values for free TSC incubations have rather low significance. In fact, all free TSCs behave more or less in the same way.

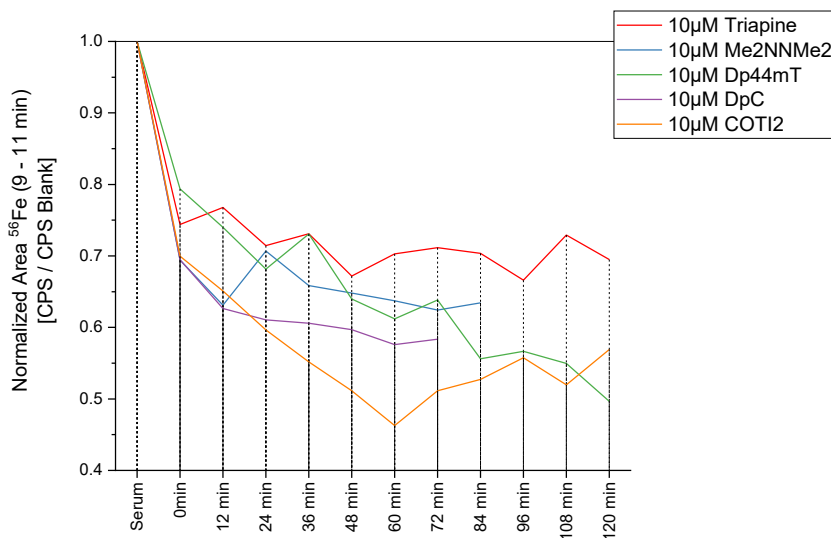


Figure 90: An iron integration comparison plot of all tested TSCs in 10uM concentration.

An interesting behavior found when investigating the Cu-TSCs was that after an initial reduction of the low molecular iron pool signal there is a faint upwards trend. This is predominantly seen in the case of Cu-Dp44mT whose incubation study was performed over a prolonged period of time. As can be seen Cu-Dp44mT might complex the iron from the low molecular iron pool and reverse the trend via an unknown reaction. A more prominent effect is seen in Me₂NNMe₂, but due to premature ending of the experiment it is incomplete.

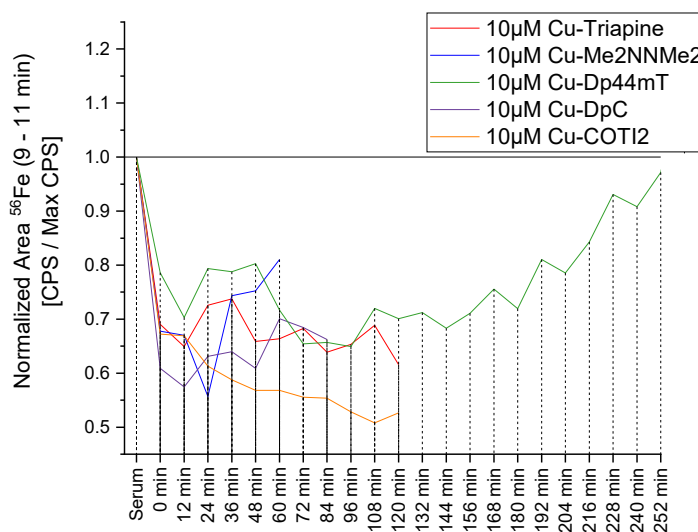


Figure 91: An iron integration comparison plot of all tested Cu-TSCs in 10uM concentration.

Zinc Integration (5-11min). Unfortunately, zinc integration values as well as raw data do not seem to have high significance as for the extremely high blank measurement variance. There is however a seemingly altered behavior of free Dp44mT and COT12 both of which cause an increase in zinc signal whereas all the other free agents show the opposite reaction (see figure 92). Judging from all the raw data (not depicted in this work) the interpretation does not seem feasible at this point. Future research might bring some new insights as zinc reactions of TSCs in biological environments are not yet fully understood.

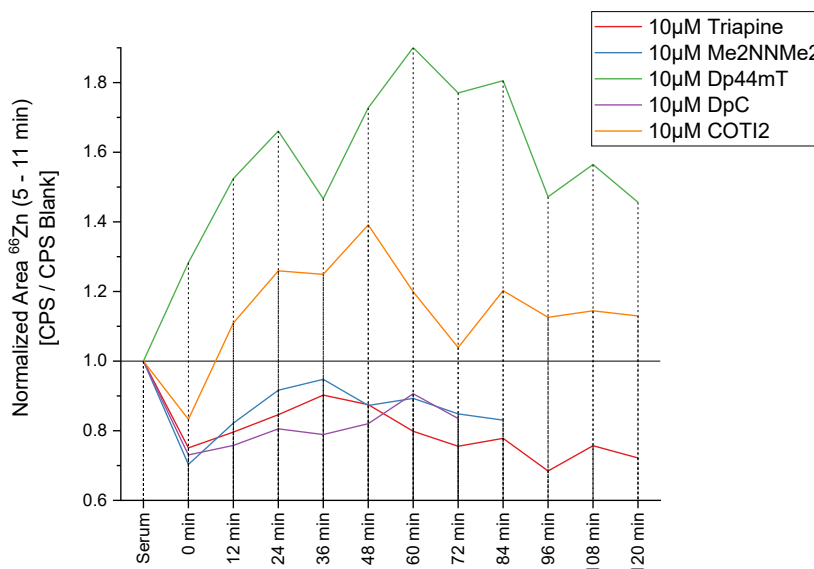


Figure 92: A zinc integration comparison plot of all tested TSCs in 10uM concentration.

The zinc integration of Cu-TSC behaves more or less sporadically as well (see figure 93 below), thereby no further meaningful discussion will be given.

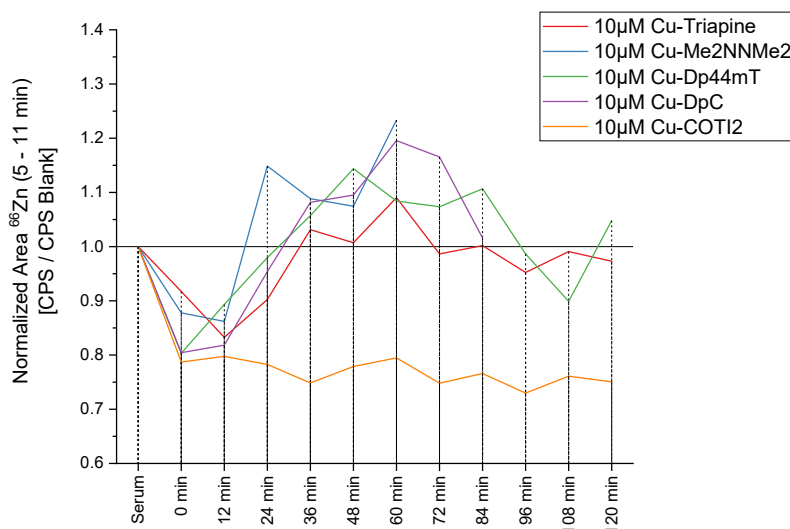


Figure 93: A zinc integration comparison plot of all tested Cu-TSCs in 10uM concentration.

The findings in the copper traces are very interesting and to further prove their significance an incubation study was conducted using only an albumin standard and two TSC agents, namely Triapine and Cu-Triapine. The aim of this experiment is to prove that TSCs in fact bind to albumin. For this purpose, Cu-Triapine was added to albumin solution in a resulting concentration of 10 μ M and analyzed in the same manner as buffered human blood serum. After 24min free Triapine was added in a resulting concentration of 10 μ M to the incubation solution. As can be seen from figure 94 the findings from human blood plasma incubations can be reproduced in a single experiment. The copper Albumin signal increases upon addition of Cu-Triapine. After addition of free Triapine the trend can be artificially reversed. This behavior raises an important question about the exact mechanism of Triapine interacting with albumin.

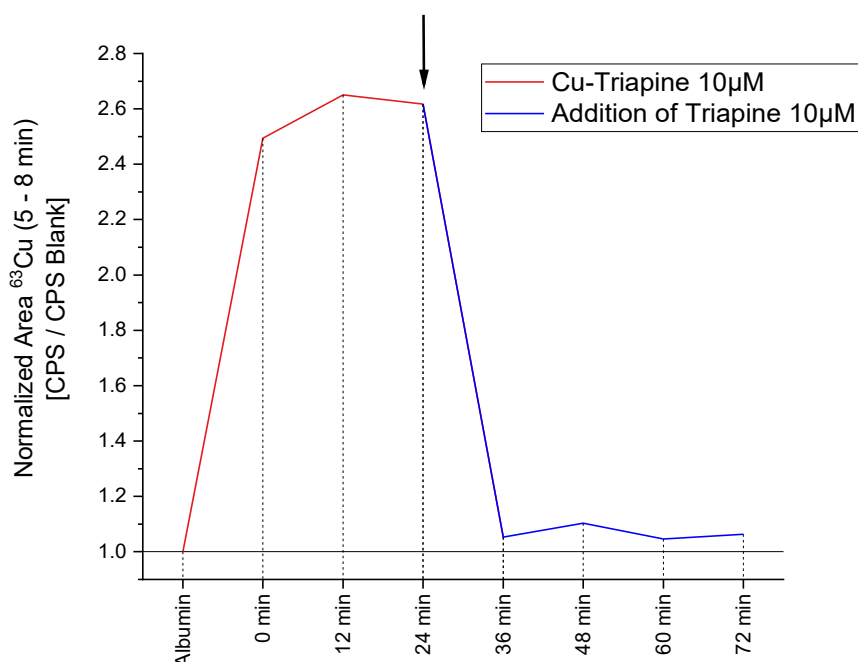


Figure 94: Incubation study of Cu-Triapine with Albumin standard. A successful reversal reaction is achieved by adding free Triapine after 24min into the experiment (marked with an arrow).

Clearly, Cu-Triapine binds to Albumin and increases its copper signal. Free Triapine however, complexes the copper from Albumin but does not stay attached to it immediately. It is assumed that the process of attaching of TSCs to albumin after complexation takes place after a longer period of time (a small evidence for this assumption was given in the experiment with Dp44mT and DpC). This question remains unanswered as my incubation studies were not conducted for long enough. The reasons for this were complicated analysis of TSC and successive worsening of separatory performance which had to be reserved for completion of the experiments.

3.7 Free TSC elution experiment using MabPac analytical column

A side experiment using Thermofischer MabPac (**MAbPac_450Å/300mm**) analytical column was conducted after the TSC's incubation studies to test if the inert PEEK column allows for elution of Thiosemicarbazones that otherwise seem to stick to metal surfaces (like in the steel column used in incubation studies). The PEEK analytical column cannot support very high pressures which rendered it unsuitable for incubation studies - For Incubation studies high flowrates needed to be achieved in order to keep every single separation experiment as short as possible.

All the components of human blood serum eluted after about 15 min completely. The free TSCs and Cu-Bound TSCs, however, could not be seen even after prolonged column elution which lasted 40minutes. This finding suggests that Thiosemicarbazones might irreversibly remain inside the analytical column (concretely inside the pores of the size exclusion stationary phase or attached to some internal structures of the column). This problem was obvious in the incubation studies, where due to TSCs not eluting, the diminishing signals could not be correlated to rising TSC signals. This issue was attributed to the column material – steel. However, the TSCs signals could be detected in flow injection studies suggesting that the problem is not attributable to HPLC system materials. This experiment shows that TSC do not elute even when using inert PEEK column material which is unexpected. Therefore, the problem might be the size exclusion material itself. Thiosemicarbazones are complicated analytes that need careful consideration in every analytical aspect in order to prevent difficulties. In the case of incubation studies performed during this master's thesis the main requirement was to ensure physiological conditions (incubation performed in buffered human blood plasma at 37°C). These requirements prevented the employment of solvent systems that could eventually keep TSCs solubilized even when encountering a favorable absorbent material like steel.

3.8 Alternative quantitation using bovine Cu-Zn Superoxide Dismutase

in this side experiment a quantitation of copper was attempted using a standard bovine Copper-Zinc-Dismutase (bCuZn-SOD) – a detailed procedural description in section 2.5.3 Experimental setup and preparation of alternative quantitation standard on page 35.

The Bovine CuZn-SOD consists of two subunits, each having around 15kDa. The whole Protein has a molecular weight of 30kDa and harbors 2 copper ions (1 Copper ion per subunit).[86]

Figure 95 illustrates a good linearity of the dilution series, which means that there were no severe issues with the dilution procedure itself. However, upon attempting to quantify copper in CRM Seronorm™ a large excess recovery was found (See figure 96).

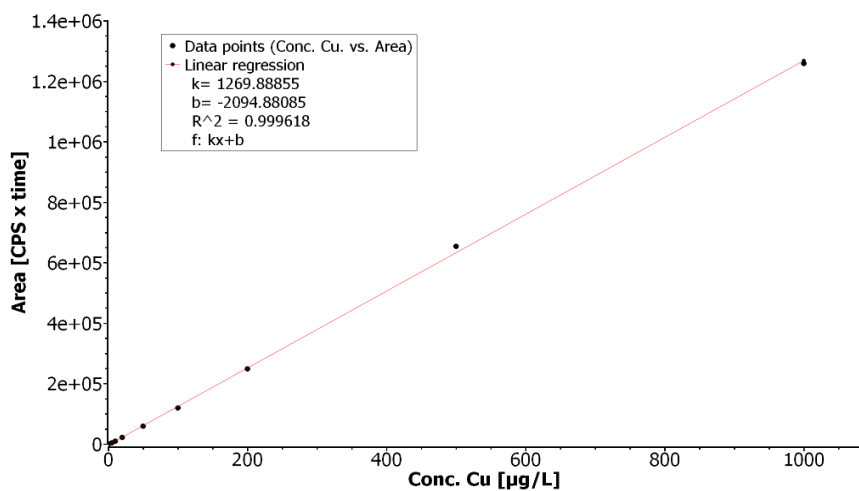


Figure 95: Analytical function resulting from measurements of copper from the dilution series of bovine Cu/Zn Superoxide dismutase. The linear regression was performed using SciDAVis software

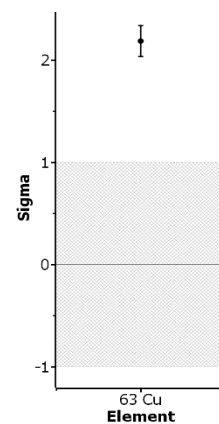


Figure 96: The quality assurance plot showing the result of copper measurement accuracy from CRM - Seronorm™

Therefore, it can be suggested that the used bCuZn-SOD was not pure. Furthermore, another issue occurred during the initial weighing of the protein – the extremely fine protein flakes easily acquired electrostatic charges. Although all involved plasticware was discharged using antistatic gun, the protein flakes were strongly repelled and no accurate weighing could be ensured. However, a quantification can be performed nevertheless, as the recovery factor can be obtained from CRM and used to correct sample results. The Recovery value is in this case 1.43 or 143%. Therefore, all results can be corrected by multiplying by the value 1/1.43 or 0.699. This approach is often avoided but it is well enough suited for semiquantitative studies as those presented in this work. Further parameters demonstrating the usability of this approach were rather low limits of detection and quantitation of copper. In this case the values were 0.159 ppb for LOD and 3.025 ppb for LOQ.

3.9 *In vivo* Incubation (Mouse) – a short metabolic study

In this experiment two mice were subjected to an incubation study for TSCs. First, control urine and blood sample were drawn from both animals. The experiment was then proceeded as described in section 2.5.7 non-lethal in-vivo experiments with Triapine in mouse on page 38. All mouse samples were chromatographically separated but unfortunately the results from blood samples did not show any significant changes when compared to control blood samples. This is probably due to fast excretion of Triapine or due to low deployed concentration of the agent. Furthermore, the behavior of treated mouse urine on the chromatographic column resembled that of aqueous thiosemicarbazone solution. This meant that free Thiosemicarbazones present in the urine eluted in an unpredictable manner rendering the separatory and analytical method unusable.

3.10 CHELEX® ion exchange for background reduction in cell culture media

This experiment should demonstrate a possible strategy for lowering the amount of copper contamination in cell culture medium and its components. Unfortunately, even after extended period of conditioning the CHELEX® resin introduced even more contaminations. Furthermore, this strategy turned out to be unelidable as the components of the cell culture medium need to be buffered to a specific pH. Filtering the components of cell culture media through the ion exchanging resin significantly changed their pH values. This was especially apparent when filtering MEME which contains a mixture of pH indicators (see figure 97 below). The change of its color indicated a decrease in pH rendering the component inapplicable.



Figure 97: Change in pH of MEME cell culture medium component after being fluxed through the ion exchange resin CHELEX®

Nevertheless, the components of cell culture medium and full cell culture media with different combinations of filtered and unfiltered components were measured using the digestion method analogically as in section 3.1.1 Contamination analysis using a digestion method (Agilent 7800) (detailed procedural description in section 2.5.1 Assessment of contaminations in cell culture media on page 33). As already mentioned, the method introduced further contaminations (all metals of interest: copper Iron and zinc). It is, therefore, advisable to pursue another cleaning strategy or using clean precursors (one of the main contaminants - sodium bicarbonate can be purchased in p.a. grade from Sigma Aldrich – Article ID **31437-M** as of July 2021)

4. Conclusions

In conclusion, in the course of this work, a reliable analytical procedure for determining metal concentrations in complex serum-like samples via an “open vessel digestion” - ICP-MS method was established and validated. Another more advanced method: SEC HPLC – ICP-MS was subsequently developed and established which made incubation studies of human blood serum with Thiosemicarbazones possible. The latter procedure created the framework for semiquantitative measurements of three metals, namely Iron, Copper and Zinc in human blood serum incubated with notoriously hard to measure Thiosemicarbazones. Although the issue with extreme systemic retention of Thiosemicarbazones was not resolved, significant results could be produced.

The main experiments – the incubation studies with human blood serum have shown very promising results. It can be argued now, that free Thiosemicarbazones are able to tendentially complex copper from blood albumin when administered. After the complexation reaction now Cu-bound Thiosemicarbazones seem to bind back to albumin as whole. This suggestion is mainly backed by the measurements of pre-complexed Cu-Thiosemicarbazones incubated with human blood serum and by the measurement of albumin standard having been incubated first with Cu-Thiosemicarbazone and then with free Thiosemicarbazone reversing the observed effects. The reaction is not well visible in the incubation experiments of free Thiosemicarbazones - there are only some slight hints that should serve as a reminder for not overinterpreting the results. The results of the other two metals of interest, namely iron and zinc in the incubation studies showed already in blank measurements lower significance. This is very unfortunate, however, there is a small hint that low molecular iron and zinc pools in human blood serum are also affected by Thiosemicarbazones by some unknown mechanisms – this discussion is therefore unfortunately closed as “indecisive”. To round off the incubation studies, a small incubation study in mice was carried out to confirm the findings from the *in-vitro*. Unfortunately, the concentration of the deployed Triapine was probably not high enough in the mouse’s bloodstream to see any significant changes. Another explanation for this finding is rapid excretion of Triapine. When investigating mouse’s urine for the presence of Triapine the unpredictable elution and strong chromatographic retention become again an unhurdled issue.

Considering the complicated character of Thiosemicarbazones being strong chelators there is a strong need to refine chromatographic techniques for effective separations. Metal-bound as well as free thiosemicarbazones currently cause big issues in liquid chromatography – They are strongly retained and elute unpredictably after long periods of time in experiments performed in this work.

A low-pressure tolerant PEEK column was also probed for applicability in the course of this work but failed due to the exact same reason as steel column (unreliable elution). This finding was surprising as the column material was expected to perform in an inert way. Therefore, new strategies and advanced analytical columns (like PEEK coated steel columns as mentioned in the introductory section 1.3 High performance liquid chromatography) should be probed in future research in order to accelerate new, precise and accurate analytical results.

In addition, it was shown that metal contaminations in media might very easily put Thiosemicarbazone research on cultivated cells in jeopardy, when the behavior of free thiosemicarbazones is being the main point of interest. This issue can be easily overcome by deploying reagents in higher purity grade (readily available). Own cleaning strategies like eluting the liquid media components through an ion exchange resin, on the other hand proved to be inadequate.

Lastly, a series of side experiments were conducted to test and probe methods for better analyzability of Thiosemicarbazones – It is clear that this class of analytes is extraordinarily demanding. Thiosemicarbazones showed in every single experiment some unwanted retention to some degree. The most convenient method for quantitation is a flow-injection method using bioinert equipment. In this case the Agilent 1260 Bioinert HPLC system performed satisfactorily. The use of inert materials is however a must. Only PEEK capillaries in place of steel capillaries perform optimally. Another side experiment involved a PEEK chromatographic column MabPac from ThermoFischer. Unfortunately, when aqueous Thiosemicarbazones were introduced, they exerted unpredictable elution behavior and strong retention.

5. References

- [1] West, Douglas X., Subhash B. Padhye, and Pramila B. Sonawane. "Structural and physical correlations in the biological properties of transition metal heterocyclic thiosemicarbazone and S-alkyldithiocarbazate complexes." *Complex Chemistry*. Springer, Berlin, Heidelberg, 1991. 1-50.
- [2] Casas, J. S., M. S. Garcia-Tasende, and J. Sordo. "Main group metal complexes of semicarbazones and thiosemicarbazones. A structural review." *Coordination Chemistry Reviews* 209.1 (2000): 197-261.
- [3] Beraldo, Heloisa, and Dinorah Gambino. "The wide pharmacological versatility of semicarbazones, thiosemicarbazones and their metal complexes." *Mini reviews in medicinal chemistry* 4.1 (2004): 31.
- [4] French, Frederic A., and Erwin J. Blanz. "The carcinostatic activity of α -(N) heterocyclic carboxaldehyde thiosemicarbazones: I. Isoquinoline-1-carboxaldehyde thiosemicarbazone." *Cancer research* 25.9 Part 1 (1965): 1454-1458.
- [5] Moore, E. Colleen, and Alan C. Sartorelli. "Inhibition of ribonucleotide reductase by α -(N)-heterocyclic carboxaldehyde thiosemicarbazones." *Pharmacology & therapeutics* 24.3 (1984): 439-447.
- [6] Nordlund, Pär, and Peter Reichard. "Ribonucleotide reductases." *Annu. Rev. Biochem.* 75 (2006): 681-706.
- [7] Eriksson, Mathias, et al. "Binding of allosteric effectors to ribonucleotide reductase protein R1: reduction of active-site cysteines promotes substrate binding." *Structure* 5.8 (1997): 1077-1092.
- [8] Sender, R., Milo, R. The distribution of cellular turnover in the human body. *Nat Med* 27, 45–48 (2021).
- [9] Nocentini, Giuseppe. "Ribonucleotide reductase inhibitors: new strategies for cancer chemotherapy." *Critical reviews in oncology/hematology* 22.2 (1996): 89-126.
- [10] Szekeres, Thomas, et al. "The enzyme ribonucleotide reductase: target for antitumor and anti-HIV therapy." *Critical reviews in clinical laboratory sciences* 34.6 (1997): 503-528.
- [11] Brockman, R. Wallace, et al. "Observations on the antileukemic activity of pyridine-2-carboxaldehyde thiosemicarbazone and thiocarbohydrazone." *Cancer research* 16.2 (1956): 167-170.
- [12] DeConti, Ronald C., et al. "Clinical and pharmacological studies with 5-hydroxy-2-formylpyridine thiosemicarbazone." *Cancer research* 32.7 (1972): 1455-1462.
- [13] Brockman, R. W., et al. "Heterocyclic thiosemicarbazones: correlation between structure, inhibition of ribonucleotide reductase, and inhibition of DNA viruses." *Proceedings of the Society for Experimental Biology and Medicine* 133.2 (1970): 609-614.
- [14] Antholine, William, et al. "Studies of the reaction of 2-formylpyridine thiosemicarbazone and its iron and copper complexes with biological systems." *Molecular Pharmacology* 13.1 (1977): 89-98.
- [15] Jungwirth, Ute, et al. "Anticancer activity of metal complexes: involvement of redox processes." *Antioxidants & redox signaling* 15.4 (2011): 1085-1127.
- [16] Richardson, Des R., et al. "Dipyridyl thiosemicarbazone chelators with potent and selective antitumor activity form iron complexes with redox activity." *Journal of medicinal chemistry* 49.22 (2006): 6510-6521.

- [17] Attia, S., Kolesar, J., Mahoney, M. R., Pitot, H. C., Laheru, D., Heun, J., ... & Holen, K. D. (2008). A phase 2 consortium (P2C) trial of 3-aminopyridine-2-carboxaldehyde thiosemicarbazone (3-AP) for advanced adenocarcinoma of the pancreas. *Investigational new drugs*, 26(4), 369-379.
- [18] Giles, Francis J., et al. "Phase I and pharmacodynamic study of Triapine®, a novel ribonucleotide reductase inhibitor, in patients with advanced leukemia." *Leukemia research* 27.12 (2003): 1077-1083.
- [19] Miah, A. B., K. J. Harrington, and C. M. Nutting. "Triapine in clinical practice." *The European Journal of Clinical & Medical Oncology* 2.1 (2010): 1.
- [20] Pelivan, Karla, et al. "Understanding the metabolism of the anticancer drug triapine: electrochemical oxidation, microsomal incubation and in vivo analysis using LC-HRMS." *Analyst* 142.17 (2017): 3165-3176.
- [21] Kowol, Christian R., et al. "Impact of stepwise NH₂-methylation of triapine on the physicochemical properties, anticancer activity, and resistance circumvention." *Journal of medicinal chemistry* 59.14 (2016): 6739-6752.
- [22] Rejmund, Marta, et al. "Piperazinyl fragment improves anticancer activity of Triapine." *PloS one* 13.4 (2018): e0188767.
- [23] Whitesell, Luke, and Susan L. Lindquist. "HSP90 and the chaperoning of cancer." *Nature Reviews Cancer* 5.10 (2005): 761-772.
- [24] Laplante, Mathieu, and David M. Sabatini. "mTOR signaling at a glance." *Journal of cell science* 122.20 (2009): 3589-3594.
- [25] Salim, Kowthar Y., et al. "COTI-2, a novel small molecule that is active against multiple human cancer cell lines in vitro and in vivo." *Oncotarget* 7.27 (2016): 41363.
- [26] Lindemann, Antje, et al. "COTI-2, a novel thiosemicarbazone derivative, exhibits antitumor activity in HNSCC through p53-dependent and -independent mechanisms." *Clinical Cancer Research* 25.18 (2019): 5650-5662.
- [27] Quach, Patricia, et al. "Methemoglobin formation by triapine, di-2-pyridylketone-4, 4-dimethyl-3-thiosemicarbazone (Dp44mT), and other anticancer thiosemicarbazones: identification of novel thiosemicarbazones and therapeutics that prevent this effect." *Molecular pharmacology* 82.1 (2012): 105-114.
- [28] Maqbool, Sundus N., et al. "Overcoming tamoxifen resistance in oestrogen receptor-positive breast cancer using the novel thiosemicarbazone anti-cancer agent, DpC." *British journal of pharmacology* 177.10 (2020): 2365-2380.
- [29] Balcaen, Lieve, et al. "Inductively coupled plasma–Tandem mass spectrometry (ICP-MS/MS): A powerful and universal tool for the interference-free determination of (ultra) trace elements–A tutorial review." *Analytica chimica acta* 894 (2015): 7-19.
- [30] Thompson, Michael. *Handbook of inductively coupled plasma spectrometry*. Springer Science & Business Media (2012).
- [31] Olesik, John W. "Elemental analysis using ICP-OES and ICP/MS." *Analytical Chemistry* 63.1 (1991): 12A-21A.
- [32] Thomas, Robert. "A beginner's guide to ICP-MS." *Spectroscopy* 16.4 (2001): 38-42.
- [33] Ammann, Adrian A. "Inductively coupled plasma mass spectrometry (ICP MS): a versatile tool." *Journal of mass spectrometry* 42.4 (2007): 419-427.
- [34] Niu, Hongsen, and R. S. Houk. "Fundamental aspects of ion extraction in inductively coupled plasma mass spectrometry." *Spectrochimica Acta Part B: Atomic Spectroscopy* 51.8 (1996): 779-815.

- [35] Pröfrock, Daniel, and Andreas Prange. "Inductively coupled plasma-mass spectrometry (ICP-MS) for quantitative analysis in environmental and life sciences: a review of challenges, solutions, and trends." *Applied spectroscopy* 66.8 (2012): 843-868.
- [36] Olesik, John W., and Lisa C. Bates. "Characterization of aerosols produced by pneumatic nebulizers for inductively coupled plasma sample introduction: effect of liquid and gas flow rates on volume based drop size distributions." *Spectrochimica Acta Part B: Atomic Spectroscopy* 50.4-7 (1995): 285-303.
- [37] Morishige, Yosuke, and Atsushi Kimura. "Ionization interference in inductively coupled plasma-optical emission spectroscopy." *SEI TECHNICAL REVIEW-ENGLISH EDITION-* 66 (2008): 106.
- [38] Bolea-Fernandez, Eduardo, et al. "Overcoming spectral overlap via inductively coupled plasma-tandem mass spectrometry (ICP-MS/MS). A tutorial review." *Journal of Analytical Atomic Spectrometry* 32.9 (2017): 1660-1679.
- [39] Peláez, Marta Vázquez, José M. Costa-Fernández, and Alfredo Sanz-Medel. "Critical comparison between quadrupole and time-of-flight inductively coupled plasma mass spectrometers for isotope ratio measurements in elemental speciation." *Journal of Analytical Atomic Spectrometry* 17.8 (2002): 950-957.
- [40] Theiner, Sarah, et al. "Single-cell analysis by use of ICP-MS." *Journal of Analytical Atomic Spectrometry* 35.9 (2020): 1784-1813.
- [41] Mueller, Larissa, et al. "Trends in single-cell analysis by use of ICP-MS." *Analytical and bioanalytical chemistry* 406.27 (2014): 6963-6977.
- [42] Dawson, Peter H., ed. *Quadrupole mass spectrometry and its applications*. Elsevier, (2013).
- [43] Miller, Philip E., and M. Bonner Denton. "The quadrupole mass filter: basic operating concepts." *Journal of chemical education* 63.7 (1986): 617.
- [44] Bozorgzadeh, M. H., R. P. Morgan, and J. H. Beynon. "Application of mass-analysed ion kinetic energy spectrometry (MIKES) to the determination of the structures of unknown compounds." *Analyst* 103.1227 (1978): 613-622.
- [45] Maher, Simon, Fred PM Jjunju, and Stephen Taylor. "Colloquium: 100 years of mass spectrometry: Perspectives and future trends." *Reviews of Modern Physics* 87.1 (2015): 113.
- [46] Domon, Bruno, and Ruedi Aebersold. "Mass spectrometry and protein analysis." *science* 312.5771 (2006): 212-217.
- [47] Lum, Tsz-Shan, and Kelvin Sze-Yin Leung. "Strategies to overcome spectral interference in ICP-MS detection." *Journal of Analytical Atomic Spectrometry* 31.5 (2016): 1078-1088.
- [48] May, Thomas W., and Ray H. Wiedmeyer. "A table of polyatomic interferences in ICP-MS." *ATOMIC SPECTROSCOPY-NORWALK CONNECTICUT-* 19 (1998): 150-155.
- [49] May, Jody C., and John A. McLean. "Ion mobility-mass spectrometry: time-dispersive instrumentation." *Analytical chemistry* 87.3 (2015): 1422-1436.
- [50] Guevremont, Roger. "High-field asymmetric waveform ion mobility spectrometry: a new tool for mass spectrometry." *Journal of Chromatography A* 1058.1-2 (2004): 3-19.
- [51] Pick, Denis, Matthias Leiterer, and Jürgen W. Einax. "Reduction of polyatomic interferences in biological material using dynamic reaction cell ICP-MS." *Microchemical Journal* 95.2 (2010): 315-319.
- [52] Brown, K. L., and G. W. Tautfest. "Faraday-Cup Monitors for High-Energy Electron Beams." *Review of Scientific Instruments* 27.9 (1956): 696-702.

- [53] Simonetti, Antonio, Larry M. Heaman, and Thomas Chacko. "Use of discrete-dynode secondary electron multipliers with Faradays—A 'reduced volume' approach for in-situ U-Pb dating of accessory minerals within petrographic thin section by LA-MC-ICP-MS." *Mineralogical Association of Canada Short Course Series 40* (2008): 241-264.
- [54] Medhe, Sharad. "Mass spectrometry: detectors review." *Chem Biomol Eng* 3 (2018): 51-58.
- [55] Feldmann, Joerg, Andrea Raab, and Eva M. Krupp. "Importance of ICPMS for speciation analysis is changing: future trends for targeted and non-targeted element speciation analysis." *Analytical and bioanalytical chemistry* 410.3 (2018): 661-667.
- [56] Sader, Jamil A., and Shawn Ryan. "Advances in ICP-MS technology and the application of multi - element geochemistry to exploration." *Geochemistry: Exploration, Environment, Analysis* 20.2 (2020): 167-175.
- [57] Limbeck, Andreas, et al. "Recent advances in quantitative LA-ICP-MS analysis: challenges and solutions in the life sciences and environmental chemistry." *Analytical and bioanalytical chemistry* 407.22 (2015): 6593-6617.
- [58] Bélanger, Jacqueline MR, JR Jocelyn Paré, and Michel Sigouin. "High performance liquid chromatography (HPLC): principles and applications." *Techniques and Instrumentation in Analytical Chemistry*. Vol. 18. Elsevier (1997). 37-59.
- [59] Snyder, Lloyd R., Joseph J. Kirkland, and John W. Dolan. *Introduction to modern liquid chromatography*. John Wiley & Sons (2011).
- [60] Meyer, Veronika R. *Practical high-performance liquid chromatography*. John Wiley & Sons, 2013.
- [61] Nawrocki, Jacek. "The silanol group and its role in liquid chromatography." *Journal of Chromatography A* 779.1-2 (1997): 29-71.
- [62] McLaren, David G., et al. "An ultraperformance liquid chromatography method for the normal-phase separation of lipids." *Analytical biochemistry* 414.2 (2011): 266-272.
- [63] Dorsey, John G., and Ken A. Dill. "The molecular mechanism of retention in reversed-phase liquid chromatography." *Chemical Reviews* 89.2 (1989): 331-346.
- [64] Sepsey, Annamária, Ivett Bacskay, and Attila Felinger. "Molecular theory of size exclusion chromatography for wide pore size distributions." *Journal of Chromatography A* 1331 (2014): 52-60.
- [65] Wu, Chi-San, ed. *Handbook of size exclusion chromatography and related techniques: revised and expanded*. Vol. 91. CRC press (2003).
- [66] Wagner, Brian M., et al. "Superficially porous particles with 1000 Å pores for large biomolecule high performance liquid chromatography and polymer size exclusion chromatography." *Journal of Chromatography A* 1489 (2017): 75-85.
- [67] Kaegi, Jeremias HR, and Andreas Schaeffer. "Biochemistry of metallothionein." *Biochemistry* 27.23 (1988): 8509-8515.
- [68] Li, Hongbin, et al. "Reverse engineering of the giant muscle protein titin." *Nature* 418.6901 (2002): 998-1002.
- [69] Anderson, N. Leigh, and Norman G. Anderson. "The human plasma proteome: history, character, and diagnostic prospects." *Molecular & cellular proteomics* 1.11 (2002): 845-867.
- [70] La Verde, Valentina, Paola Dominici, and Alessandra Astegno. "Determination of hydrodynamic radius of proteins by size exclusion chromatography." *Bio-protocol* 7.8 (2017): e2230-e2230.

- [71] De Pra, Mauro, et al. "Effects of titanium contamination caused by iron-free high-performance liquid chromatography systems on peak shape and retention of drugs with chelating properties." *Journal of Chromatography A* 1611 (2020): 460619.
- [72] Chen, Xin, and Ying Ge. "Ultrahigh pressure fast size exclusion chromatography for top-down proteomics." *Proteomics* 13.17 (2013): 2563-2566.
- [73] Denko, Charles W. "Protective role of ceruloplasmin in inflammation." *Agents and Actions* 9.4 (1979): 333-336.
- [74] Peters Jr, Theodore. *All about albumin: biochemistry, genetics, and medical applications*. Academic press, (1995).
- [75] Hellman, Nathan E., and Jonathan D. Gitlin. "Ceruloplasmin metabolism and function." *Annual review of nutrition* 22.1 (2002): 439-458.
- [76] Ahmed, Farid E. "Sample preparation and fractionation for proteome analysis and cancer biomarker discovery by mass spectrometry." *Journal of separation science* 32.5-6 (2009): 771-798.
- [77] Butler, John E. "Bovine immunoglobulins: A review." *Journal of Dairy Science* 52.12 (1969): 1895-1909.
- [78] Wassell, Julie. "Haptoglobin: function and polymorphism." *Clinical laboratory* 46.11-12 (2000): 547-552.
- [79] Bormio Nunes, Julia H., et al. "Cancer Cell Resistance Against the Clinically Investigated Thiosemicarbazone COTI-2 Is Based on Formation of Intracellular Copper Complex Glutathione Adducts and ABCC1-Mediated Efflux." *Journal of medicinal chemistry* 63.22 (2020): 13719-13732.
- [80] <http://www.lymphomation.org/tests-immunoglobulins.htm>
- [81] Mänttari, Matti, et al. "Serum ferritin and ceruloplasmin as coronary risk factors." *European heart journal* 15.12 (1994): 1599-1603.
- [82] Asselta, R., S. Duga, and Maria Luisa Tenchini. "The molecular basis of quantitative fibrinogen disorders." *Journal of Thrombosis and Haemostasis* 4.10 (2006): 2115-2129.
- [83] Aliyazicioğlu, Yüksel, et al. "Reference values of cord blood transferrin, ceruloplasmin, alpha-1 antitrypsin, prealbumin, and alpha-2 macroglobulin concentrations in healthy term newborns." *The Turkish journal of pediatrics* 49.1 (2007): 052-054.
- [84] Ziring, Barry, S. "Preoperative Assessment for the Healthy Patient." *Medical Management of the Surgical Patient*. WB Saunders, 2008. 15-33.
- [85] Punnonen, Kari, Kerttu Irjala, and A. Rajamäki. "Iron-deficiency anemia is associated with high concentrations of transferrin receptor in serum." *Clinical chemistry* 40.5 (1994): 774-776.
- [86] Richardson, J. S., et al. "Crystal structure of bovine Cu, Zn superoxide dismutase at 3 Å resolution: chain tracing and metal ligands." *Proceedings of the National Academy of Sciences* 72.4 (1975): 1349-1353.

List of Tables

Table 1: Interferences of some relevant analyte ions. excerpt from Thomas W.May and Ray H.Wiedmeyer, "A Table of Polyatomic Interferences in ICP-MS", (1998)	15
Table 2: All reagents, chemicals and standards that were used in the course of this research thesis.....	23
Table 3: A tabular overview on the general setup and settings of the 7800 mass spectrometer in the direct infusion experiments (samples: standard reference materials, Cell culture media).....	29
Table 4: A tabular overview on the general setup and settings of the 8800 mass spectrometer in the main experiments (Flow-injection and HPLC-MS/MS Experiments).....	31
Table 5: A tabular overview on the used settings of the HPLC setup in the main experiments part.....	32
Table 6: A tabular overview on selected metals and their respective limit of detection and limit of quantitation in the direct infusion experiments performed on the 7800 mass spectrometer.....	40
Table 7: Summarized values on Limits of detection and limits of quantitation in the investigated solvent systems.....	45
Table 8: Comparison table for digestion method (Agilnet 7800) and flow-injection method (Agilent 8800). Values in [$\mu\text{g}/\text{kg} = \text{ppb}$]	46
Table 9: Results from the analysis of copper content in cell culture media (flow-injection method) Values in [$\mu\text{g}/\text{kg} = \text{ppb}$].....	47
Table 10: An overview of the main contents of minimal essential meadium eagle (MEME)	47
Table 11: An overview table on the theoretical and calculated (MLR) protein concentrations in human blood plasma	64
Table 12: The integration data from sulfur traces integrated over the elution time between 4min and 8min	66
Table 13: The integration data from iron traces integrated over the elution time between 8min and 11min	67
Table 14: The integration data from copper traces integrated over the elution time between 4min and 8min.....	68
Table 15: The integration data from zinc traces integrated over the elution time between 4min and 11min.....	69

List of Figures

Figure 1:	General structure of Thiosemicarbazones.....	1
Figure 2:	General structure of α -N-Heterocyclic TSCs.....	1
Figure 3:	Structures of several methyl-derivated TSCs from the publication “Impact of Stepwise NH ₂ -Methylation of Triapine on the Physicochemical Properties, Anticancer Activity, and Resistance Circumvention” by C. Kowol et al. that were systematically tested for anticancer activity on cancer cell lines.....	4
Figure 4:	Periodic table of elements with denotation about ionizability by means of ICP. Table was redrawn and altered from: Pröfrock, Daniel, and Andreas Prange. "Inductively coupled plasma-mass spectrometry (ICP-MS) for quantitative analysis in environmental and life sciences: a review of challenges, solutions, and trends." Applied spectroscopy 66.8 (2012): 843-868.....	7
Figure 5:	General construction of the ICP torch	7
Figure 6:	General construction of a spray chamber being fed via peristaltic pump. The waste of the spray chamber is also pumped away via peristaltic pump.....	8
Figure 7:	schematic construction of a quadrupole. Two opposing rods sharing the same potential resulting in quadrupole electric field as shown in figure 3.	9
Figure 8:	Electrical fields of a quadrupole	9
Figure 9:	Stability diagram from Mathieu equations of a given m/z species. Graph was redrawn from Heinrich, Johannes. “A Be ⁺ ion trap for H ₂ ⁺ spectroscopy.” Diss. Sorbonne université, (2018), p.15	11
Figure 10:	Stability diagrams of three theoretical charged species with ascending order of their m/z values	12
Figure 11:	Schematic graph of a single quadrupole mass analyzer setup and ICP as means of ionization.....	12
Figure 12:	Schematic graph of a triple quadrupole mass analyzer and ICP as means of ionization.....	13
Figure 13:	Schematic figure of a gravity driven liquid chromatography column packed with stationary phase.....	18
Figure 14:	Schematic figure of a pump-driven HPLC system	18
Figure 15:	Chemical structure of silica (normal stationary phase).....	19
Figure 16:	Chemical structure of silica modified with alkyl-silyl chains, that allow hydrophobic interactions on the surface of the stationary phase (reversed stationary phase)	19
Figure 17:	Common steel analytical column Source: https://www.waters.com/webassets/cms/category/media/snapshot/sec_hplc_group_yellow_fobs.jpg	21
Figure 18:	An analytical column made from PEEK Source: https://assets.thermofisher.com/TFS-Assets/CMD/product-images/MabPac%20SCX%20Columns%20Horizontal%20white.jpg-650.jpg	21
Figure 19:	A graphical overview on the selected thiosemicarbazones used in the incubation studies section of this master thesis. The thiosemicarbazones are denoted with their respective names, molecular formulas and average molecular masses.....	26
Figure 20:	A schematic figure on the measurement method. The sample is introduced from the on-site autosampler via a direct infusion method to the Agilent 7800 spectrometer	28
Figure 21:	Agilent 8800 triple quadrupole setup	30

Figure 22: A schematic depiction of the measurement setup consisting of the Agilent 1260 Bioinert HPLC interfaced with Agilent 8800 Mass spectrometer. The measurement mode is either Flow-injection mode bypassing an analytical column or HPLC mode with an installed analytical column	31
Figure 23: A Pasteur pipette filled with CHELEX® ion exchanger material for background reduction experiment with cell culture media.....	37
Figure 24: The Python code used for Multilinear regression employed in a side experiment with protein standards commonly found in human blood serum emulating human blood serum chromatogram measured separately	39
Figure 25: Analytical function plot: Concentration of iron in ppb against counts per second in the experiments on 7800 mass spectrometer. Linear regression performed using SciDAVis.....	41
Figure 26: Analytical function plot: Concentration of copper in ppb against counts per second in the experiments on 7800 mass spectrometer. Linear regression performed using SciDAVis.....	41
Figure 27: A quality assurance plot for the standard reference material measurement of LakeOntario water. All depicted elements are certified as their mean values correspond to the mean value of the certified reference material with an uncertainty margin of $\pm 1\sigma$	41
Figure 28: A quality assurance plot for the standard reference material measurement of Lake Ontario water. Most depicted elements are certified except for ^{63}Cu [no gas mode], ^{66}Zn [no gas mode] and ^{78}Se [no gas mode] which are almost certified (and can easily be corrected by using recovery factors). This is not an issue as these elements are certified in other measurement modi or via their sister isotopes.....	42
Figure 29: Results chart for the 10 analyzed samples showing the amount of Iron in the units of $\mu\text{mol}/\text{kg}$. This experiment was performed on the 7800 mass-spectrometer.....	43
Figure 30: Results chart for the 10 analyzed samples showing the amount of Copper in the units of $/\text{kg}$. This experiment was performed on the 7800 mass-spectrometer	43
Figure 31: Calibration function of copper in solvent system: 0.1% Formic Acid	45
Figure 32: Elution profile of Seronorm™ in flow injection experiment performed on the 8800 Agilent mass spectrometer.....	45
Figure 33: A quality assurance plot for the standard reference material measurement of Seronorm™. Comparison of the digestion method performed on the Agilent 7800 mass spectrometer against flow injection method performed on the Agilent 8800 mass spectrometer.....	46
Figure 34: Elution profile of Triapine in flow injection experiment performed on the 8800 Agilent mass spectrometer. The peak is substantially broader than for example Seronorm™ peak in the same experiment.....	48
Figure 35: The sulfur trace of the separatory experiment with human blood serum on the AcqUHPLC_125Å/150mm analytical column.....	50
Figure 36: The iron trace of the separatory experiment with human blood serum on the AcqUHPLC_125Å/150mm analytical column	50
Figure 37: The copper trace of the separatory experiment with human blood serum on the AcqUHPLC_125Å/150mm analytical column	50

Figure 38: The combined trace of the separatory experiment with human blood serum on the AcqUHPLC_125Å/150mm analytical column.....	50
Figure 39: The sulfur trace of the separatory experiment with human blood serum on the MAbPac_450Å/300mm analytical column	51
Figure 40: The iron trace of the separatory experiment with human blood serum on the MAbPac_450Å/300mm analytical column.....	51
Figure 41: The copper trace of the separatory experiment with human blood serum on the MAbPac_450Å/300mm analytical column	51
Figure 42: The combined trace of the separatory experiment with human blood serum on the MAbPac_450Å/300mm analytical column.....	51
Figure 43: The sulfur trace of the separatory experiment with human blood serum on the AcqUHPLC_200Å/300mm analytical column.....	52
Figure 44: The iron trace of the separatory experiment with human blood serum on the AcqUHPLC_200Å/300mm analytical column.....	52
Figure 45: The copper trace of the separatory experiment with human blood serum on the AcqUHPLC_200Å/300mm analytical column.....	52
Figure 46: The combined trace of the separatory experiment with human blood serum on the AcqUHPLC_200Å/300mm analytical column	52
Figure 47: The sulfur trace of the separatory experiment with human blood serum on the AcqUHPLC_200Å/150mm analytical column	53
Figure 48: The iron trace of the separatory experiment with human blood serum on the AcqUHPLC_200Å/150mm analytical column	53
Figure 49: The copper trace of the separatory experiment with human blood serum on the AcqUHPLC_200Å/150mm analytical	54
Figure 50: The combined trace of the separatory experiment with human blood serum on the AcqUHPLC_200Å/150mm analytical column	54
Figure 51: Comparison of the background signal of copper for all tested analytical columns.....	54
Figure 52: Comparison of the background signal of iron for all tested analytical columns...	54
Figure 53: Additional experiment sulfur trace: separatory performance of the selected AcqUHPLC_200Å/300mm on a mix of protein standards.....	55
Figure 54: Additional experiment iron trace: separatory performance of the selected AcqUHPLC_200Å/300mm on a mix of protein standards	55
Figure 55: Additional experiment copper trace: separatory performance of the selected AcqUHPLC_200Å/300mm on a mix of protein standards.....	55
Figure 56: Additional experiment combined traces: separatory performance of the selected AcqUHPLC_200Å/300mm on a mix of protein standards	55
Figure 57: Stacked chromatograms (Sulfur traces) of 10 of the investigated protein standards.....	56
Figure 58: An overlay plot of the human blood serum chromatogram (sulfur trace) with 10 of the investigated protein standards.....	57
Figure 59: Stacked chromatograms (copper traces) of 10 of the investigated protein Standards.....	58
Figure 60: An overlay plot of the human blood serum chromatogram (copper trace) with 10 of the investigated protein standards. Only 2 of the protein are significant in the copper trace.....	58

Figure 61: Stacked chromatograms (Iron traces) of 10 of the investigated protein standards	59
Figure 62: An overlay plot of the human blood serum chromatogram (Iron trace) with 10 of the investigated protein standards. Only 4 of the proteins are significant in the Iron trace	60
Figure 63: Stacked chromatograms (Zinc traces) of 10 of the investigated protein standards	60
Figure 64: An overlay plot of the human blood serum chromatogram (Zinc trace) with 4 significant protein standards, namely Albumin, Ceruloplasmin, Hatoglobine and a1-Antitrypsin.....	61
Figure 65: Sulfur trace of human blood serum (black line) and calculated sulfur trace from pure analyzed proteins by means of multilinear regression (red line)	62
Figure 66: Sulfur trace of human blood serum (black line) and calculated sulfur trace from pure analyzed proteins by means of multilinear regression (red line).....	63
Figure 67: The error plot constructed from the error matrix. This plot depicts, where is the highest relative error in the calculation (Multilinear regression)	63
Figure 68: Sulfur trace of the blank incubation (no TSC agent) of human blood serum.....	65
Figure 69: Iron trace of the blank incubation (no TSC agent) of human blood serum. Integrated values are highlighted blue	67
Figure 70: Copper trace of the blank incubation (no TSC agent) of human blood serum. Integrated values are highlighted green	68
Figure 71: Zinc trace of the blank incubation (no TSC agent) of human blood serum. Integrated values are highlighted grey	69
Figure 72: Chromatograms from 10 μ M Triapine incubation Study (sulfur traces)	72
Figure 73: Chromatograms from 10 μ M Triapine incubation Study (copper traces).....	72
Figure 74: Chromatograms from 10 μ M Triapine incubation Study (iron traces)	72
Figure 75: Chromatograms from 10 μ M Triapine incubation Study (zinc traces)	72
Figure 76: A comparison plot: Integration of signals in an elution time of 5-8min in the copper traces of Triapine agents.....	73
Figure 77: A comparison plot: Integration of signals in an elution time of 9-11min in the iron traces of Triapine agents.....	74
Figure 78: A comparison plot: Integration of signals in an elution time of 5-11min in the zinc traces of Triapine agents.....	75
Figure 79: Me2NNMe2 Copper traces	76
Figure 80: A comparison plot: Integration of signals in an elution time of 5-8min in the copper traces of Me2NNMe2 agents.....	76
Figure 81: A comparison plot: Integration of signals in an elution time of 9-11min in the copper traces of Me2NNMe2 agents.....	77
Figure 82: A comparison plot: Integration of signals in an elution time of 5-8min in the copper traces of Dp44mT agents.....	78
Figure 83: A comparison plot: Integration of signals in an elution time of 9-11min in the copper traces of Dp44mT agents.....	79
Figure 84: A comparison plot: Integration of signals in an elution time of 5-8min in the copper traces of DpC agents.....	80
Figure 85: A comparison plot: Integration of signals in an elution time of 9-11min in the iron traces of DpC agents.....	81

Figure 86: A comparison plot: Integration of signals in an elution time of 5-8min in the copper traces of COTI2 agents	82
Figure 87: A comparison plot: Integration of signals in an elution time of 9-11min in the Iron traces of COTI2 agents.....	82
Figure 88: A copper integration comparison plot of all tested TSCs in 10uM concentration.....	83
Figure 89: A copper integration comparison plot of all tested Cu-TSCs in 10uM concentration.....	83
Figure 90: An iron integration comparison plot of all tested TSCs in 10uM concentration.....	84
Figure 91: An iron integration comparison plot of all tested Cu-TSCs in 10uM concentration.....	84
Figure 92: A zinc integration comparison plot of all tested TSCs in 10uM concentration.....	85
Figure 93: A zinc integration comparison plot of all tested Cu-TSCs in 10uM concentration.....	85
Figure 94: Incubation study of free Triapine with Albumin standard. A successful reversal reaction is achieved by adding Cu-Triapine after 24min into the experiment.....	86
Figure 95: Analytical function resulting from measurements of copper from the dilution series of bovine Cu/Zn Superoxide dismutase. The linear regression was performed using SciDAVis software.....	88
Figure 96: The quality assurance plot showing the result of copper measurement accuracy from CRM - Seronorm™	88
Figure 97: Change in pH of MEME cell culture medium component after being fluxed through the ion exchange resin CHELEX®	90